



저작자표시-비영리-변경금지 2.0 대한민국

이용자는 아래의 조건을 따르는 경우에 한하여 자유롭게

- 이 저작물을 복제, 배포, 전송, 전시, 공연 및 방송할 수 있습니다.

다음과 같은 조건을 따라야 합니다:



저작자표시. 귀하는 원저작자를 표시하여야 합니다.



비영리. 귀하는 이 저작물을 영리 목적으로 이용할 수 없습니다.



변경금지. 귀하는 이 저작물을 개작, 변형 또는 가공할 수 없습니다.

- 귀하는, 이 저작물의 재이용이나 배포의 경우, 이 저작물에 적용된 이용허락조건을 명확하게 나타내어야 합니다.
- 저작권자로부터 별도의 허가를 받으면 이러한 조건들은 적용되지 않습니다.

저작권법에 따른 이용자의 권리는 위의 내용에 의하여 영향을 받지 않습니다.

이것은 [이용허락규약\(Legal Code\)](#)을 이해하기 쉽게 요약한 것입니다.

[Disclaimer](#)

August 2015

PhD Thesis

Lightweight Algorithms for Reliable Personalized Health Monitoring

Graduate School of Chosun University

Department of Computer Engineering

Olufemi Oluwole Adeluyi

신뢰할 수있는 개인 건강
모니터링을위한 경량 알고리즘의
설계

2015 년 8 월 25 일

조선대학교 대학원

컴퓨터학과

아델루이 올루페미 올루월이

Lightweight Algorithms for Reliable Personalized Health Monitoring

Advisor: Prof Jeong-A Lee

**This Thesis is submitted to the Graduate School of Chosun
University in partial fulfillment of the requirements for
the award of a PhD degree**


2015 년 4 월


Graduate School of Chosun University


Department of Computer Engineering


Olufemi Oluwole Adeluyi

Olufemi Oluwole Adeluyi 의 박사학위논문을 인준함

위원장 조선대학교 교수 모상만 

위 원 조선대학교 교수 이지은 

위 원 조선대학교 교수 문인규 

위 원 전남대학교 교수 김철홍 

위 원 조선대학교 교수 이정아 

2015년 6월

조선대학교 대학원

Dedication

*I dedicate this thesis to my darling wife- Ese and
wonderful children- Daniel and Gabrielle. Your
unflinching support and sacrifice gave me strength
for the journey. Thank you very much.*

Acknowledgements

I will start by acknowledging the role of my Advisor- Prof. Jeong-A Lee. Her mentorship, support and belief played an important role in my research journey. I deeply appreciate all her help.

I am grateful to my professors and the members of my thesis committee (professors Sangman Moh, Inkyu Moon, Jieun Lee and Cheol-Hong Kim) for their guidance and support. I also wish to thank Prof. Kiseon Kim of the Gwangju Institute of Science and Technology (GIST) for his great support in my EEG research.

I thank my labmates for their camaraderie. My family and I made many friends during my PhD program and this made Korea a home away from home. I am also grateful to the management team of the National Information Technology Development Agency (NITDA) for their support.

On a personal note, I would like to thank my parents, parents-in-law and siblings for their immense support and encouragement. I am also grateful for the encouragement that I received from my relatives and friends that reside outside Korea.

I am very grateful to my wife- Ese and children- Daniel and Gabrielle. Their love, sacrifice and presence enabled me to endure the challenging seasons.

I wish to conclude by giving great thanks to God for his wisdom and wonderful support.

Table of Contents

Dedication	i
Acknowledgements	ii
Table of Contents	iii
List of Tables	v
List of Figures	vi
Abbreviations	vii
Abstract	x
요 약	xii
I. Introduction	1
A. Overview	1
B. Motivation	5
C. Contributions	7
D. Thesis Outline.....	7
II. Related Work	8
A. Medical Instrumentation.....	8
B. Analysis of Search Results	10
C. PHM: Key Issues and Prospects.....	23
D. Application of the Information to this Thesis.....	25

III. A Bioinspired Algorithm for Lightweight Neural Telemetry	26
A. Telemonitoring of Neural Signals	29
B. The Basics of Electroception.....	29
C. Bio-inspired electroreceptive Compressive System (BeCoS).....	31
D. System Model and Performance Metrics	33
E. Porting Key Electroceptive Features into BeCoS	37
F. Results	43
IV. R-READER: An Algorithm for Lightweight Detection of Fiducial	
Points in the Cardiovascular Domain	59
A. Detection of R-peaks in ECG Signals	59
B. The R-READER Process.....	65
C. Performance.....	71
V. Conclusion and Future Work.....	76
A. Conclusion.....	78
B. Future Work.....	79
Refernces.....	80
Appendix A	91

List of Tables

(Table 1) Sensors used for PHM.....	11
(Table 2) Examples of Virtual Sensing in PHM	13
(Table 3) Monitoring Scenarios for the Cardiovascular Disease Domain	17
(Table 4) Common Algorithms used in MVIs	21
(Table 5) Comparison of BSBL-BO and BeCoS Coherence Values.....	44
(Table 6) Comparison of BSBL-BO and BeCoS Compression Ratios	46
(Table 7) Comparison of the Power and FPGA Resource Utilization for the BO and BeCoS Core Engines	48
(Table 8) Comparison of BSBL-BO and BeCoS CW-SSIM	51
(Table 9) Effect of Numerical Methods on Signal Reconstruction.....	53
(Table 10) R-peak Points in R-READER and Annotation for Record #100.....	73
(Table 11) R-peak Points in R-READER and Annotation for Record #108.....	74
(Table 12) Accuracy of the R-READER Algorithm	75

List of Figures

(Figure 1) A Typical PHM System.....	1
(Figure 2) Location of PHM Systems on Healthcare Delivery Research Space.....	2
(Figure 3) OECD ALE at Birth (1970-2011).....	3
(Figure 4) Healthcare Cost as a % of GDP.....	4
(Figure 5) Search Strategy.....	9
(Figure 6) Platforms used in MVIs.....	13
(Figure 7) Communication Protocols used for PHM at the Patient-end.....	15
(Figure 8) Remote-PHM Communication Protocols.....	16
(Figure 9) Disease Domains.....	16
(Figure 10) Examples of Signature Signals used for Electroreception.....	Error! Bookmark not defined.
(Figure 11) BeCoS Sensing Approach.....	31
(Figure 12) Conceptual Diagram of the BeCoS System Model.....	33
(Figure 13) System Diagram for Testing Models: (a)BSBL-BO and (b) BeCoS.....	35
(Figure 14) Steps for generating an optimized signature signal.....	Error! Bookmark not defined.
(Figure 15) Coherence across the frequency spectrum.....	45
(Figure 16) Top level block diagram of the BeCoS compression engine.....	47
(Figure 17) Top level block diagram of the BSBL-BO compression engine.....	48
(Figure 18) CW-SSIM for Ch7 [1:700].....	52
(Figure 19) CW-SSIM for Ch1 [3000:3650].....	52
(Figure 20) CW-SSIM for Ch4 [6300:6900].....	53
(Figure 21) Effect of Numerical Methods on Signal Reconstruction.....	55
(Figure 22) A Model of the Variatio Generated by Numerical Methods.....	56

(Figure 23) The Effect of Variation on SSIM	57
(Figure 24) The Effect of Variation on CW-SSIM.....	57
(Figure 25) A Typical ECG Signal Showing the Fiducial Points.....	60
(Figure 26) Steps in the Pan & Tompkins Algorithm	62
(Figure 27) R-READER's Selection of Fiducial and R-peak points for Record #100	66
(Figure 28) Flowchart of Steps in the R-READER Process	69
(Figure 29) Accuracy Comparison for the 2 Algorithms	76
(Figure 30) +P Comparison for the 2 Algorithms	76
(Figure 31) Se Comparison for the 2 Algorithms	77

Abbreviations

AAL: Ambient Assisted Living
 AC: Alternating Current
 ADC: Analog to Digital Converter
 ADL: Activities of Daily Life
 BAN: Body Area Network
 BeCoS: Bioinspired electroceptive Compressive System
 BP: Blood Pressure
 BRAM: Block Random Access Memory
 BSBL-BO: Block Sparse Bayesian Learning-Bound Optimization
 BT: Bluetooth
 CLB: Configurable Logic Block
 CPU: Central Processing Unit
 CS: Compressive Sensing
 CVD: Cardiovascular diseases
 CW-SSIM: Complex Wavelet Structural Similarity Index
 DAC: Digital to Analog Converter
 DCT: Discrete Cosine Transform
 DICOM: Digital Imaging and Communications in Medicine
 ECG: Electrocardiography
 EEG: Electroencephalography
 FF: Flip Flop
 FN: False Negatives
 FP: False Positives
 FPGA: Field Programable Gate Arrays
 GA: Genetic Algorithm
 GSM: Global System for Mobile Communications
 HR: Heart Rate
 I/O: Input/Output
 IOB: Input Output Blocks
 ICU: Intensive Care Unit
 LRV: Linear Regression Variation
 LUT: Look Up Table
 MVI: Medical Virtual Instrument
 NN: Neural Networks
 OECD: Organisation for Economic Co-operation and Development
 p-a-i-d: peak-adjacency-interval-detector
 PAN: Personal Area Network
 PHM: Personalized Health Monitoring
 P-T: Pan-Tompkins
 RAM: Random Access Memory
 R-READER: Rapid-Ramp Effective Algorithm for Detection of ECG R-peaks
 ROM: Read Only Memory

SBA: Simple Bus Architecture
SOC: System On Chip
SpO₂: Saturation of Peripheral Oxygen
SVM: Support Vector Machine
TN: True Negatives
TP: True Positives
VCD: Value Change Dump
WAN: Wide Area Network
WT: Wavelet Transform

Abstract

Lightweight Algorithms for Reliable Personalized Health Monitoring

By: Olufemi Oluwole Adeluyi

Advisor : Prof Jeong-A Lee, Ph. D

Department of Computer Engineering

Graduate School of Chosun University

Patient monitoring techniques are fast evolving from the traditional curative, doctor-centered approach to one that is preventive and patient-centered. A number of factors have influenced this transition; notable among these are the spiraling costs of healthcare management, the ageing of society and the advances in sensor technology. Personalized Health Monitoring Healthcare (PHM) systems play an important role in this new approach.

PHM systems are usually implemented in resource constrained environments such as embedded systems running on limited battery power. As such, any algorithm used for diagnosing and classifying diseases should be lightweight and reliable.

The cardiovascular and neurologic domains were used for the analysis in this thesis. For the neurologic domain we proposed an algorithm known as Bio-inspired electroceptive Compressive System (BeCoS). BeCoS was inspired by wave-type active electroreception used by weakly electric fish. It was used for the sensing, processing, telemetry and reconstruction of neural signals. BeCoS was compared with the well regarded Block Sparse Bayesian Learning-Bound Optimization (BSBL-BO) and it gave higher quality results. BeCoS resulted in coherence, average latency, compression ratio and estimated per epoch power values that were 35.38%, 62.85%, 53.26% and 13mW better than BSBL-BO, respectively, while structural-similarity was only 6.295% worse. The original and reconstructed signals still remain visually similar.

The identification of the R-peaks of electrocardiograms (ECG) represents one of the most important steps for the successful monitoring of cardiovascular health. The Pan-Tompkins (P-T) algorithm has been used as a key reference in the design and testing of algorithms used for the detection of R-peaks. The P-T algorithm uses a cascade of filters to process the ECG signals prior to the identification of the R-peaks. This filtration process results in a large overhead. A Rapid-Ramp Effective Algorithm for Detection of ECG R-peaks (R-READER) has been proposed as an alternative to P-T. It is an intuitive algorithm that uses ECG slopes and inflexion points as a basis for the identification of R-peaks without the need to pass the signals through the filters used in traditional approaches. R-READER gave average accuracy, positive predictivity and sensitivity values of 97.79%, 98.23% and 99.54% when compared to values of 87.47%, 88.57% and 98.59% for the P-T algorithm.

In this dissertation we demonstrate that the BeCoS and R-READER algorithms provide reliable and lightweight alternative for health monitoring in the neurologic and cardiovascular domains respectively. Experimental results also demonstrate a potential for significant performance enhancements when compared to the main algorithms used in the domains.

[KEYWORDS]: personalized health monitoring, reliable computing, lightweight processing, electrocardiogram, encephalogram

요 약

신뢰할 수 있는 개인 건강 모니터링을 위한 경량 알고리즘

아델루이 올루페미 올루월이

지도교수 : 이정아

컴퓨터공학과

조선대학교 대학원

환자 모니터링 기술은, 의사 중심적인 치료 위주의 전통적 접근법에서, 환자 중심적인 예방 위주의 새로운 접근법으로 빠르게 진화하고 있다. 헬스케어 관리 비용의 증가, 사회의 노령화와 센서 기술의 발달 등이 이러한 변화에 영향을 미치는 요소들이다. 개인 맞춤형 건강 모니터링 헬스케어 (PHM) 시스템은 이러한 새로운 접근법에서 중요한 역할을 하고 있다.

제한된 배터리 전력으로 작동하는 embedded 시스템과 유사하게, PHM 시스템은 통상적으로 자원이 제한된 환경에서 구현 되기 때문에, 질병을 진단하고 분류하는 알고리즘은 신뢰성은 물론이고, 연산처리량이 가벼워야 한다.

본 논문에서는 신경계 및 심혈관 영역에서 신뢰성을 유지하면서도 연산처리량을 가볍게 하는 알고리즘을 제안한다. 신경계 영역에서는 Bio-inspired electroceptive Compressive System (BeCoS)라는 알고리즘을 제안한다. BeCoS의 개념은 약한 전기를 사용하는 어류의 파동형(wave-type) 활성 전기인식(electroreception)에서 착안하였다. 이 알고리즘은 신경 신호의 감지, 처리, 원격 측정 그리고 신호 복원을 위해 사용되었다. BeCoS 알고리즘은 잘 알려진 Block Sparse Bayesian Learning-Bound Optimization (BSBL-BO)와 비교했을 때 보다 높은 품질의 결과를 제공하였다. BeCoS는 BSBL-BO보다 62.85% 증가한 일관성, 35.38% 감소한 평균 처리시간, 53.26% 증가한 압축비, 13mW 감소한 추정 epoch 당 전력값을 보였고, 구조적 유사성에서는 6.295% 감소하였지만, 원래 신호와 복원된 신호는 시각적 유사성을 유지했다.

심혈관 영역에서는, 심혈관 건강의 성공적 모니터링에 가장 중요한 단계들 중 하나인, 심전도 R-peaks의 검출에 중점을 두었다. 주요 비교대상으로 Pan-Tompkins (P-T) 알고리즘을 활용하면서, R-peaks을 찾기 위한 경량 알고리즘을 설계하고 실험하였다. P-T 알고리즘은 R-peaks의 확인 이전에 ECG 신호를 처리하기 위해 연속적인 필터를 사용하는데, 이 과정이 큰 오버헤드(overhead)를 초래한다. 본

논문에서는 P-T 알고리즘의 대안으로 ECG R-peaks 의 발견을 위한 Rapid-Ramp Effective 알고리즘, R-READER 를 제안한다. R-READER 는 R-peaks 검출 기반으로, 전통적 접근법이 사용하는 필터가 아닌, ECG 의 기울기와 만곡점(inflexion point)을 사용하는 직관적 알고리즘이다. R-READER 는, P-T 알고리즘이 보인 각각 87.47%, 88.57%, 그리고 98.59%의 평균 정확성, 긍정적 예측도 그리고 감도 값과 비교할 때, 각각 97.79%, 98.23% 그리고 99.54% 값을 제공했다.

본 논문에서는, 신경계 및 심혈관 영역에서의 건강 모니터링을 위하여, 신뢰성을 유지하면서도 연산처리량이 가벼운 대안으로 BeCoS 와 R-READER 알고리즘을 제시하였으며, 이 영역들에서 사용된 기존의 주요 알고리즘과 비교해 보았을 때, 제시된 BeCoS 와 R-READER 알고리즘의 성능이 향상됨을 실험 결과를 통하여 보였다.

[KEYWORDS]: 개인 맞춤형 건강 모니터링(PHM), 신뢰할 수 있는 계산, 경량 프로세싱, 심전도, 뇌파기록

I. Introduction

A. Overview

Health monitoring refers to a systematic approach for keeping track of the health status of any given entity. It can refer to both animate and inanimate objects. For example, the process of monitoring the degradation of infrastructure like bridges and buildings falls under this category, as does the process of monitoring the health of a human being. The former is usually referred to as structural health monitoring (SHM) [1], while the latter is called personalized health monitoring (PHM) [2].

In this thesis, PHM refers to the process of using wearable sensors to monitor a patient's biosignals over an extended period in order to track, predict and maintain their health. PHM usually takes place in uncontrolled environments outside the confines of a hospital [3, 4]. It is more useful for monitoring signals that change over time rather than those that rarely change or those that do not change such as a patient's genotype. Fig 1 shows the common parts of a PHM system.

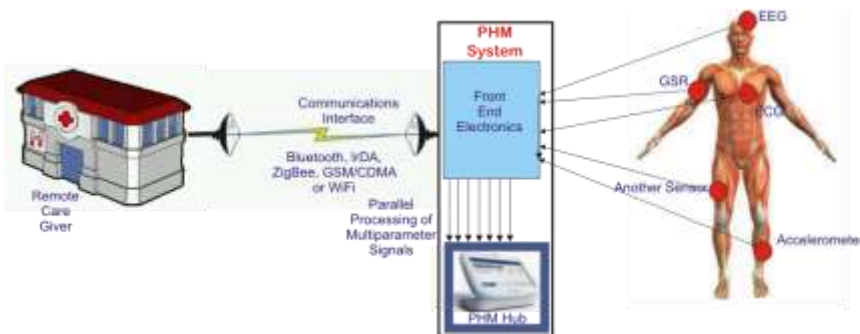


Figure 1: A Typical PHM System

The global healthcare industry has evolved from one that places an emphasis on a curative, doctor-centered healthcare approach to a patient-centered approach that focuses on prevention [5, 6]. This paradigm shift has increased the importance of diagnostic health monitoring and has played a role in making PHM a core part of today’s healthcare delivery system. Fig 2 shows the approximate location of PHM systems in the healthcare delivery research space; toward the top ends of preventive and automated medicine.

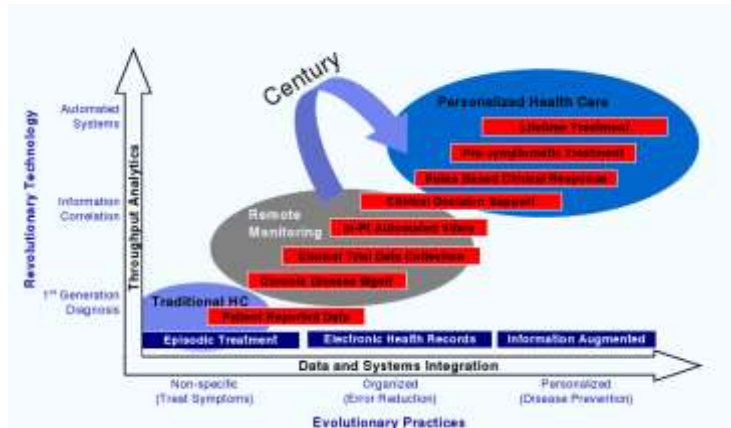


Figure 2: Location of PHM Systems on the Healthcare Delivery Research Space [7]

In addition to the effect of the paradigm shift, three (3) main developments have led to the popularity of PHM:

1. The Rapid Ageing of Society
2. The Rising Cost of Healthcare and the Dwindling Budgets
3. The Availability of Cost-effective Enabling Technologies

The Rapid Ageing of Society

Recent demographic studies have indicated an increase in the Average Life Expectancy (ALE) in many developed countries. As shown in Fig 3, the 2011 ALE at birth for countries in the Organisation for Economic Co-operation and Development (OECD) is now 80.1 years [8]. This represents an average increase of 10.1 years from 1970, with the Republic of Korea and

Turkey having the largest individual increase of 19.0 and 20.4 years respectively.

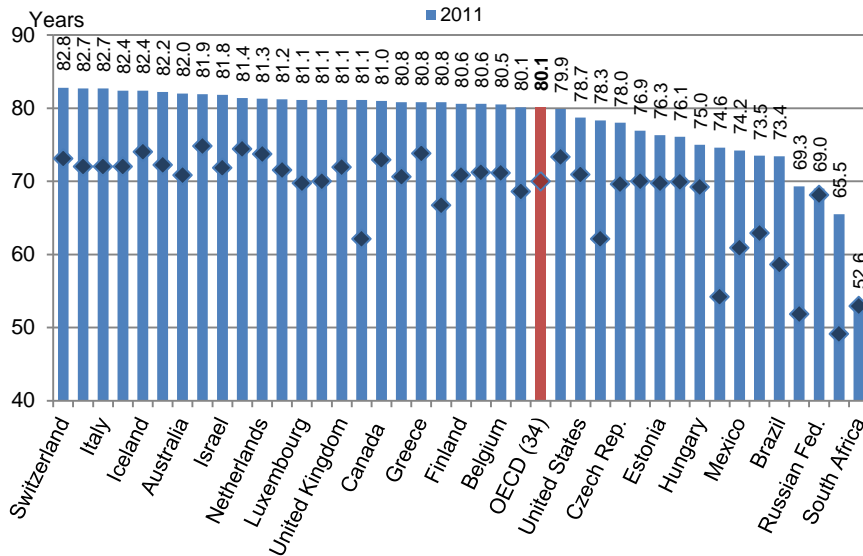


Figure 3: OECD ALE at Birth (1970-2011) [8]

The Rising Cost of Healthcare and the Dwindling Budgets

Healthcare is traditionally perceived as a key determinant of the general quality of life of people and it usually forms a significant part of a country's economy [9]. As shown in Fig 4, there has been a steady increase in the amount of healthcare costs as a percentage of GDP. In 2009, the average share of the total healthcare expenditure as a part of GDP in OECD countries was 9.6%. The United States, Netherlands, Italian and Korean GDP shares were 17.7%, 11.9%, 9.2% and 7.4% respectively [8].

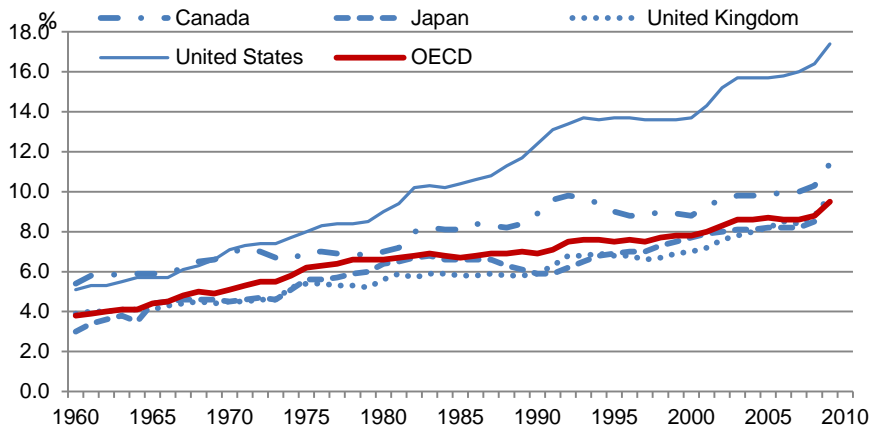


Figure 4: Healthcare Cost as a % of GDP [10]

This increase has not led to a rise in healthcare budgets as many governments have adopted a more frugal approach to government spending in virtually every sector of the economy, including the healthcare sector. For example, in the United Kingdom there was a shortfall of 630million GBP in the 2013/2014 budget for the National Health Scheme (NHS) [11]. Many governments now view the use of technology as a viable option for reducing healthcare costs [12].

The Availability of Cost-effective Enabling Technologies

Recent technological advances in areas such as the sensors, memory, wireless communication and digital signal processing have aided the deployment of PHM systems [13, 14]. Semiconductor technologies like Micro-Electro-Mechanical Systems (MEMS) and Nano-Electro-Mechanical-Systems (NEMS) have also enabled the design of devices with high levels of functionality and miniaturization [15]. As a result of these advances, sensors and actuators have become smaller, cheaper, more sensitive and less power hungry [16].

B. Motivation

Current PHM systems have been generally limited to fitness applications and do not play a significant role in clinical decision making [17, 18]. This is because a number of the systems do not provide the level of reliability required of standard medical systems [19]. Current PHM systems also focus on intermittent monitoring and detection of abnormal signals rather than on the continuous long term monitoring of the entire signals as is common in standard devices at the hospital [20, 21].

PHM systems, unlike their hospital-based equivalents, have to operate under a number of resource constraints [22]. Many PHM systems use batteries to meet their energy requirements [23] and these batteries would be easily depleted when the systems are designed to support long term monitoring and more reliable analysis.

In addition to pattern recognition and disease classification, PHM systems need to support the telemetry of the signals to the physician [24]. These wireless systems usually have limited bandwidths and may experience interference. This would increase the amount of *latency* required to transmit the signals and would restrict the system's ability to support real time monitoring.

PHM systems have a limited storage capacity but they process biosignals, many of which have a high temporal resolution [25]. This leads to very big datasets which require a large amount for storage sometimes beyond the storage capacity of the systems. These challenges have led to research efforts that are aimed at developing PHM systems whose computational requirements are more sensitive to the resource constraints. Such systems should be lightweight in terms of their power, storage and latency profiles.

The algorithms for processing and classifying the signals play an important role in determining the level of complexity of the PHM systems [26, 27]. As such, a proper design of the algorithms is a suitable approach for ensuring that the systems are lightweight. Physicians base their decisions on inferences drawn from the biosignals of the patients. For PHM systems to be reliable they must provide results that are similar to the results obtained by using standard medical devices. Reliability refers to the ability of a system to deliver a service that can justifiably be trusted and the ability to avoid failures that are more frequent and more severe than is acceptable [28, 29].

As a result of the sensitive nature of healthcare, the ultimate decision of the medical choices that are made lies with the physicians. However, a lot will depend on the reliability of the data that is made available to them by the PHM systems.

Ideally PHM systems can be used to monitor signals from any part of the human body. However, this research will focus on two key domains- cardiovascular and neurologic. The cardiovascular domain was selected because it is the leading cause of global deaths. In 2012, it accounted for 17.5 million deaths- 31% of the total number of global deaths [30].

Neurologic disorders now constitute a significant global disease burden [31] and they account for 35% of the global disease burden. An estimated cost of 798 billion EUR was spent on this burden in Europe in 2010 [32]. As a result of its growing importance a number of research efforts around the world now focus on reducing this burden [33, 34].

The research presented in this thesis deals with issues involving lightweight processing and reliability of PHM systems in general, with a greater emphasis on PHM systems in the cardiovascular and neurologic domains.

C. Contributions

In this thesis, we have described a suite of lightweight algorithms for reliable personalized health monitoring. The main contributions are as follows:

- A systematic analysis of the present state, inhibiting challenges and future outlook of medical instrumentation in personalized health monitoring
- Identification of key requirements for lightweight and reliable personalized health monitoring
- Design of a bioinspired lightweight and reliable multichannel algorithms for continuous long term monitoring of neural signals
- Design of an intuitive lightweight and reliable algorithm for continuous long term monitoring of the main fiducial point in cardiovascular signals

D. Thesis Outline

The rest of this thesis is organized as follows: A systematic review of the current body of work on PHM is given in Chapter 2. It identifies the key disease domains, sensors, platforms, algorithms, communication protocols and challenges of PHM systems.

Chapter 3 describes BeCoS- an algorithm for the lightweight sensing, processing, transmission and reconstruction of neural signals. The R-READER algorithm is described in Chapter 4. It is a lightweight approach for identifying the R-peaks of an ECG signal without a need for the noise filtering used in traditional techniques. The conclusions and proposed future work are given in Chapter 6.

II. Related Work

A. Medical Instrumentation for PHM

PHM systems aim to attain a level of reliability comparable to the reliability of medical instruments based at the hospital. Insights on the key requirements for these PHM systems was gained from a systematic literature search that focused on the present state, inhibiting challenges and future outlook of medical instrumentation used for personalized health monitoring.

A total of 915 main articles were reviewed from a search on instrumentation and health monitoring that covered the following databases- Cochrane Library (1992 – August 2014: 40 articles were selected), Web of Science (1973 – August 2014: 233 articles were selected) and MEDLINE (1996 – August 2014: 642 articles were selected). The objective of this systematic review is to give an overview of the current body of work covering instrumentation used for personalized health monitoring.

The emphasis is on the identification of key architectures used for such systems in terms of the type of sensors, modality, type of communication interface and network model. Second, it describes the important application domains of PHM, its level of adaptation and the common algorithms utilized. Third, it outlines the key outcomes of PHM systems, as well as the current challenges and the anticipated future research directions for the field.

Selection Process

The 915 articles generated from the search were further narrowed using a selection process based on the following 5-stage strategy:

1. Deletion of doubles
2. Title scan
3. Abstract scan
4. Cursory full text scan
5. Detailed full text scan

The search strategy is shown in Fig. 5.

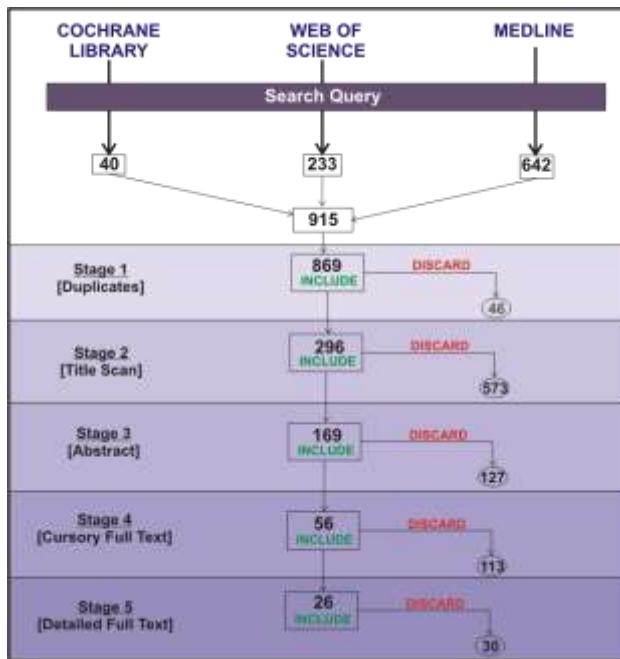


Figure 5: Search Strategy

There were 46 articles that were duplicated and these were deleted before the articles were screened based on their titles. Titles that indicated contents very different from research related to PHM were discarded. There were 573 articles discarded at this stage, leaving a total of 296 articles for the abstract-scan stage. During the abstract scan we eliminated articles that did not align with the theme of medical instrumentation in PHM; 127 articles were filtered out at this stage.

The remaining 169 articles were subjected to a cursory scan of the full text which essentially involved identifying the sections, as well as reading the introduction, discussion and conclusion sections. Articles that did not give sufficient details on the items relating to the theme were discarded. After this stage there were 56 articles that were subjected to a detailed full text scan out of which a further 39 articles were discarded. The criteria included the ones listed in the previous stage and for articles that contained similar ideas we chose the one that outlined the idea with the greatest level of detail. A preference was also given to articles that covered multiple domains, those that addressed unique applications and those which described the instrumentation process in some detail. After these stages we retained 26 core articles for the review. A description of each of these articles is given in Appendix A.

B. Analysis of Search Results

From the analysis of the 26 research articles included in this review, we identified a number of key features that characterize the use of instrumentation for PHM. These features will be discussed in the subsequent sections under the following groupings:

- Architecture
- Application
- Outcomes

Architecture of PHM Systems

The architecture describes the hardware portion of the PHM system and the communication interface. It comprises the sensors, system platform and the communication interface utilized for both the local and remote ends of the MVI.

Sensors and Sensing

The sensors capture the analog biosignals from the patient and condition it for further

processing. The sensing technology plays an important role in the utility of PHM systems. The sensors used in PHM systems can be categorized based on the level of invasiveness.

Table 1: Sensors used for PHM

S/No.	Sensor	Cases	%
1	Electrocardiogram [35, 39, 44, 45, 46, 47, 48, 51, 54, 55]	10	38.50%
2	Blood Pressure [35, 39, 45, 49, 51, 53]	6	23.10%
3	Accelerometer [38, 46, 50, 51, 53, 56]	6	23.10%
4	Oxygen Saturation [38, 45, 51, 53]	4	15.40%
5	Temperature [38, 49, 53, 54]	4	15.40%
6	Microphone [39, 52, 54, 61]	4	15.40%
7	Posture [38, 45, 53]	3	11.50%
8	Pressure [40, 49, 59]	3	11.50%
9	Weight [35, 45]	2	7.70%
10	Cardiac Implantable Electronic Device [36, 43]	2	7.70%
11	Gyroscope [38, 56]	2	7.70%
12	Blood Glucose [57, 60]	2	7.70%
13	Photodiode [41, 53]	2	7.70%
14	Surface Electromyography [37]	1	3.80%
15	Electroencephalography [58]	1	3.80%
16	Tilt [46]	1	3.80%
17	Camera [54]	1	3.80%
18	Pedometer [56]	1	3.80%
19	Gastrocnemius Expansion [56]	1	3.80%
21	Electro Dermal Activity [61]	1	3.80%
22	Chest Impedance [45]	1	3.80%

Invasiveness refers to a need for a puncture of a patient's skin or the introduction of a foreign

body into a patient in order to monitor some signal. Thus, the sensors can be classified as non-invasive or invasive. Tab. 1 shows the type of sensors used in the selected articles and the percentage of the 26 studies where they were used.

At 38.5%, Electrocardiogram (ECG) sensors represent the most extensively used sensors for PHM and when one includes the Cardiac Implantable Electronic Device (CIED) sensors this rises to 46.2%, implying that close to half of PHM systems monitor heart signals. Blood pressure (BP) sensors and accelerometers are the next most prevalent at 23.1% each. It is interesting to note that a number of some of these sensors measure signals as a proxy for another signal of interest and are thus known as virtual sensors.

Virtual sensors [42] are fast becoming an important part of the PHM architecture. They refer to sensors that are based on software rather than hardware and they infer their readings from the relevant hardware sensor(s). These virtual sensors enable patients to monitor biosignals for which it is either impractical to have access to the signal of interest or for which the sensors or related equipment may be too expensive. From the reviewed articles, there were 13 cases (or half) that used virtual sensing. The actual sensors used for this process are listed in Tab 2.

Platform

Many PHM systems do not use a personal computer (PC) as their platform (only one uses the PC [41]). Most of them use a custom device [38, 39, 40, 44, 45, 46, 47, 49, 50, 51, 52, 53, 56, 58, 59, 60, 61] or a mobile phone/personal digital assistant (PDA) [35, 37, 48, 54, 55, 57] as their platform of choice as shown in Fig. 6. The 2 cases of Cardiac Implantable Electronic Devices (CIEDs) [36, 43] were not included since they only use mobile phones for communicating with a remote system.

Table 2: Examples of Virtual Sensing in PHM

S/No.	Virtual Sensor	Actual Sensor	No of Cases
1	Respiratory Rate [38, 50, 53, 59]	ECG, Accelerometer, Pressure	4
2	Heart Rate [53, 55]	ECG	2
3	Respiratory Input Impedance [40]	Pressure	1
4	Blood Flow Velocity [41]	Optical	1
5	Drowsiness Analysis [61]	EDA	1
6	Gait Analysis [56]	Gastrocnemius Expansion Measurement Unit (GEMU)	1
7	Parkinson's Disease Progression [39]	Microphone	1
8	Obstructive Sleep Apnea Syndrome (OSAS) [52]	Microphone	1
9	Consciousness Awareness [58]	EEG	1
	Total		13

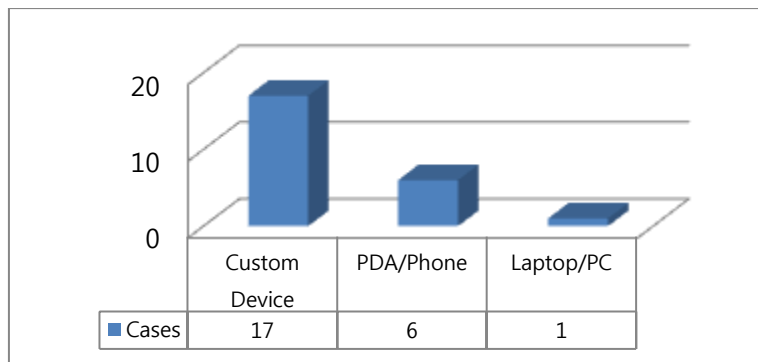


Figure 6: Platforms used in MVIs

Network Models and Communication System

All the PHM systems in the reviewed articles were based on a client-server network model. In most of the systems, the sensed signals were forwarded from the local (or patient) end to an access point device in close proximity to the sensors for onward transmission to a remote server at the remote (or physician) end. In many cases the platforms described in the previous section were used as the access points.

One trend worth noting about PHM network models involves the direct connection between the output of the biosignals and a remote webserver or cloud service, rather than a connection to a specific remote server at the physician's end. Five (5) of the reviewed articles [46, 52, 55, 60, 61] used such a model. A number of advantages can be derived from this approach. One such advantage is the potential of “geographically decoupling” the biosignals [60]. In other words, it reduces the mobility restrictions on the patients since their signals can be streamed to the webserver while they move around freely. The platforms need to be configured as a webserver and should have access to the Internet. Another advantage of this approach is that the signals can be simultaneously viewed by different authorized people (such as the physician and the care giver). The approach can also exploit the memory and processing capabilities of a web or cloud service while reducing the computational complexity of the PHM system at the patient end.

Communication in PHM systems can either be within the modules at the local (patient) end or between the instruments at the patient end and those at the remote (physician) end. As shown in Fig. 7, the wireless protocol was the most common for local-PHM communication and was used in 73.9% of the cases. This included 26.1% for Bluetooth [35, 45, 54, 55, 57, 58], 8.7% for ZigBee [46, 48] and 39.1% of wireless protocols that were not specified [36, 43, 44, 47, 49, 52, 53, 56, 57]. There were 8.7% of the cases that used RS-232 protocols [38, 61] and another

17.4% that used other methods [39, 40, 44, 50]. Some articles did not specify the communication protocol [41, 51, 59].

The cellular networks were the most common approach of for communication in PHM systems between the patient-end and the physician-end. They were used in 56% of the cases [35, 36, 37, 38, 43, 44, 45, 48, 51, 52, 53, 54, 57, 60]. It was followed by the wireless approach (36%, of which 28% were for WiFi [37, 40, 44, 46, 50, 55, 56] and another 8% for unspecified wireless techniques [40, 47]). Digital Subscriber Lines (DSL) were used in 8% of the references [40, 45]. The details are shown in Fig. 8. Some articles used multiple techniques for remote communication and others did not specify the communication protocol [41, 49, 50, 51, 58, 59, 61].

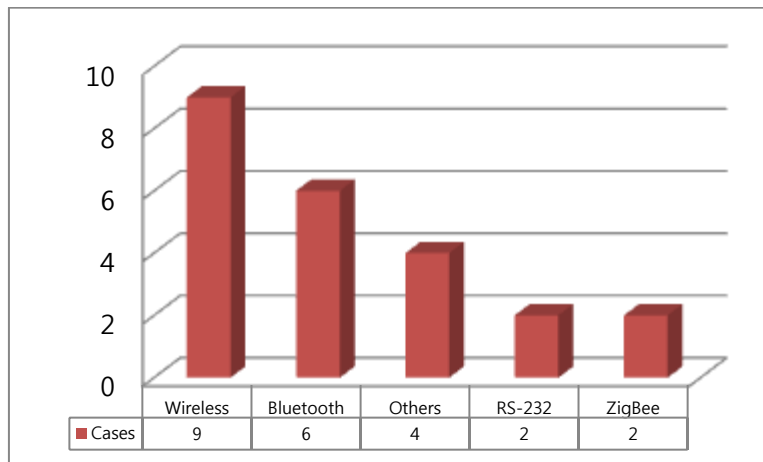


Figure 7: Communication Protocols used for PHM at the Patient-end

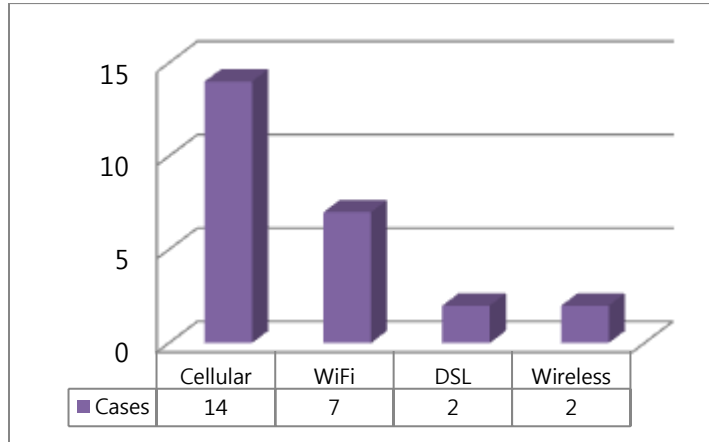


Figure 8: Remote-PHM Communication Protocols

Applications

PHM applications refer to the disease domains, adopted modality, level of system adaptability and algorithms that govern the operation of the instrument.

Disease Domains

PHM systems can be used for medical research applications, clinical applications, healthcare information management systems and mathematical modeling of physiologic systems [63], to name but a few domains of application. However, an analysis of the research articles in this review showed that PHM systems focus on some specific disease domains (Fig 9).

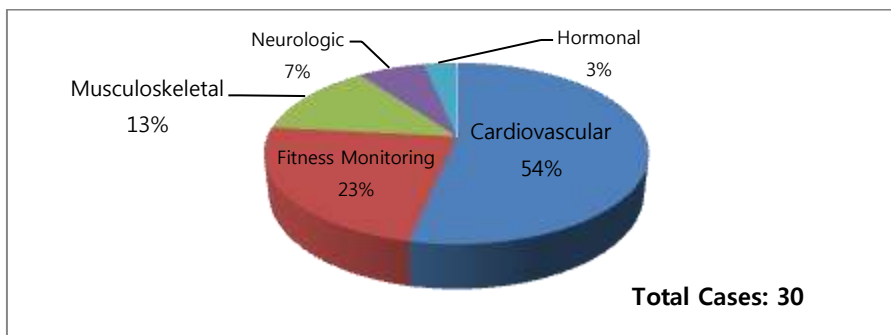


Figure 9 Disease Domains

The Cardiovascular Disease (CVD) domain accounts for over half of the cases. This is understandable since CVDs are the largest single contributor to global mortality. This domain covers the monitoring of biosignals that give an insight into the state of the patient’s heart.

Fitness monitoring refers to cases where the PHM did not target a specific domain. These cases were basically for monitoring general health and fitness. They accounted for about a quarter of the cases. The musculoskeletal domain addressed areas like fall detection, gait analysis and back pain.

Table 3: Monitoring Scenarios for the Cardiovascular Disease Domain

S/No.	Monitoring Scenario	No of Cases
1	Heart Monitoring [35, 43, 44, 47, 48, 55, 58]	7
2	Chronic Heart Failure [35, 45]	2
3	Spirometry [40, 53]	2
4	Hypertension [49]	2
5	Blood Flow Velocity [42]	1
6	Snoring [59]	1
7	Obstructive Sleep Apnea [52]	1
	Total	16

The cases under the neurologic domain focused on mental health monitoring using EEG sensors in one case [48] and using an EDA sensor [51] as a virtual sensor for monitoring drowsiness in the second case. The hormonal disease domain involved a case where blood glucose levels were monitored for the management of diabetes [47].

The constituent monitoring scenarios classified under the cardiovascular domain are shown in Tab 3.

Modality

The modality refers to the expected effect on the state of health of the patient. An overwhelming number of the cases reviewed (24 cases or 92.3%) focused solely on extracting, analyzing and reporting a patient's biosignals. Only 2 PHM systems (7.7%) triggered some form of therapeutic activity in response to the results of the analysis. The first case controlled the delivery of insulin to the diabetic patient [47] and the second case involved a stimulation to help the sleeping patient to stop snoring [52].

System Adaptability

The theme 'personalized health monitoring' presupposes a need to have systems that are personalized to suit the individual needs of a patient. This requires that the systems support some level of adaptability. In the literature review there were 11 (or 42.3%) of the articles that supported some level of adaptation [36, 37, 45, 47, 51, 52, 53, 55, 57, 58, 60]. Most of these were based on adaptation at the communication and architectural levels rather than at the patient level. Five of the six cases with adaptation at the patient level [36, 52, 53, 57, 58] were based on the patient's clinical profile while the sixth was based on the activity state of the patient [61].

Algorithms

The algorithms used in PHM systems refer to a step-by-step procedure for diagnosing and classifying a disease using a finite number of steps [63]. They help patients and physicians to make sense of the biosignals generated by the patient. The choice of the algorithm depends on

the type of diseases to be diagnosed, type of input parameters available for the process and the available resources for the computation.

Several algorithms can be used with PHM systems. A number of the main algorithms used across the various disease domains are either a subset or a combination of the following categories: Derivative-based, Support Vector Machine (SVM), Genetic Algorithm (GA), Threshold-based, Wavelet-based, Neural Networks and Compressive Sensing.

An SVM is a supervised learning model that uses data points (support vectors) closest to the decision surface (hyperplane) of the expected diagnosis to classify new data [64]. It provides a deterministic approach for obtaining an accurate classification that is unique and global. However, the algorithm can tend to be complex and it has high memory requirements [65]. In [66], SVM is used for classify the risk of epilepsy in patients based on their EEG signals.

A GA is a bio-inspired approach that is based on adaptive heuristics. It mimics the process of natural selection in nature and implements the classification using a fitness function. This algorithm is conceptually simple and useful for scenarios where there are several input parameters. The inductive nature of GA means that it can work with internal rules and does not need to know or work with the problem-specific rules. As a result, GAs can be used for several types of problems. It also has the advantage of being robust to dynamic changes in the system environment but cannot integrate problem specific information [67]. GA was used to predict the presence of heart disease in [68].

For many of the biosignals it is possible to predict the presence or absence of a disease based on a given level in the signal and this level is known as the threshold. Algorithms based on the thresholds classify the disease based on some pre-specified or adaptive threshold. These types

of algorithms provide a heuristic approach that is straight forward and generally simpler to implement than the other types of algorithms. Threshold based algorithms were used with ECG signals in [69] and for fall detection in [70].

The NN is a nondeterministic algorithm that was inspired by the interconnection of the neurons in the brain. Its classification is based on simple but highly connected processing elements whose weights are dynamically modified in response to incoming signals based on some learning rule. It is an accurate, robust and highly parallel technique. However, it is comparatively slower than other algorithms and tends to be resource intensive for systems with large input data sets [71]. It was used to screen for heart diseases in [72].

Compressive sensing (CS) is an emerging paradigm for energy efficient sensing, data compression and transmission of biosignals [73, 74]. The CS approach involves the transformation of the sensed data into a domain where the data is sparse in order to reduce the signal processing requirements. It is quite useful for applications where data capture is expensive in terms of time and power. Compressive sensing is discussed in more detail in the next chapter.

Tab 4 shows a list of the algorithms that were explicitly stated by the authors of the reviewed articles. The Pan-Tompkins algorithm featured in the most number of cases (3) and was used for systems targeting the cardiovascular domain. It was proposed in the late 1980s but has remained relevant today because of its suitability for real-time and resource-light processing of ECG signals. It is a first-derivative method that detects the R-peaks of the ECG signals using thresholding techniques following a series of filter stages. This algorithm is described in greater detail in Chapter IV. Peak detection algorithms also were also used in 3 of the systems.

Evaluation Metrics

The choice of the algorithm to use for a given disease domain depends on the following metrics- accuracy, precision, training time, speed, robustness, scalability, specificity and selectivity [75, 76].

The *accuracy* refers to the proximity of the measured value to the actual value. In the field of medicine the accuracy of the measurement has a greater level of importance as it may well be the difference between life and death for the patient. The accuracy is a ratio of the correct readings (true positives and true negatives) to all the readings taken as shown in Eq 1.

Table 4: Common Algorithms used for PHM

Algorithm	Cases
Pan-Tompkins [45, 48, 51]	3
Peak detection [38, 50, 58]	3
Thresholding [38, 39]	2
Wavelet transform [55, 59]	2
Correlation [41, 43]	2
Fuzzy-based [44]	1
Machine learning [54]	1
Least squares [40]	1
Edge detection [50]	1

$$\text{Accuracy} = \frac{\text{Number of correct assessments}}{\text{Number of total assessments}} = \frac{\text{TN}+\text{TP}}{\text{TN}+\text{TP}+\text{FN}+\text{FP}} \quad (1)$$

Precision refers to the consistency of the results under unchanged conditions. It is the ratio of the true positives to the total number of positives (true and false). The true positives refer to the number of positive outcomes that were correctly identified while the true negatives refer to the number of negative outcomes that were correctly identified. Conversely, the false positives (FP) and the false negatives (FN) refer to those incorrectly identified as positive and negative respectively.

Speed refers to the duration it takes to complete the classification process and this includes the time used in the training process for the classifier algorithm. For many medical signals this training process is needed to ensure proper analysis and classification. The *robustness* of an algorithm describes how much the performance is independent of the type and distribution of the input signals.

Scalability refers to the ability of the system to maintain its level of performance as the size of the input signal increases. In medical diagnosis, the specificity is the proportion negative classifications that are correctly made while the sensitivity refers to the proportion of positive classifications that are correctly made. As such specificity focuses on correct exclusions while sensitivity focuses on correct detections. The specificity and sensitivity can be calculated using Eq 2 and Eq 3 respectively.

$$\text{Specificity} = \frac{\text{Number of true negative assessments}}{\text{Number of all negative assessments}} = \frac{\text{TN}}{\text{TN}+\text{FP}} \quad (2)$$

$$\text{Sensitivity} = \frac{\text{Number of correct assessments}}{\text{Number of all positive assessments}} = \frac{\text{TN}+\text{TP}}{\text{TP}+\text{FN}} \quad (3)$$

C. PHM: Key Issues and Prospects

There are five (5) themes that were identified from the review as the key issues in the design and development of PHM systems, namely:

1. The need for personalization based on the profile of the patient
2. The need for more diverse PHM systems
3. The need for resource-light systems that support reliable long-term monitoring
4. The need for more non-invasive and non-intrusive PHM systems
5. The need for a greater degree of system miniaturization, virtualization and for more cloud based applications

Personalization for PHM Systems

Personalization is one of the main motivations for PHM [77]. It is a trend away from the sometimes ineffective “one-size-fits-all” approach used in standard medicine to a more effective approach that is customized for the specific needs of a given patient. The conclusion of The Human Genome Project [78] in 2001 has significantly increased interest in the area of personalized medicine, where diagnostic routines are used to determine the best treatment approach that can suit a specific patient. Many research efforts are exploring approaches that would enable PHM systems to adapt themselves to the unique profile of the patient in areas such as the patient’s genetic information or other biomedical data unique to the patient [79, 80].

Diversity for PHM Systems

More research effort is needed to increase the variety of PHM systems, away from devices that mainly focus on cardiovascular health and general fitness monitoring. For example, mental health is becoming a big global healthcare concern. It has been reported that one in four people now experience a mental health problem in their lifetime [81]. EEG sensors provide a low cost option for monitoring brain signals and researchers need to take advantage of this.

Reduced Processing Complexity and Long Term Monitoring

The requirement for mobility in PHM systems comes with a need for flexible and less power hungry applications since many of these systems use batteries as their power sources. The current need for continuous biosignal monitoring puts an additional strain on the limited resources of the PHM systems [82, 83, 84, 85]. As such, lightweight algorithms are required to ensure reliable health monitoring within the constraints imposed by these systems. Such algorithms must be lightweight with regard to the following metrics:

- (i) Power
- (ii) Memory
- (iii) Bandwidth
- (iv) Latency

Non-invasiveness and Non-intrusiveness

Non-invasive and non-intrusive are two words that describe the desired type of sensors for PHM systems [86]. It is desirable to provide comfortable sensors for the patients since the PHM systems are expected to support long term monitoring. Many PHM systems are non-invasive and these include systems that use ECG, EEG and accelerometer based sensors. In addition to a need to support non-invasive sensing, recent PHM systems go a step further by supporting non-intrusive sensors. The goal of a non-intrusive PHM system is to sense biosignals without intruding into the activities of daily living of the patient. A common approach involves the use of non-contact and capacitive sensors that are embedded into clothing, furniture, watches or jewelry [87, 88, 89].

Another approach involves the use of proxy or virtual sensors. For example, [59] uses a virtual sensor based on a pressure sensor embedded in a pillow. By using this approach, the

authors avoided the need for expensive, complex and intrusive polysomnography equipment by inferring its readings from the virtual sensor.

D. Application of the Information to this Thesis

In this thesis we will focus on the third key issue of PHM- the need resource-light systems that support reliable long-term monitoring. The thesis addresses two main domains- the dominant domain for PHM systems (the cardiovascular domain) and one of the fastest growing domains of interest (the neurologic domain).

The approach involved studying these two domains and identifying the unique features of the relevant biosignals that can be exploited to develop an intuitive approach for reducing the complexity of signal processing. we identified the main lightweight approaches used for long term monitoring of biosignals in these domains, located the most computationally intensive portions of the algorithms and devised a way around them without sacrificing the reliability of the system. Algorithms have been developed for the two domains and compared with the current leading lightweight algorithms.

III. A Bioinspired Algorithm for Lightweight Neural Telemetry

A. Telemonitoring of Neural Signals

Neural signals usually result in a very large dataset, the processing and transmission of which require much energy, storage and processing time. In this chapter we present a Bio-inspired electroceptive Compressive System (BeCoS) as an approach for minimizing these penalties. It is a lightweight and dependable system for the compression, transmission and reconstruction of neural signals inspired by active electroceptive sensing used by weakly-electric fish. It uses a signature-signal and a sensed pseudo-sparse differential signal to transmit and reconstruct the neural signals remotely.

Some signals from a 64-channel EEG dataset have been used to compare BeCoS with the Block Sparse Bayesian Learning-Bound Optimization (BSBL-BO) technique - a popular compressive sensing technique used for low energy and reliable wireless telemonitoring of EEG signals. This research explores the possibility of using BeCoS as a lightweight and dependable approach for the compression and recovery of non-sparse EEG signals.

Compressive Sensing

Traditional sensing techniques are based on the Nyquist theorem [90] and this requires signals to be sampled at a frequency equal to at least double their bandwidth in order to perfectly capture the signal. Compressive sensing (CS) techniques approach the challenge of sensing in a much different way.

In CS, the goal is to find a base, γ , to transform a high dimensional analogue data, \mathbf{x} , of dimension N , into a k -sparse analogue data set, \mathbf{x}^* using the Eq (4).

$$\mathbf{x} = \boldsymbol{\gamma} \mathbf{x}^* \quad (4)$$

The next step in CS involves the use of a user defined sensing matrix, Φ , to generate \mathbf{y} , a compressively sensed representation of \mathbf{x} using Eq (4) and (5).

$$\mathbf{y} = \Phi \mathbf{x} \quad (5)$$

The original signal, \mathbf{x} , is then reconstructed at the remote receiver using \mathbf{y} and Φ . \mathbf{y} is a compressively sensed representation of \mathbf{x} when $\boldsymbol{\gamma}$ and Φ are incoherent. This condition is met when Φ is chosen as a random matrix. The CS approach is effective when there is a sparse representation of the original signal. In this approach, the greater the level of sparsity of the sensing matrix, Φ , the greater the potential compression ratio and the lower the energy requirements.

CS [91] provides a good option for the lightweight sensing, processing, transmission and reconstruction of signals. However, CS systems need to use signals that are sparse in the time or transformed domains in order to reconstruct the signals with a high level of fidelity. EEG signals are neither sparse in the time nor the transformed domains and this makes the traditional CS- based EEG telemonitoring approach inadequate for clinical applications.

For non-sparse signals, it is necessary to use a sparsifying dictionary matrix, \mathbf{D} , to obtain a sparsified form of \mathbf{x} (\mathbf{x}^d) as shown in Eq (6). Eq (5) can thus be replaced by Eq (7).

$$\mathbf{x} = \mathbf{D} \mathbf{x}^d \quad (6)$$

$$\mathbf{y} = \Phi \mathbf{D} \mathbf{x}^d \quad (7)$$

Again, the success of the approach depends on the system's ability to find a sparse representation of \mathbf{x} . This underscores the importance of finding an appropriate user defined dictionary matrix, \mathbf{D} . This process can be challenging for arbitrary signals like EEG since general dictionary matrices are unable to sparsify them sufficiently.

Block Sparse Bayesian Learning Bound Optimization (BSBL-BO)

The Block Sparse Bayesian Learning (BSBL) framework has recently been proposed as a lightweight approach for processing biosignals in a way that avoids the requirement of an optimal dictionary matrix. It is based on the premise that most natural signals have a rich structure and can be represented as a concatenation of blocks [92] as shown in Eq(8). It uses user defined block partitions and assumes that most of these blocks are sparse.

$$\mathbf{s} = \left[\underbrace{[s_1, \dots, s_{l_1}]}_{s_1^T}, \dots, \underbrace{[s_{l_{g-1}+1}, \dots, s_{l_g}]}_{s_g^T} \right]^T \quad (8)$$

where s_i describes the block interval i of length l_i .

BSBL-BO is a fast learning BSBL based on the bound-optimization method [92]. It has been effectively applied as a lightweight solution for the reconstruction of temporally correlated EEG signals [93]. The authors' empirical results showed that non-sparse EEG signals can be reconstructed with a high level of fidelity by using BSBL-BO with standard dictionary matrices.

In [93], the solution was based on the use of a sparse binary matrix as the sensing matrix, Φ , and an inverse Discrete Cosine Transform (DCT) as the dictionary matrix, \mathbf{D} . The use of this type of dictionary matrix created a system that was 2.58 times faster than a system which did not use the dictionary matrix [93]. BSBL-BO has been used as the reference technique for

comparing BeCoS.

B. The Basics of Electroreception

Electroreception, also known as electroreception, refers to the ability to perceive natural electrical stimuli. Lampreys, bees, sharks, cockroaches and rays are examples of species that use electroreception either for communication or location of objects [94]. Some of these species are highly sensitive to changes in the electric field around them. For example, the shark can detect changes as low as $1 \times 10^{-10} \text{V/m}$ [95].

Electroreception can either be active or passive. In passive electroreception the sensing species detects a field originating from another species while in active electroreception the specie senses its environment by generating an electric field and detecting the distortions made to it by the field of another animal or object. The biological sensors used for the detection are known as the “Ampullae of Lorenzini”[94]. The generated electric field, also known as its signature signal, may be modulated to make it unique to the sending species. It can give information of the fish’s individual identity, sex, social and non-social behavior [96].

The weakly electric fish is a good example of an animal that uses active electroreception [95, 97]. This approach can either be based on small pulses (pulse-type) or a quasi-sinusoidal discharge (wave-type) and it allows the specie to identify the properties of the sensed object. For example, a weakly electric fish can detect and discriminate objects based on their ohmic and capacitive properties [94, 95, 98, 99]. The signature signal of the fish has *very large intraspecific waveform variability and usually has a triangular or sawtooth pattern* [100]. Fig 10 shows some examples of signature signals.

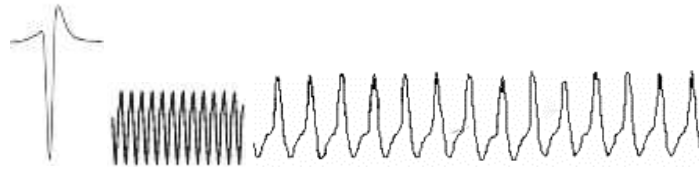


Figure 10: Examples of Signature Signals used for Electroreception [96, 102, 103]

Similar electrolocation techniques are used by bats and in radar technology. In those approaches there is a Doppler shift as a result of a relative motion between the source and the target. However, in electroreception there is *no frequency shift* due to the movement of electric signals [103].

The fish makes the process of sensing more efficient by *matching the impedance* between itself and its sensing environment. This way it can use a minimal amount of energy to sense its environment. The impedance, Z , is a combination of the resistance, R , and the capacitive reactance, X_C as shown in Eq (9). All living organisms have considerable capacitive properties that filter the signature signal in a way that *maintains the phase* [104].

$$Z = R + X_C \quad (9)$$

The resistance is independent of frequency while the capacitive reactance is inversely proportional to the product of the frequency and capacitance. The fish detects the distortions to the electric field that reflect the conductivity of the sensed object. The change is measured as a change in the *transepidermal voltage gradient* in the area next to the skin of the prey [103]. It was also noted that good conductors increase the transepidermal voltage while insulators have a decreasing effect. Also, *the detection of object waveforms relies on a purely temporal (and not spectral frequency) analysis.* [100].

A description of the key features of electroreception used in BeCoS is given in the section on ‘Porting Key Electroceptive Features into BeCoS’.

C. Bio-inspired electroreceptive Compressive System (BeCoS)

The BeCoS approach utilizes the electroreceptive approach for the sensing, compression and transmission of physiological signals as shown in Fig. 11. The approach is based on the wave-type active electroreception option. The modulated vector derived from this approach contains a high proportion of elements whose amplitude is close to zero. The Results section of this chapter provides further details about this.

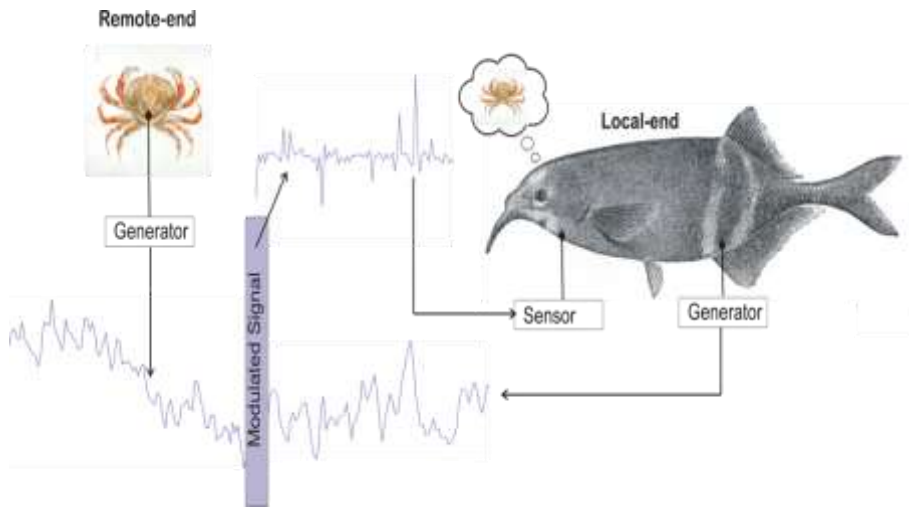


Figure 11. BeCoS Sensing Approach

BeCoS assumes that the *signature signal* vector (of length, E), originates from H , analogous to the local-end of the weakly electric fish. The \mathbf{h} vector is transmitted in the direction of R , analogous to the position of the object to be sensed, which generates an \mathbf{r} vector (of length, Z). $Z \gg E$ and $Z = wE$ (where w is a positive integer).

A modulated vector, \mathbf{p} , is generated when the \mathbf{h} and \mathbf{r} vector waves interact. The vector, \mathbf{p} , is given by Eq (10):

$$\mathbf{p} = [p_1, p_2, \dots, p_w] = \left[\frac{d\mathbf{r}_{jE+1, jE+2, \dots, E(1+j)}}{d\mathbf{h}} \right] \Big|_{j=0,1,2, \dots} \quad (10)$$

where each vector \mathbf{p}_w has a length, E which is the size of each epoch of the neural signals.

In this approach, $\frac{d\beta}{d\alpha}$ is a numerical differentiation given as the gradient between two adjacent points and defined as shown in Eq. (11).

$$\frac{df(\alpha)}{d\alpha} = \frac{f(\alpha+\Delta\alpha) - f(\alpha)}{(\alpha+\Delta\alpha) - (\alpha)} \quad (11)$$

The neural signals of interest are usually measured and stored as time series data. As such, there is a need to compute modulated signal, $\mathbf{p} = \frac{d\mathbf{r}}{d\mathbf{h}}$ by using the differentiation-by-part as shown in Eq (12):

$$\mathbf{p} = \frac{d\mathbf{r}}{d\mathbf{h}} = \frac{d\mathbf{r}}{d\mathbf{t}} \div \left[\frac{d\mathbf{h}}{d\mathbf{t}} + \delta \right] = \dot{\mathbf{r}} / (\dot{\mathbf{h}} + \delta); \quad \delta = \begin{cases} 1 \times 10^{-6}, & \dot{\mathbf{h}} = 0 \\ 0, & \dot{\mathbf{h}} \neq 0 \end{cases} \quad (12)$$

where δ is a small positive stabilizer that prevents numerical instability when $\dot{\mathbf{h}} = 0$

Similarly, \mathbf{r} is reconstructed by integration as shown in Eq (13). The cumulative trapezoidal numerical integration method was used.

$$\mathbf{r}_{\text{recon}} = \int \mathbf{p} d\mathbf{h} = \int \mathbf{p} \mathbf{h} d\mathbf{t} \quad (13)$$

D. System Model and Performance Metrics

The BeCoS model is shown in Fig. 12. The multi-channel physiological signals are captured in real-time using appropriate sensors at the patient's end- the local end of the Medical Virtual Instrument (MVI). A sparse differential signal is then generated in quasi real time. For each channel, a vector (\mathbf{h}) of length E is selected as the signature signal and all subsequent signals are differentiated with respect to the appropriate signature signal. This differential signal (\mathbf{p}) is wirelessly transferred to the physician's end- the remote MVI. Here, the differentiated signal is integrated with respect to $d\mathbf{h}$ in order to reconstruct the original signals. An Additive White Gaussian Noise (AWGN) channel with an SNR of 0dB is assumed. The reconstructed signals ($\mathbf{r}_{\text{recon}}$) are then compared to the original signal using a set of performance metrics.

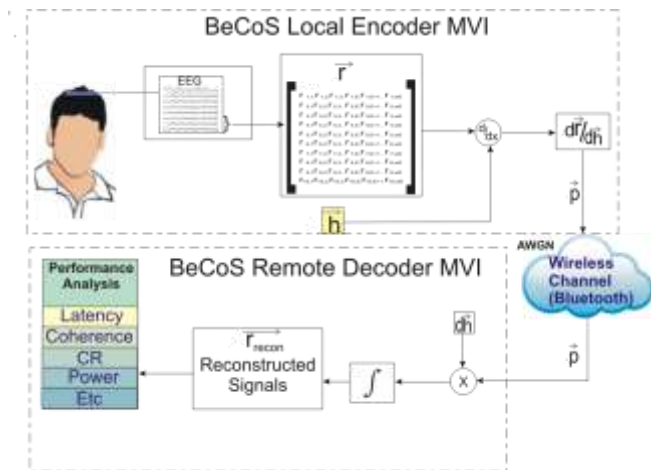


Figure 12: Conceptual Diagram of the BeCoS System Model

The \mathbf{r} vector is segmented into w equal non-overlapping segments, each representing an epoch block, with a length equal to the length of the signature signal vector, \mathbf{h} , as shown in Eq

(14).

$$\mathbf{r} = [\underbrace{u_1, \dots, u_E}_{1\text{st seg}}, \underbrace{u_{E+1}, \dots, u_{2E}}_{2\text{nd seg}}, \dots, \underbrace{u_{E(w-2)+1}, \dots, u_{(w-1)E}}_{(w-1)\text{th seg}}, \underbrace{u_{E(w-1)+1}, \dots, u_{wE}}_{w\text{th seg}}] \quad (14)$$

where u_i is the i^{th} element of \mathbf{r}

Dataset of Physiological Signals

Standard EEG databases have been used for this work. The EEG signals were taken from a 64-channel EEG Motor Movement/Imagery Dataset. It was obtained from an arrangement of sensors based on the international 10-10 system and provided on the Physionet website [105].

The Physionet signals were sampled at 160 samples/s and the following 8 channels were used for the analysis- Fc5, Fc3, Fc1, Fcz, Fc2, Fc4, Fc6 and C5, as channels 1-8 respectively. Each channel had a sequence length of 9,760 data points. An epoch length, E , of 244 was used and this resulted in 40 epochs, (w) .

The signals were used to simulate a typical signal compression, transmission and reconstruction scenario for EEG signals as shown in Fig 13. An Analog to Digital Converter (ADC) is used to emulate the signal acquisition phase. Location A refers to the patient-end of the MVI, where resource-constrained portable and mobile instruments are used. The instruments are usually powered by batteries. By contrast, location B refers to the physician-end of the MVI, where the signals are reconstructed on desktop computers or servers and powered by AC power.

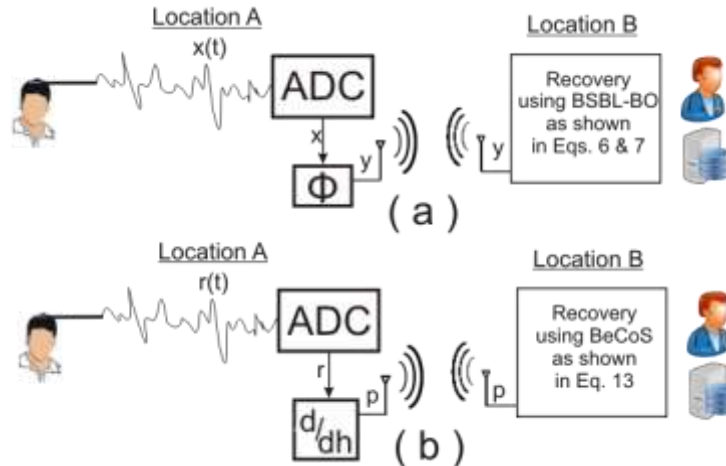


Figure 13: System Diagram for Testing Models: (a) BSBL-BO and (b) BeCoS

Performance Metrics

Five performance metrics have been chosen to evaluate the BeCoS approach. They are coherence, latency, compression ratio (CR), power and structural similarity as described in this section.

Coherence

EEG signal processing techniques are reliant on the frequency content of the signal [106]. As such, it is important to take the frequency content into consideration when comparing the signals at the local and remote ends. Spectral coherence provides this type of comparison. It is a measurement of the linear correlation between two neural electrodes [107] as a function of frequency and it is very useful for comparing EEG signals [108]. It computes the amount of synchrony between 2 stationary signals at a specific frequency [106]. The coherence metric compares the signals sensed at location A of Fig 13 with the signals reconstructed at location B of the same figure. The magnitude squared Coherence, C_{XY} , of two signals X and Y is given by Eq (15).

$$C_{XY}(f) = \frac{|P_{XY}(f)|^2}{P_{XX}(f)P_{YY}(f)} \quad (15)$$

P_{XX} and P_{YY} are the power spectral densities of X and Y respectively. P_{XY} is the cross spectrum of X and Y.

It is calculated based on the standard Welch's averaged periodogram method [109]. A Hamming window size of 125 was used for the computation.

Latency

The latency is calculated as the time between the acquisition of the sensed signal at location A and its reconstruction at location B of Fig 13. A zero delay over the noiseless wireless channel has been assumed. The learning phase of the BSBL-BO algorithm takes place at location B, prior to reconstruction. Many PHM systems require real-time monitoring and it is important to keep the latency at a minimum.

Compression Ratio

The compression ratio, CR, refers to the ratio of the dimensionality of the original signal to that of the sparsified sensed signals. The dimensionalities (non-sparseness) of the sensed and original signals are given as m and n respectively. CR is given in Eq (16). The compression takes place at location A of Fig 13.

$$CR = 1 - \frac{m}{n} \quad (16)$$

Power Consumption

Power consumption is a major consideration for health monitoring systems as they are likely to depend on batteries for their energy requirements [93, 110, 111]. According to [92], low energy

health monitoring systems are lighter and more comfortable for patients since they use smaller, longer lasting batteries. Power is important at the patient-end (location A) due to the use of batteries but it is not an important consideration at location B. The patient side core-engines of BeCoS and BSBL-BO were implemented in a Xilinx Virtex 5 FPGA and used to calculate the power consumption.

Structural Similarity

The frequency content of EEG signals has already been identified as an important feature for neural signal processing. The second important feature is the structural similarity of the reconstructed waveform with respect to the original signal [112]. A Structural Similarity (SSIM) index [93] is the standard metric for quantifying this. However, it has been shown in [112] that even a slight translation, scaling or rotation of the reconstructed signals can greatly affect the SSIM value. [112] went further to propose a Complex-Wavelet SSIM (CW-SSIM) as a more robust metric for comparison. The CW-SSIM index has been chosen as the metric since the BeCoS approach scales and translates the signals. CW-SSIM is calculated using Eq (17).

$$\tilde{A}(s_x, s_y) = \frac{2|\sum_{i=1}^N s_{x,i} s_{y,i}^*| + j}{2\sum_{i=1}^N |s_{x,i} + s_{y,i}^*| + j} \quad (17)$$

where s_x and s_y are the coefficients extracted from the same spatial locations of the same wavelength sub-bands of the two images being compared; s^* is the complex conjugate of s . j is a small positive constant (stabilizer)

E. Porting Key Electroceptive Features into BeCoS

This section shows how BeCoS integrates the most relevant features of the electroception discussed in the section entitled “The Basics of Electroception”. Some of these features were *italized* for emphasis in that section. The features have been identified and discussed below:

1. Same Type: The signature signal should be of the same type as the monitored signal. This requires the following:

- The signal should be of the same length as the signal being monitored. In the case of long term monitored signals, BeCoS requires the biosignal to be monitored in segments equal to the length of the signature signal
- The signal should be a similar biosignal to the biosignal of interest. As such, an EEG signal will be used for monitoring EEG signals
- More importantly, there should be a good level of ‘impedance matching’ between the signature signal and the segments of the biosignal of interest. This feature is further described in feature #4.

2. Signal Sparsification: The signature signal of the electric fish significantly sparsifies the monitored signals. BeCoS also uses a similar signature signal to achieve sparsification without a need for the base or dictionary matrices shown in Eqs (4-7). The level of sparsity can be further increased through the design of a signature signal with very large gradients at specific points as determined by the designer.

As shown in Eq (12), the modulated sparse signal, \mathbf{p} , is computed by dividing the inter-signal gradient of the sensed signal by that of the signature signal. As such, the designer can generate a very sparse signal, by choosing a signature signal, \mathbf{h} , with many large swing gradients (those that are very large compared to the corresponding gradient of the sensed signal, $\dot{\mathbf{r}}$).

3. Support for Sample Rate Conversion: The design of a signature signal described in #2 can also be used for downsampling of the sensing process and for sampling rate conversion without the need for the measurement matrix used in standard CS techniques. By noting the points in

the signature signal where there are very large gradients, the sensing protocol can avoid sampling those points since \mathbf{p} , will always be close to zero at those points.

For example the sampling rate can be halved by ensuring that the signature signal has very large swings at every other point or a third of the sampling rate can be used if two out of every three points have large swings.

4. Impedance Matching: As mentioned previously, the weakly electric fish uses an impedance matching between the local and remote ends in order to ensure an efficient sensing process. As shown in Eq 18, this impedance has both ohmic (R) and reactive components (X_C). In the ‘Basics of Electroception’ section we highlighted the fact that electroreception is not affected by shifts in frequency and it maintains the phase of the signature frequency.

$$Z = R + X_C \quad (18)$$

This suggests that the impedance matching in electroreception aims to maintain the ohmic value, while keeping the frequency dependent reactance at a minimum. The transfer function of a system is a mathematical function relating the output or response of a system to the input or stimulus [113]. For systems that have the same impedance, the transfer function is equal to 1. This appears similar to a scenario where input and output EEG signals are matched. In such a scenario the coherence is also equal to 1. As such, for BeCoS we will use a coherence term to represent the ohmic resistance.

The capacitive reactance, X_C , for capacitance, C , at frequency, f , is computed [114] as shown in Eq (19):

$$X_C = \frac{1}{2\pi fC} \quad (19)$$

The capacitance, C , can be calculated [114] as shown in Eq (20) and Eq (21):

$$C = I / \frac{dV}{dt} \quad (20)$$

$$C = \epsilon_o \epsilon_r \frac{A}{d} \quad (21)$$

Where I is the current in amps, $\frac{dV}{dt}$ is the voltage swing rate in Volts/second, ϵ_r is the dielectric constant, ϵ_o is the permittivity of free space ($\approx 8.854 \times 10^{-12}$ Farad/m). A is the overlap area between the two objects and d is the distance (in meters) between the two objects.

The brain can be modeled as a constant current source [115] and in electroception the overlap area between the fish and the prey is relatively constant. The dielectric constant and the permittivity of free space do not change. As such only d and $\frac{dV}{dt}$ may vary and these are the parameters that can be adjusted to alter the capacitance. Both terms need to be low in order to keep C high. This is logical since the fish would prefer sensing prey located at a close distance to it. The EEG signals do not provide any d parameter but the voltage swing rate can be calculated as shown in Eq 22:

$$Swing = \frac{1}{t} \sum_0^t |x_t - x_{t-1}| \quad (22)$$

where x_t is the EEG signal at time, t

The Swing Ratio (SR) is the ratio of the voltage swing of the system response (EEG signal being sensed) to the voltage swing of the stimulus (signature signal). The impedance equation shown in Eq (18) can be re-written to indicate the parts for coherence and SR as shown in Eq

(23). BeCoS does not work with impedance per se, as such, another term will be used to describe this similarity- *zygosity* (Z_{BeCoS}). The name was inspired by a similar term used to describe the degree of identity in the genome of twins [116].

$$Z_{\text{BeCoS}} = \frac{R}{\propto C_{XY}} + \frac{X_C}{\propto SR} \quad (23)$$

Minimize

Z_{BeCoS} is dependent on the coherence and SR as shown in Eq (24):

$$Z_{\text{BeCoS}} \propto (C_{XY}, SR) \quad (24)$$

From Eqs (23) and (24), an ideal optimized signature signal for BeCoS should have the following properties:

1. Have a high level of coherence to the sensed signal
2. Have a low swing ratio (ie the voltage swing of the signature signal should be high when compared to the voltage swing of the original EEG signal)

The second property can be attained by making using a signature signal that follows a pattern similar to the pattern of the natural signature signal used by weakly electric fish- the sawtooth waveform pattern. However, this signal still needs to be coherent with the sensed signal in order to meet the first requirement.

According to [116] it is possible to maintain a high level of coherence between two signals with different amplitudes and/or phases as long as the phase difference tends to remain constant. In calculating coherence it is necessary to know how stable the phase between two waves is and how quickly it changes with time. In [117], the coherence of a high-order harmonic spectrum was controlled by adjusting the sawtooth shape parameter.

EEG signals reflect the personalized information about the unique anatomical and functional attributes of a patient’s brain, including personality traits and genetic information [118, 119, 120, 121]. The signal coherence of EEG signals was used as a biometric in a recent study [107]. As such, the signature signal should have a high coherence when compared to a signal segment taken from the measured EEG signal.

Based on the foregoing discussions a procedure for designing an ideal optimized signature signal is presented in the next section.

Designing an Optimized Signature Signal

In this section we describe the process for designing an ideal optimized signature signal that satisfies the primary requirement of high coherence and the secondary requirement of a large swing ratio as described in the previous section. The process is shown in Fig 14.

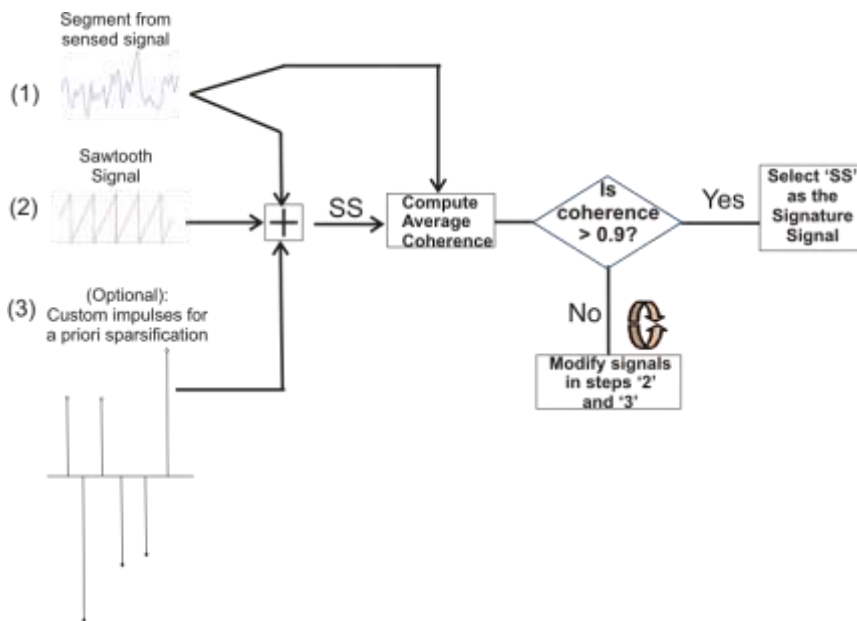


Figure 14 : Steps for generating an optimized signature signal

The following are the steps for generating an ideal optimized signature signal for BeCoS:

1. The first option for getting a non-optimized signature signal involves the selection of a signal that is highly coherent with the signal to be sensed. A segment of the sensed signal can be used as the seed signal. In this study the first epoch is used as the seed signal.
2. The second option for a more optimized signature signal requires the addition of a sawtooth signal with a known voltage swing to the coherent signature signal used in the first option. This composite signal should still be coherent to the measured signal.
3. A third option for an ideal optimized signal requires the addition of high valued input pulses to the summation of the seed signature signal and sawtooth signal. The output of step 3, called 'SS', is then compared with the seed signal to determine the coherence. If the average coherence is high enough (≥ 0.9), then SS is chosen as the signature signal. If the coherence is less than 0.9, steps '2' and '3' are iteratively modified until an 'SS' with the required coherence is attained. This gives an ideal optimized signature signal but the process has extra computational requirements.

F. Results

The EEG datasets were used to compare BSBL-BO and BeCoS based on the 5 metrics described in the previous section. The tests were conducted on a Xilinx Virtex 5 FPGA and an Intel Pentium 4 system, with a 3.0GHz CPU and 2GB RAM. For the BSBL-BO experiments a 122 x 384 sparse binary sensing matrix, Φ , was used and a 244 x 244 inverse DCT matrix as the dictionary matrix, \mathbf{D} .

Coherence

The average coherence value for BeCoS and BSBL-BO were compared (Table 5). The average coherence was also compared across a frequency range of 0-90Hz (Fig. 15). BeCoS had an average coherence of 0.949 across the 8 channels while BSBL-BO had an average of 0.701. Also, BeCoS maintained a near optimum coherence between 2.1Hz and 84.38Hz. On the other hand, BSBL-BO fluctuated across the spectrum with a peak of 0.996 at 0.7Hz and a trough of 0.497 at 90Hz.

Table 5: Comparison of BSBL-BO and BeCoS Coherence Values

BSBL-BO	BeCoS	% Increase
0.701	0.949	35.38%

Overall, BeCoS had 35.38% better average values. BSBL-BO is an adaptive learning approach that exploits the intra-block correlation of the signals. This is less linear than the BeCoS approach and increases the power of the noise in the reconstructed signal. BeCoS generates a reconstructed signal that is linearly dependent on the original signal since the differential and integral operators used have a linear time invariant property in the Fourier domain.

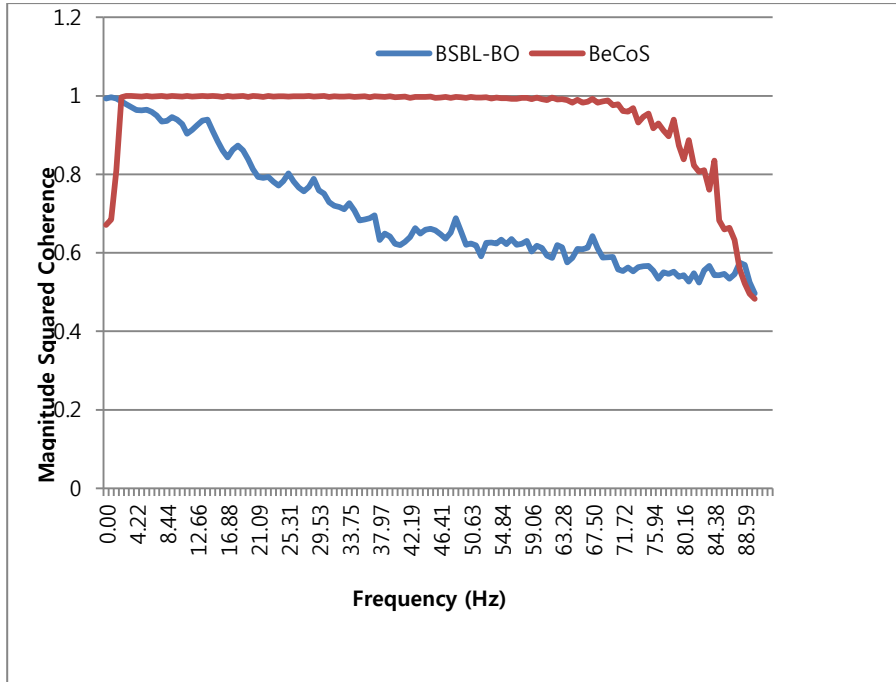


Figure 15: Coherence across the frequency spectrum

Latency

The latency refers to the time taken for sensing, processing, transmitting and reconstructing the neural signals. In BSBL-BO it involves these stages as well as the learning stage as discussed earlier. For BeCoS, it involves the steps shown in Eqs (12-13). The sensing, processing and reconstruction phases of BeCoS basically involve a few additions and multiplications. For the BSBL-BO it involves additions on the accumulators that result from the sparse binary sensing matrix, the multiplications with the inverse DCT dictionary matrix and the learning process.

With BeCoS we had an average of 0.117ms for processing each epoch, compared to 5.869ms that was used by BSBL-BO. As such, BeCoS used just 1.99% of the processing time used by BSBL-BO. The processing time we got was similar to the time reported in the reference BSBL-BO paper [93], where 105ms was used to process an epoch. The epoch length used in

that paper was 384 data points for 32 channels. This results in 0.273ms per data point or 2.085ms per epoch. That paper also used a 192x384 sparse binary matrix to sparsify the signal while we used a 122x244 sparse binary matrix for this work. By factoring in this ratio of 2.477, one can estimate that the process described in the reference paper would have taken about 5.165ms/epoch for the experimental setup used in this paper. Also, the system used in the reference paper had a 2.8GHz CPU and 6GB RAM while a system with a 3GHz CPU and a 2GB RAM was used in this research. This may also explain why the result in the reference paper was slightly faster than the BSBL-BO processing results obtained in this research.

Compression Ratio

By representing the sensed signal with respect to a pre-specified signature signal, the BeCoS approach reduces a large portion of the original values to values that are close to zero. Values of the sensed signal, x , where $|x| < 0.99\text{mV}$ were taken to be sparse. This pseudo-sparsity reduces the dimensionality of the transmitted signal and increases the effective compression ratio (see Eq. 16). The comparison was based on the same optimal configuration for BSBL-BO used to attain a low-cost EEG system in [93] (compression ratio of 50%). As seen in Table 6, BeCoS achieved an average compression ratio of 76.63% or 53.26% better than BSBL-BO, even though the non-optimized signature signal was used for the analysis.

Table 6: Comparison of BSBL-BO and BeCoS Compression Ratios

BSBL-BO	BeCoS	% Increase
50%	76.63%	53.26%

Power and Hardware Resource Consumption

Previous research [95] already shows that weakly electric fish use the electroceptive approach

to maximize the energy efficiency of their sensing process and we have also used it for the efficient sensing, processing and transmission of the neural signals. We implemented the core compression engines of BeCoS and BSBL-BO in hardware in order to get a realistic estimation of the power consumption at the patient-end of the telemonitoring system.

The Simple Bus Architecture (SBA) [122] was used for both designs. The SBA is lightweight computer architecture that implements a minimum essential subset of the open source Wishbone signals interface [123]. It consists of software tools and intellectual property (IP) cores that are interconnected by buses and it enables the implementation of a System on Chip (SoC). The availability of the essential blocks enable the system designer to concentrate on the core design and this helps to speed up the design process and makes it portable across different FPGA platforms. The master core is a special state machine that performs basic dataflow like a microprocessor without the high resource utilization that characterizes soft processor.

The top level block diagrams for the BeCoS and BSBL-BO compression engines are shown in Fig 16 and 17 respectively.

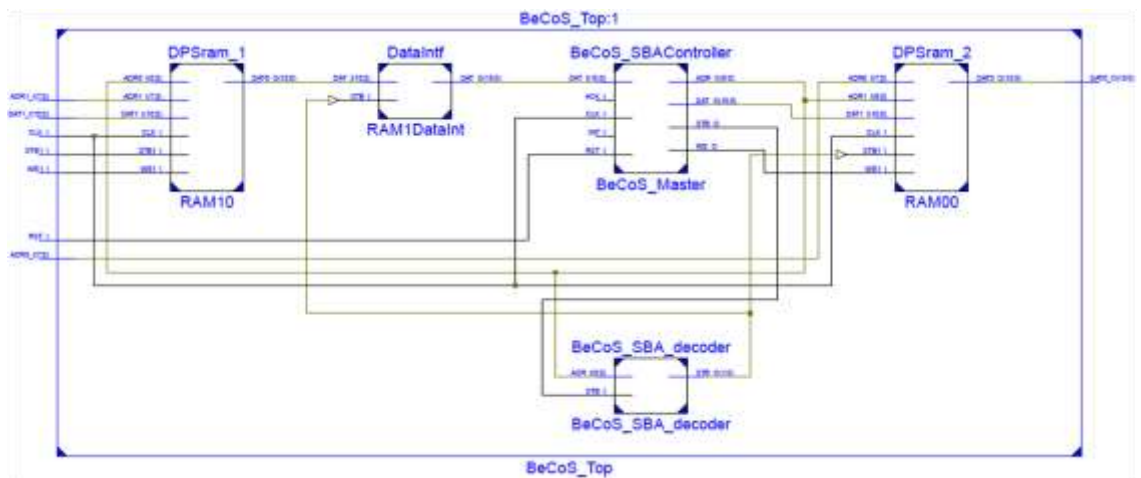


Figure 16: Top level block diagram of the BeCoS compression engine

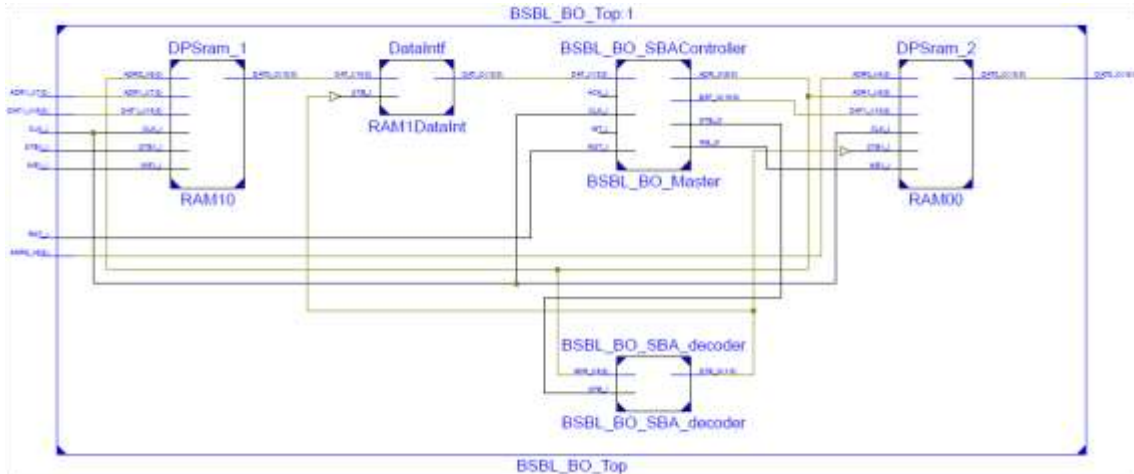


Figure 17: Top level block diagram of the BSBL-BO compression engine

The following blocks and signal names were used for the BeCoS engine (Fig 16):

- SBA Controller: Master System Controller
- SBA Decoder: SBA Address Decoder
- DPSram: Dual Port Single Clock RAM
- DataInf: Data Output Bus Interface
- CLK_I: Main clock (1 bit)
- RST_I: Active high reset (1 bit)
- ADR0_I: Address output bus (8 bit)
- DAT0_O: Data output bus (16 bit)
- WE1_I: Write Enable (16 bit)
- STB1_I: Strobe acknowledgement (1 bit)
- ADR1_I: Address input bus (1 bit)
- DAT1_I: Data input bus (8 bit)
- INT-I: Interrupt (16 bit)
- RAM 10 (0-255, for EEG data values)
- RAM 00 (0-255 for output values)

Similarly, the following blocks and signal names were used for the BSBL-BO engine (Fig 17):

- SBA Controller: Master System Controller
- SBA Decoder: SBA Address Decoder
- DPSram: Dual Port Single Clock RAM
- DataInf: Data Output Bus Interface
- CLK_I: Main clock (1 bit)
- RST_I: Active high reset (1 bit)

- ADR0_I: Address output bus (8 bit)
- DAT0_O: Data output bus (16 bit)
- WE1_I: Write Enable (16 bit)
- STB1_I: Strobe acknowledgement (1 bit)
- ADR1_I: Address input bus (1 bit)
- DAT1_I: Data input bus (8 bit)
- INT-I: Interrupt (16 bit)
- RAM 10 (0-255, for EEG data values)
- RAM 00 (0-127 for output values)

A master clock of 160Hz was used. At each rising edge of the clock one EEG signal was sent as an input to the compression engine. This process mimics the data acquisition process in a live PHM system where an EEG sensor captures signals at a given sampling rate. The epoch EEG data was stored in a RAM (RAM 10) with a resolution of 16bits. The BeCoS engine stores 245 consecutive EEG signals in RAM 10 per epoch while the BSBL-BO engine stores 244 EEG signals. Both systems used two banks of double port memories. The first was for the input data while the second was for the output data.

The BeCoS engine uses 3 internal buffers (IB1, IB2 and IBS). At each rising clock edge, an EEG signal is fed into the first internal buffer (IB1). At the second rising edge, the content of IB1 is transferred to IB2 and the next EEG signal is fed into IB2. On the third cycle, the difference (IB2-IB1) is computed and stored in IBS (see Eq 11). The BSBL-BO engine has 244 internal buffers because all 244 EEG values must be obtained in order to compute the output signals for each epoch.

For BSBL-BO, at each rising edge of the clock a new consecutive EEG signal is stored in the internal buffers consecutively from IB1 to IB244. For BeCoS, only two consecutive signals are required to compute the corresponding output signal. For example, the 1st and 2nd EEG signals are used to compute the 1st output, the 13th and 14th EEG signals are used to compute

the 13th output and the 244th output signal can be computed when the 244th and 245th EEG values are in the internal buffers. The buffers were implemented using Configurable Logic Blocks (CLBs).

To compute the output signal, the BeCoS engine divides the value of the BS buffer with the corresponding signature signal as shown in Eq. 12. The signature signals were stored in a ROM table. The BSBL-BO output signals were computed using a sparse binary sensing matrix (Φ) as shown in Eq. 5. Each column of the sensing matrix contained just two non-zero entries to allow the use of accumulator registers, rather than multipliers. The resulting output signals were then generated based on the sensing matrix. The BeCoS engine has an output of 244 signals while the BSBL-BO has an output of 122. As such, the BeCoS system has 244 output registers (OR) while the BSBL-BO approach has 122 output registers.

Table 7: Comparison of the Power and FPGA Resource Utilization for the BSBL-BO and BeCoS Core Engines

	FFs	LUTs	IOBs	BRAMs	Power
Total No of FPGA Resources	69,120	69,120	640	148	-
BSBL-BO (% Utilization)	3,981 (5.8%)	1,743 (2.52%)	51 (7.97%)	2 (1.35%)	1.204W
BeCoS (% Utilization)	123 (0.18%)	881 (1.27%)	52 (8.13%)	3 (2.03%)	1.191W

The hardware synthesis report is shown in Tab. 7 and it gives the resource utilization for both systems using a Xilinx Virtex 5 FPGA (XUPV5-LX110T). The table shows the amount of

Flip Flops (FF), Look Up Tables (LUTs), Input Output Blocks (IOBs) and Block RAMs (BRAMs) used.

The Value Change Dump (VCD) was used with the Xilinx Power Analyzer to calculate the power consumption of both systems. The results are also shown in Table 7. BeCoS used 13mW less power than BSBL-BO to process one epoch of EEG signals at the patient’s end. To put this figure in better perspective, let us assume the system at the patient’s end is running on a Samsung Galaxy 4 phone with an Li-Ion battery rated at 2100mAh and 3.8V. This battery would serve the BSBL-BO system for 8,837 hours and the BeCoS system for 8,933hours- a difference of 96 hours or 4 days.

Structural Similarity

The average CW-SSIM values for both BSBL-BO and BeCoS are shown in Tab. 8.

Table 8: Comparison of BSBL-BO and BeCoS CW-SSIM

BSBL-BO	BeCoS	% Increase
0.969	0.908	-6.295%

Tab 8 shows that BeCoS has an average CW-SSIM decrease of 6.295%. As noted in the metrics section of structural similarity, the SSIM is highly altered by the scaling of the signal. Similarly, its enhancement (CW-SSIM) still gets affected by scaling and rotation, even though it is more robust than SSIM. There is a degree of scaling in the BeCoS approach as a result of the numerical integration during the reconstruction phase and this invariably lowers the CW-SSIM.

However, as seen in Figs 18-20, regardless of the scaling and translation, the structure of the

reconstructed signal using the BeCoS approach is still strikingly similar to the original EEG signal.

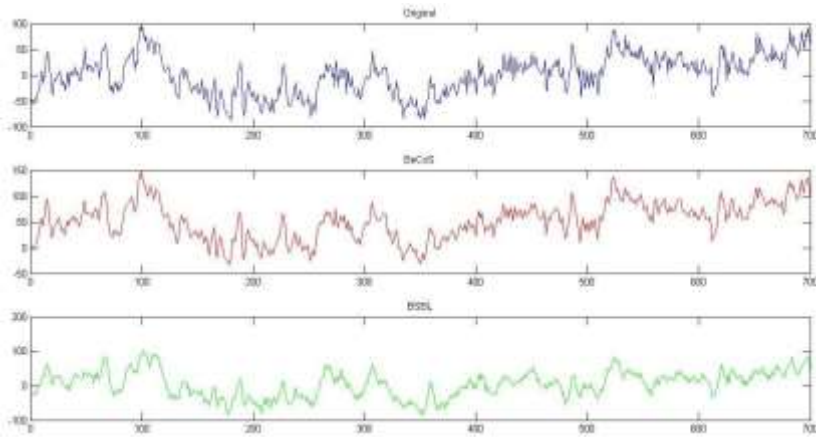


Figure 18: CW-SSIM for Ch7 [1:700]

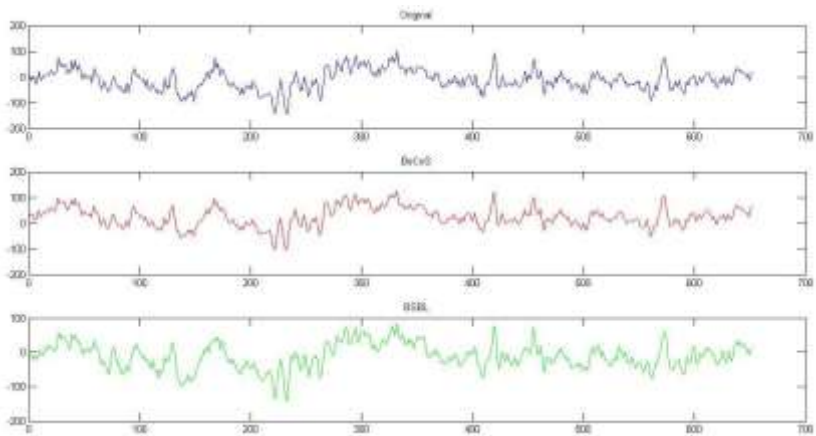


Figure 19: CW-SSIM for Ch1 [3000:3650]

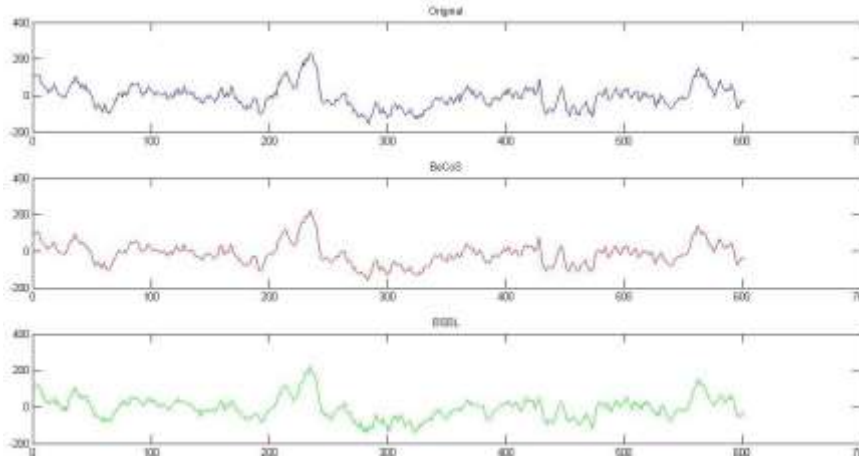


Figure 20: CW-SSIM for Ch4 [6300:6900]

Effects of Variations on SSIM and CW-SSIM

To further explain the lower CW-SSIM value for BeCoS, consider a random sample shown in Tab 9 with columns for the original sample, its numerical differentiation, numerical integration, numerical integration plus the offset value and the variation. Numerical integration, as opposed to analytical integration, uses approximations and introduces a non-uniform variation when compared to the original signals. In order to use analytical approaches the exact equation of the signal must be known in advance and this is not possible for real time physiological signals. As such, a numerical integration method is the most feasible integration approach that can be used for such signals.

Table 9: Effect of Numerical Methods on Signal Reconstruction

Original	Num Diff	Num Int	Num Int + Offset	Variation
40	1.2	0	40	0
41.2	1	1.1	41.1	0.1
42.2	1	2.1	42.1	0.1
43.2	0.8	3	43	0.2

44	0.8	3.8	43.8	0.2
44.8	0.6	4.5	44.5	0.3
45.4	0.6	5.1	45.1	0.3
46	0.5	5.65	45.65	0.35
46.5	0.3	6.05	46.05	0.45
46.8	0.3	6.35	46.35	0.45
47.1	0.2	6.6	46.6	0.5
47.3	0	6.7	46.7	0.6
47.3	0	6.7	46.7	0.6
47.3	-0.1	6.65	46.65	0.65
47.2	-0.2	6.5	46.5	0.7
47	-0.3	6.25	46.25	0.75
46.7	-0.5	5.85	45.85	0.85
46.2	-0.5	5.35	45.35	0.85
45.7	-0.6	4.8	44.8	0.9
45.1	-0.7	4.15	44.15	0.95
44.4	-0.8	3.4	43.4	1
43.6	-0.9	2.55	42.55	1.05
42.7	-1	1.6	41.6	1.1
41.7	-1.1	0.55	40.55	1.15
40.6	-1.2	-0.6	39.4	1.2
39.4	-1.3	-1.85	38.15	1.25
38.1	-1.4	-3.2	36.8	1.3
36.7	-1.5	-4.65	35.35	1.35
35.2	-1.6	-6.2	33.8	1.4
33.6	-1.7	-7.85	32.15	1.45
31.9	-1.8	-9.6	30.4	1.5
30.1	-1.9	-11.45	28.55	1.55
28.2	-2	-13.4	26.6	1.6
26.2	-2	-15.4	24.6	1.6
24.2	-2.2	-17.5	22.5	1.7
22	-2.3	-19.75	20.25	1.75
19.7	-2.4	-22.1	17.9	1.8
17.3	-2.5	-24.55	15.45	1.85
14.8	-2.5	-27.05	12.95	1.85
12.3	-2.7	-29.65	10.35	1.95

9.6	-2.8	-32.4	7.6	2
6.8	-2.8	-35.2	4.8	2
4	-3	-38.1	1.9	2.1
1	-3.1	-41.15	-1.15	2.15
-2.1	-3.1	-44.25	-4.25	2.15
-5.2	-3.3	-47.45	-7.45	2.25
-8.5	-3.3	-50.75	-10.75	2.25
-11.8	-3.5	-54.15	-14.15	2.35
-15.3	-3.5	-57.65	-17.65	2.35
-18.8	-3.7	-61.25	-21.25	2.45

Fig 21 shows the original sample and sample reconstructed by numerical integration as well as this reconstructed sample value plus an addition of the initial offset.

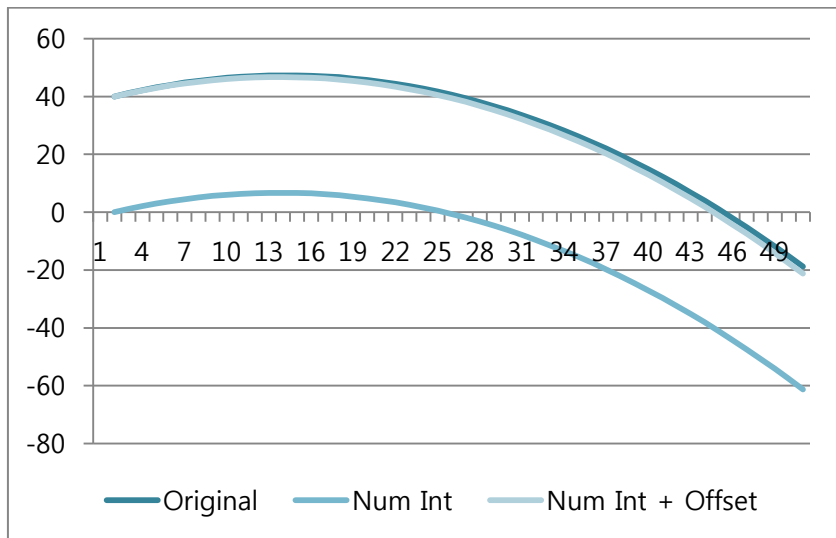


Figure 21: Effect of Numerical Methods on Signal Reconstruction

The figure clearly shows that all three signals have a similar structure. The variation is shown in Fig. 22. A regression analysis was used to generate a Linear Regression Variation (LRV) model in order to estimate the equation of this variation and we obtained the following

equation:

$$y=0.049011x+(-0.02478)$$

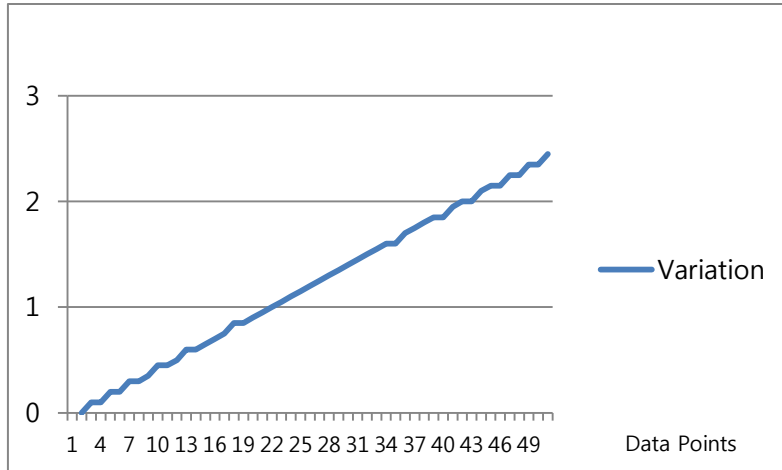


Figure 22: A Model of the Variation Generated by Numerical Methods

We have used the data in channel 1 of the EEG signals used in this research to visualize the effect of variations on the SSIM and CW-SSIM values. The SSIM and CW-SSIM were calculated by comparing the data in channel 1 with the following samples:

- (i) Original sample (comparing it with itself, Or)
- (ii) Original sample minus 1mV (Or-1)
- (iii) Original sample plus 1mV (Or+1)
- (iv) Original sample minus 5mV (Or-5)
- (v) Original sample plus 5mV (Or+5)
- (vi) Original sample plus 10mV (Or+10)
- (vii) Original sample plus 20mV (Or+20)
- (viii) Original sample plus 50mV (Or+50)
- (ix) Original Sample plus Linear Regression Variation model (Or+LRV)
- (x) Original Sample plus Linear Regression Variation model, treating it one epoch at a time (Or+LRV, 1 epoch)

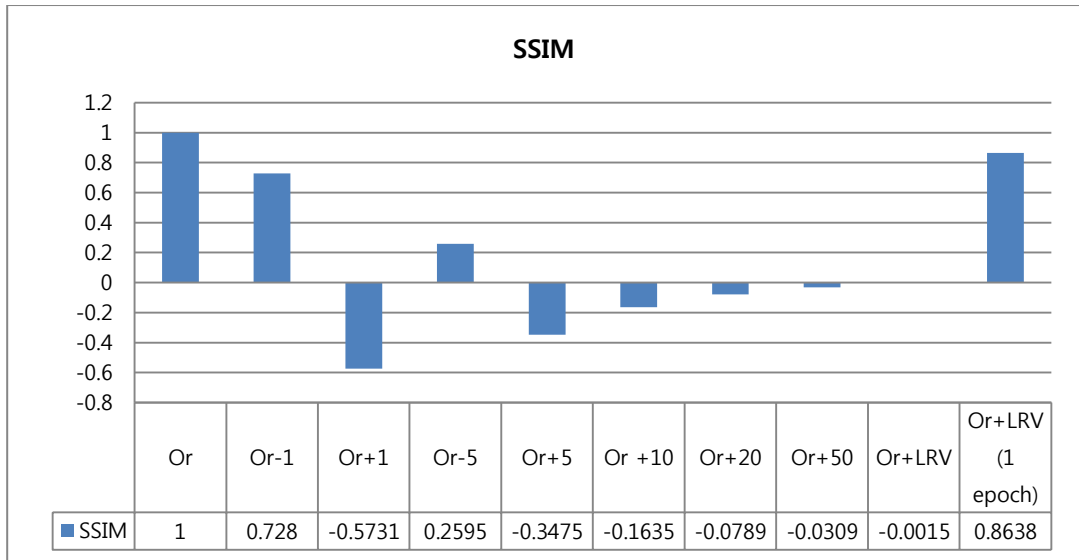


Figure 23: The Effect of Variation on SSIM

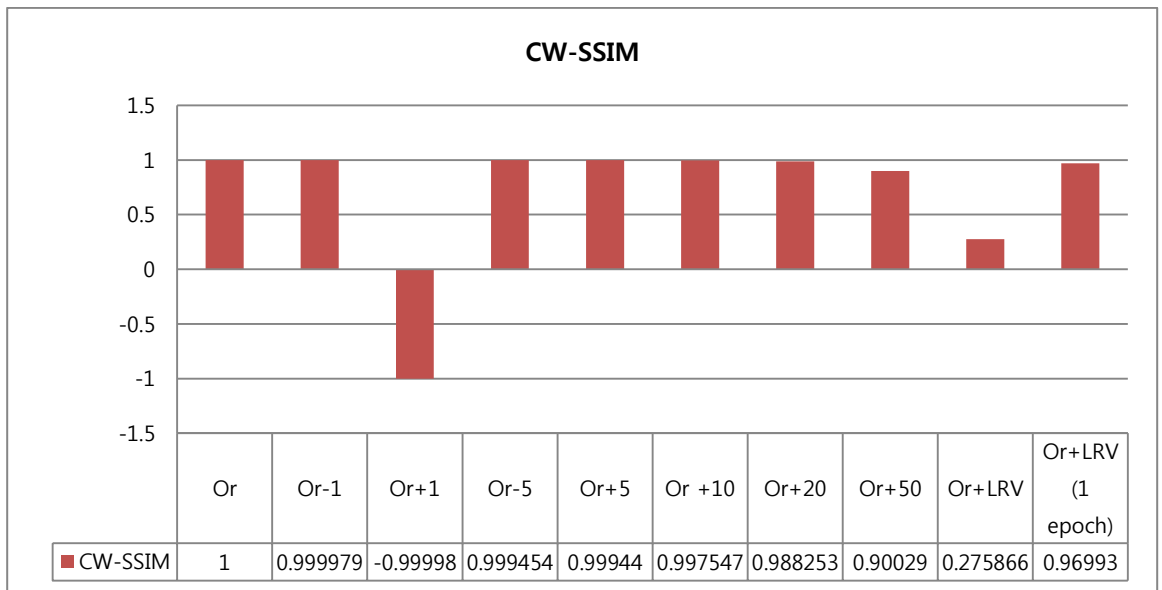


Figure 24: The Effect of Variation on CW-SSIM

As seen from Fig 23, any variation beyond 1mV significantly diminishes the SSIM values. The SSIM value for Or+LRV is almost zero but it gives a better result when it is treated epoch

by epoch.

The CW-SSIM measurements are fairly stable for different variations. The degradation becomes more apparent for higher variations as well as for the model that uses LRV. Such a model is feasible in practice since PHM systems are likely to fall under the LRV model. This is because the noise level experienced by the system can be affected by the location of the patient as well as the condition of the sensors.

The CW-SSIM calculation in the BeCoS approach is similar to the LRV based model and this explains why the values are lower than the CW-SSIM values for the BSBL-BO approach even though the reconstructed signals look similar. The CW-SSIM was used for the analysis in this research because it is currently regarded as one of the most robust approaches for measuring structural similarity. However, in the future it may be necessary for researchers to develop a new type of structural similarity index that is more robust to variations such as LRV.

A Combination of BeCoS and BSBL-BO for Personalized Health Monitoring

The following points succinctly describe how BeCoS relates to traditional CS techniques used for the telemonitoring of biosignals:

1. BeCoS can be used as a lightweight approach for significantly sparsifying an otherwise non-sparse signal. We obtained a compression ratio of at least 75% in each case. After this stage the sparse biosignal can be suited to traditional CS techniques
2. BeCoS can be used as a *stand alone* technique as an alternative to conventional CS techniques used for the telemonitoring of 'costly-to-sparsify' biosignals.

IV. R-READER: An Algorithm for Lightweight Detection of Fiducial Points in the Cardiovascular Domain

A. Detection of R-peaks in ECG Signals

The accurate identification of the R-peak of an electrocardiogram (ECG) cycle is the first step towards automated classification of the cycle. In this chapter we present a lightweight algorithm, known as R-READER: a Rapid-Ramp Effective Algorithm for Detection of ECG R-peaks. It is based on an intuitive and effective identification of inflexion points in the ECG cycle through the calculation of adjacent slopes between the signals. Traditional techniques require a number of expensive filtration stages in order to detect the R-peaks.

The R-READER approach significantly reduces the amount of filters and takes advantage of the unique shape and fiducial features of the ECG signal to accurately identify the R-peaks. It is compared with the Pan-Tompkins (P-T) algorithm - a popular lightweight algorithm used for the detection of R-peaks. The MIT-BIH Arrhythmia database was used for the analysis.

The Fiducial Points of an Electrocardiogram

An ECG signal is a record of the electrical activity of the heart and it is the basic cardiologic test used to analyze the condition of a patient's heart [124, 125]. It gives a graphic representation of the readings obtained from electrodes that are placed on the surface of the human skin and near the heart. [126]. The ECG signal is made up of a number of regions/fiducial points, namely the P-wave, Q-R-S complex and the T-wave as shown in Fig. 25. It traces a morphology identified by P, Q, R, S and T peaks and troughs [127]. The QRS-complex is the most distinguishing feature of the ECG and it serves as the basis for detection

and analysis. The peak of this complex is known and the R-peak and it is the most important point in virtually every ECG algorithm. The ECG signal has the most unique fiducial points when compared to other biosignals and R-READER takes advantage of this attribute.

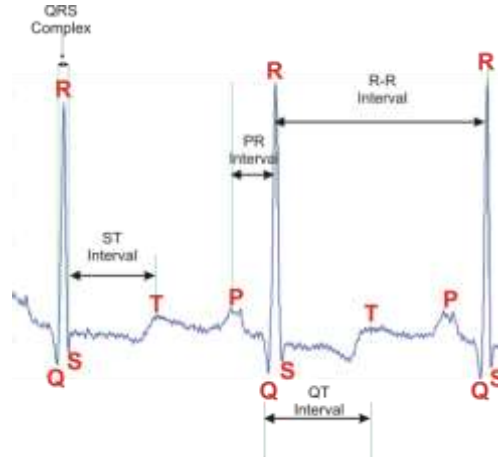


Figure 25: A Typical ECG Signal Showing the Fiducial Points

Automated R-peak Detection

As stated earlier, personalized health monitoring has become an important approach to patient care and ECG monitoring is the most common feature of this approach. The R-peak is the most striking point in the QRS complex. In general, the R-peak of an ECG cycle is that point in the cycle where the highest (or lowest) amplitude occurs. Its detection is the most important step in the diagnosis of cardiac disorders and is the basis for virtually all ECG algorithms [128]. The heart rate variability (HRV) can say a lot about a person's health. For example, diabetes, arrhythmias, sleep apnea, congestive heart failure, neonatal sepsis and even Post-traumatic stress disorder (PTSD) can be inferred from the heart rate and heart rate variability (HRV), all of which can be computed when the locations of the R-peaks are known [129, 130, 131, 132, 133].

There are a number of automated methods for the detection of the R-peaks of the ECG signals already in literature. A common approach for most existing methods involves the use of two stages, namely the preprocessor stage and the decision phase. The preprocessor phase is used to improve the general quality of the ECG signal; a major part of which is the denoising of the signal. After this is complete, the decision phase is activated for the selection of the per-cycle R-peak based on some given algorithm.

A range of techniques currently being used for these phases are based on *Derivatives & Digital Filters*, *Wavelet Transformation*, Neural Networks and Genetic algorithms amongst others [134, 135]. The Derivatives & Digital Filters approaches are the most common. This approach is based on the fact that typical ECG signals have frequency components between the ranges of about 10Hz to 25Hz. A filter stage is thus used to suppress components outside this range. The most well known algorithm in this approach is the algorithm proposed by Pan & Tompkins [136, 137]. Most research papers that focus on algorithms for the real-time detection of R-peaks compare themselves to the Pan-Tompkins algorithm. The paper has been cited 793 times [138].

The P-T algorithm uses a set of filters to extract a noise free ECG signal before the detection of R-peaks and the QRS complex. Prior to the detection phase, the P-T passes the ECG signal through low and high pass filters, followed by a differentiator, a squaring operator and a moving window integrator. These stages are shown in Fig. 26.

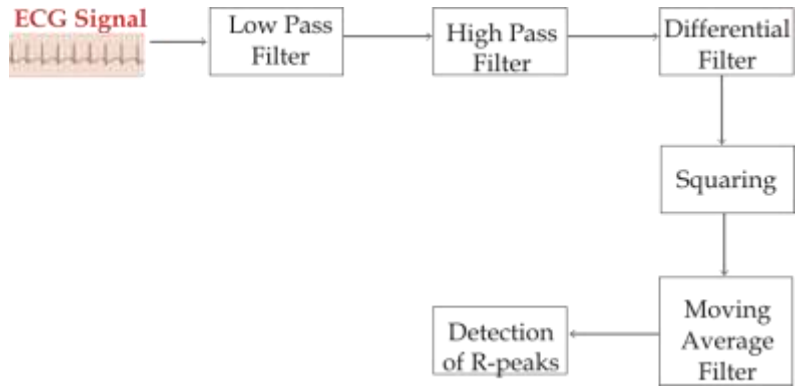


Figure 26: Steps in the Pan & Tompkins Algorithm

It also takes advantage of the fact that there is a steep slope in the region surrounding the QRS complex. The use of thresholds, θ and θ_2 , make up a major part of the P-T algorithm. These thresholds are determined after two learning phases and QRS complexes are only searched for in regions that exceed the thresholds; θ is the primary threshold of interest and θ_2 (which is a fixed fraction of θ) is only used as a backup threshold if no values exceed the primary threshold after a given time interval.

Noise and the ECG Signal

It is common to have ECG records that include noise from many sources [139]. Such noises include noise from sources like muscle movements and powerline interference. Muscle movement noise results from the patient’s movement, while power line interference is the 50/60Hz noise that is due to the presence of power lines around the location of the patient. The fiducial points in a noise-contaminated ECG signal may be obscured to such a point that detection can become difficult. An ECG analyzer performs many tasks, but its task of dealing with the noise has been identified as the major problem faced by system designers [140].

Traditional methods of dealing with noise involve the use of one or more types of filters- high pass low pass filters. However, the use of such methods presents two challenges; the first is that it increases the computational complexity of the system, along with the hardware and software resources required to obtain a reliable result. The second challenge is that the accuracy of the filtering depends on an accurate or near accurate knowledge of the *type(s)* of noise present in the ECG signal. The coloration of the noise can play an important role in the accuracy of the results. The ideal situation is for the system designer to know the type of noise(s) affecting the signal. However this is not always feasible. Also, the growing trend of ambulatory PHM of ECG signals further limits the designer's knowledge of the noise experience by the system in such a situation.

The R-READER approach has been designed to support lightweight and dependable analysis of ECG signals in the presence of different kinds of noise without the need to filter the signal prior to analysis.

Overhead and Complexity of Filtering Techniques

As mentioned earlier, the complexity of the preprocessing stage of the P-T algorithm introduces some overhead in the detection process. These overheads fall under different categories, including overhead in terms of time and memory. A total of four filtration steps are present in the P-T Algorithm, namely the low pass filter, high pass filter, differential filter and moving window integrator filter. The P-T algorithm uses approximate integer filter and this makes it suitable for lightweight real-time R-peak detection. An integer filter is a special type of filter that has only integer coefficients [141].

The P-T algorithm is widely acknowledged to be one of the ECG processing algorithms with the least degree of processing complexity. It uses approximate integer filters. This makes it

suitable for lightweight real-time R-peak detection and for use in PHM systems. However, the overhead incurred in the filtration phases still accounts for a significant amount of processing overhead.

Algorithms can be implemented in either software or hardware (usually with FPGAs), with the FPGAs generally considered to have better performance in terms of speed. By using integer filters the P-T algorithm is suitable for implementation in hardware. However, even with this advantage there is still a considerable penalty.

For example, with a Xilinx Spartan® xc3s5000 FPGA, an average delay of 16 samples is introduced in the low pass filter, 6 samples from the high pass filter, 2 samples from the derivative filter, 7 samples from the squaring and 16 samples from the moving window integrator [142]. This gives a total of 47 sample delays or a 235s delay at a sampling rate of 200Hz. Again, this inhibits the goal of a lightweight real-time PHM system.

Another penalty worth noting is the memory penalty. It depends on the amount of previous samples required to make a decision about a fiducial point. The preprocessor stage of the P-T algorithm requires at least 32 previous samples in order to determine a fiducial point. More often, due to possible delays in the processing stage, memory capacity in excess of this amount is required; [142] used 60 samples. These samples are stored in the system's RAM. These overheads do not even include the additional overhead required to implement the various filters.

MIT-BIH Arrhythmia Database

The Massachusetts Institute of Technology- Beth Israel Hospital (MIT-BIH) Arrhythmia database [143] contains 48 two-channel ambulatory ECG recordings that last for 30minutes each. They were sampled at 360 samples per second and have a resolution of 11 bits over a

10mV range. Each of the records includes a detailed annotation by experts and this provides a vital guide during the analysis of the accuracy of ECG algorithms. Most of the research articles focused on ECG algorithm use this as the test database [144]. The best (least noisy) record- Record #100 and the worst (most noisy) record- Record #108, were used to analyze R-READER and P-T algorithms.

B. The R-READER Process

The design of R-READER has been guided by the objectives of having a light-weight, fault (noise) tolerant, latency reducing and quasi-realtime ECG analyzer for rapid and dependable analysis even in resource constrained environments, such a mobile phones and personal digital assistants (PDAs). Thus, R-READER has been designed to strike a balance between the complexity of the algorithm and the dependability of the analysis. Many previous algorithms expend a lot of overhead on the preprocessor stages, especially the filtering of the signals. As such, a prime motive for this work is the design of a technique that reduces or eliminates the need for signal filtering without sacrificing the accuracy of the results.

R-READER is based on the characteristics of the slopes of adjacent ECG signals and the identification of inflection points in the signal. As shown in Fig 25, the ECG signal is comprised of 3 major parts, the most prominent of which is the QRS complex, with the R-peak being the distinguishing feature of the complex.

A close observation of an ECG signal shows that the absolute values of the ECG signals in the QRS complex have the greatest values when compared to the signals of the other regions. It gives a sloping surface between the interconnection levels, also known as a ramp, and this inspired our choice of the name for the algorithm. Using these varying slopes as a basis, we have developed an algorithm that can rapidly detect the QRS-complex region, especially the

start-of-complex, R-peak and end-of-complex. An example of the selection of fiducial points for one of the cycles in record #100 is shown in Fig. 27.

The slope, s , between any two signals, x , is given by Eq (25):

$$S = \frac{x_n - x_{n-1}}{t_n - t_{n-1}} \quad (25)$$

where x is the signal and t is the corresponding time

The time between samples is given by the sampling period and this is the inverse of the sampling frequency. In effect, every adjacent signal is separated by the same constant interval- the sampling period. This makes it possible to simplify the equation by removing the denominator to get a modified slope, s_m , for use in R-READER as shown in Eq (26). This approach reduces the complexity involved in implementing the algorithm.

$$S_m = x_n - x_{n-1} \quad (26)$$

where x is the signal

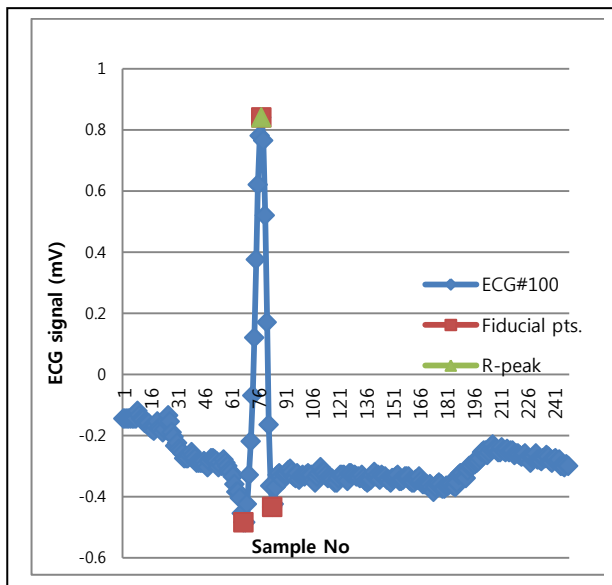


Figure 27: R-READER’s Selection of Fiducial and R-peak points for Record #100

Each of the fiducial points of the ECG signal occurs at an *inflexion* point. An inflexion point is a point on a graph where the slope *changes* sign. This simple point enables us to streamline the algorithm to obtain an efficient and accurate algorithm devoid of unnecessary complexity.

The steps are described below:

- (i) Find the modified slope, s_m , between two adjacent signals x_n and x_{n-1}
- (ii) Detect the presence of inflexion points from the slopes; inflexion points exist if there is a sign change between the adjacent modified slope values, $s_{m,n}$ and $s_{m,n-1}$
- (iii) Store the ECG signal x_n corresponding to the presence of a positive modified slope $s_{m,n+}$ as the candidate cycle-r-peak; also store its associated sample time, t_n
- (iv) Store the average maximum R-peak, R_{pmax} for the cycles 11-20 (the first 10 cycles are omitted to enable us obtain a R_{pmax} that reflects the overall ECG signal rather than the transients at startup)
- (v) Determined the peak-adjacency-interval-detector (p-a-i-d) as the average of the intervals between the first 10 R-peak values analyzed
- (vi) Subject the subsequent analysis to the following conditions:
 - a. the absolute value candidate cycle-r-peak must be greater than the R-peak threshold, R_{p-Th} , where $R_{p-Th} > 0.6 * R_{pmax}$
 - b. adjacency between candidate r-peaks must be at least 0.5 of the p-a-i-d, but not greater than 1.5 of the p-a-i-d
 - c. recompute R_{pmax} and/or p-a-i-d if the preceding 10 detected values fall below 0.8 of the current R_{pmax} and/or p-a-i-d of after 500 detected R-peaks, whichever comes first
- (vii) For multiple inflexion points in the region of interest, the following *4-point sieving criteria* is used:

- a. choose the maximum value closest to the p-a-i-d interval signal from the last selected R-peak
 - b. first priority is given to signals that are ± 5 samples from the p-a-i-d interval signal from the last selected R-peak
 - c. second priority is given to signals that are ± 5 inflexion points from the p-a-i-d interval signal from the last selected R-peak
 - d. third priority is given to signals that are ± 10 inflexion points from the p-a-i-d interval signal from the last selected R-peak
- (viii) Compare the R-peak signal points to the R-peak points in the annotated result
- (ix) Determine the accuracy, sensitivity and positive predictivity

The post-training steps in the R-READER 2.0 algorithm are depicted in the flowchart shown in Fig.28.

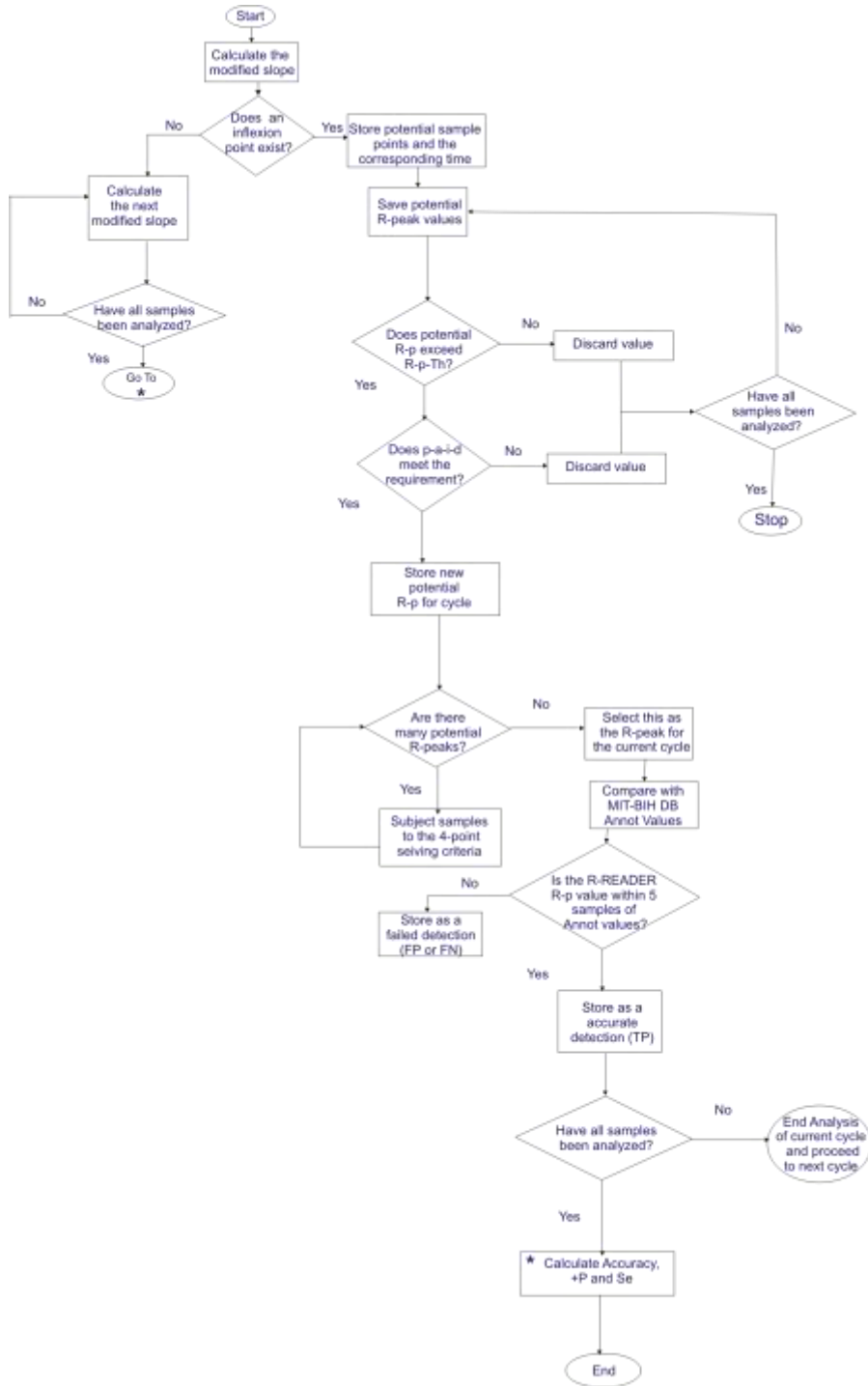


Figure 28: Flowchart of Steps in the R-READER Process

The R-READER Training Process, p-a-i-d and R_{pmax}

A training process, also known as learning phase, is an important requirement in many adaptable algorithms. It allows a designer to obtain an optimized result for any given scenario. The R-READER training process involves the implementation of the algorithm to detect the R-peaks in the first 20 cycles. For this phase, an initial R_{pmax} value of 0.6 is used.

For the R-READER algorithm there are two key parameters upon which the decisions are based- namely the R_{pmax} and the p-a-i-d. The R_{pmax} is the median maximum R-peak for a given set of cycles being reviewed. It gives a good estimate of the expected range of the R-peak in subsequent cycles and enables the selection of a threshold value as a fraction of the R_{pmax} . An initial value is determined at the onset of the execution of the algorithm and is used for the remainder of the analysis. However, R-READER is an adaptable algorithm, as such, a new calculation of R_{pmax} can be initiated by the system designer or automatically if the preceding 10 R-peaks of the current analysis all fall below 0.8 of the current R_{pmax} or after 500 detected peaks, whichever comes first.

The next important parameter is the peak-adjacency-interval-detector (or p-a-i-d). This parameter is also very crucial as it helps the algorithm to eliminate potential R-peaks that occur too soon after a selected R-peak. The basis of using this parameter stems from the fact that is physiologically impossible for a patient to encounter an R-peak within a given time window after a previous R-peak. The p-a-i-d value takes precedence over the R-p-Th in the determination of the R-peak for a given cycle. Again, the p-a-i-d value is obtained after the training process at the onset of the execution of the algorithm and a recalculation can be initiated automatically or by the system designer, similar to the case with R_{pmax} .

In both cases the training values from the first 10 cycles are discarded and the decisions are made based on the values obtained from cycles 11-20. This is to rule out the effect of transient values that are possibly obtained during the start of the ECG readings in preference for values that are likely to better reflect the overall ECG signals.

R-READER and Filtering Process

A key goal of the various filtering steps used in P-T and related algorithms is the accentuation of the fiducial points. Since all these fiducial points occur at inflexion points, R-READER focuses on locating all the existing fiducial points without filtering and these points are used as a basis for decision making in the R-READER process.

At a sampling rate of 200Hz, each ECG sample point occurs 5ms after the preceding sampled point. Noise, regardless of its coloration, occurs for a finite duration of the ECG signal and when it occurs it affects a group of succeeding samples, rather than just an individual sample. As such, it is still possible to accurately determine the relative inflexion points in an ECG signal even in the presence of noise.

C. Performance Evaluation

To assess the performance of R-READER, we have selected some records from the MIT-BIH Arrhythmia Database. In particular, we have chosen the best (least noisy) record- #100 and the worst (most noisy) record- #108. Both records run for approximately 30 minutes and include 650,000 samples, containing an average of over 2,000 cycles each. The #100 is from a 69 year old male patient, while the #108 is from an 87 year old female patient. Record #108 is widely acknowledged as being a very noisy signal [145].

The R-READER is compared with the popular Pan Tompkins algorithm using the following metrics:

- Average Accuracy
- Positive Predictivity and
- Sensitivity

In line with convention, the accuracy has been determined as the proportion of the true positives (TP), which is the number of right R-peak locations detected within ± 5 samples from the peak chosen by the annotators of the database [140]. The failed detections are the false positives (FP) and false negatives (FN). The false positives refer to detections made by R-READER that were not chosen by the annotators while the false negatives are the peaks that were not detected by R-READER but were identified by the annotators. The accuracy can be calculated by Eq (27).

$$\text{Accuracy} = \frac{1 - \text{Failed Detections}}{\text{Total Beats Given in Annotation}} \quad (27)$$

The positive predictivity, +P, is given by Eq (28):

$$+P = \frac{TP}{TP+FP} \quad (28)$$

The sensitivity, Se, is given by Eq (29):

$$S_e = \frac{TP}{TP+FN} \quad (29)$$

Tables 10 and 11 compare the R-peak positions chosen by R-READER for the first 20 cycles and the ones chosen by the annotators for records #100 and #108 respectively. It also gives the deviation between the R-READER detected values and those detected by the annotators.

Table 10. R-Peak Points in R-READER and Annotation for Record #100

Cycle #	R-READER R-peak	Annotated R-peak	Deviation
1	78	77	1
2	371	370	1
3	664	662	2
4	948	946	2
5	1232	1231	1
6	1516	1515	1
7	1810	1809	1
8	2046	2044	2
9	2404	2402	2
10	2707	2706	1
11	2999	2998	1
12	3284	3282	2
13	3561	3560	1
14	3864	3862	2
15	4172	4170	2
16	4467	4466	1
17	4766	4764	2
18	5062	5060	2
19	5348	5346	2
20	5635	5633	2

Table 11. R-Peak Points in R-READER and Annotation for Record #108

Cycle #	R-READER R-peak	Annotated R-peak	Deviation
1	23	23	0
2	88	89	1
3	442	442	0
4	789	791	2
5	1155	1156	1
6	1493	1493	0
7	1821	1822	1
8	2157	2158	1
9	2517	2518	1
10	2889	2890	1
11	3238	3238	0
12	3593	3594	1
13	3924	3926	2
14	4105	4104	1
15	4197	4198	1
16	4602	4604	2
17	4971	4972	1
18	5350	5351	1
19	5715	5716	1
20	6115	6115	0

Table 12 compares the R-READER and P-T algorithms for records #100 and #108 in terms of true positives, false positives, false negatives, accuracy, positive predictivity and sensitivity. Graphical comparisons of the accuracy, positive predictivity and sensitivity are shown in Fig. 27, Fig. 28 and Fig. 29 respectively.

Table 12. Accuracy of the R-READER Algorithm

Record#100							
<i>Algorithm</i>	<i>Total Number of ECG Cycles</i>	<i>TP</i>	<i>FP</i>	<i>FN</i>	<i>Accuracy</i>	<i>+P</i>	<i>S_e</i>
P-T	2273	2273	0	0	100.00%	100.00%	100.00%
R-READER	2273	2273	0	0	100.00%	100.00%	100.00%
Record #108							
<i>Algorithm</i>	<i>Total Number of ECG Cycles</i>	<i>TP</i>	<i>FP</i>	<i>FN</i>	<i>Accuracy</i>	<i>+P</i>	<i>S_e</i>
P-T	1763	1542	199	22	87.47%	88.57%	98.59%
R-READER	1763	1724	31	8	97.79%	98.23%	99.54%
Average Accuracy of Both Records							
<i>Algorithm</i>					<i>Accuracy</i>	<i>+P</i>	<i>S_e</i>
P-T					93.74%	94.29%	99.30%
R-READER					98.90%	99.12%	99.77%

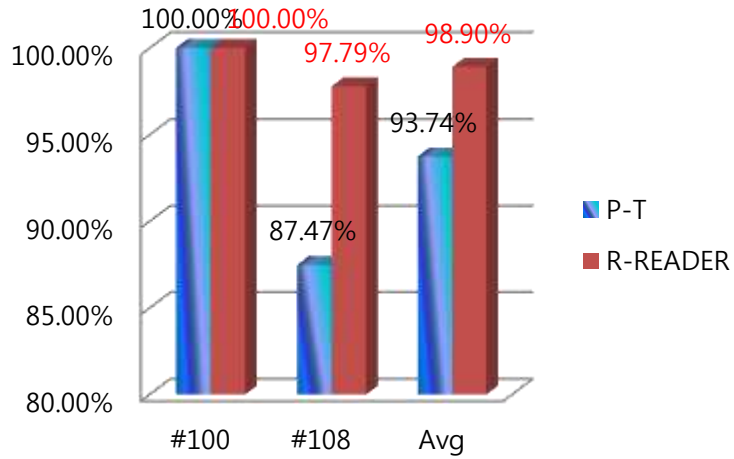


Figure 29: Accuracy Comparison for the 2 Algorithms

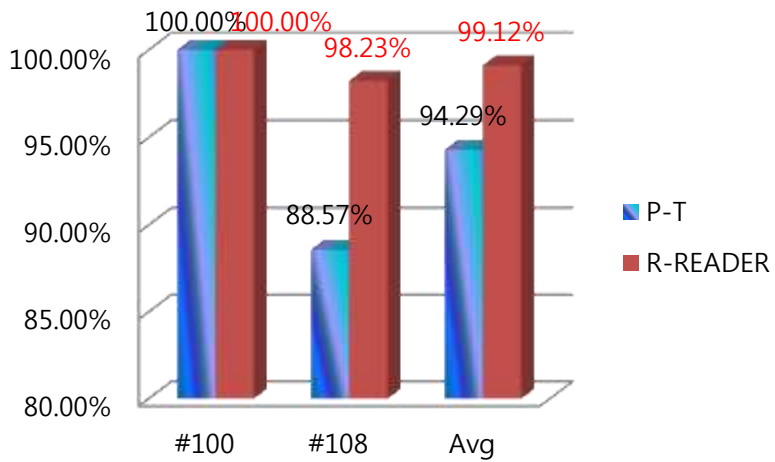


Figure 30: +P Comparison for the 2 Algorithms

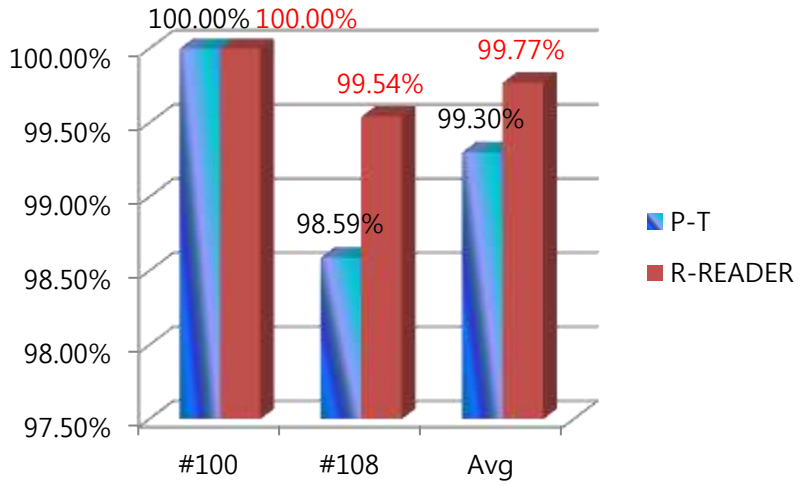


Figure 31: S_e Comparison for the 2 Algorithms

V. Conclusion and Future Work

A. Conclusion

In this thesis we have dealt with the design considerations for developing PHM systems. In particular, we have focused on the need for lightweight processing as a means of reducing the complexity of such systems. We noted the importance of system dependability in PHM systems and proposed some techniques that satisfy the need for lightweight processing as well as the need for system dependability.

The Cardiovascular and Neurologic domains were chosen as the main domains of interest. The former was chosen because it accounts for a large proportion of current PHM systems. The latter was chosen because of the growing interest in the domain as a result of the steep rise in the number of people with neurologic disorders around the world. We proposed a lightweight technique for each of the domains.

The Rapid-Ramp Effective Algorithm for Detection of ECG R-peaks (R-READER) algorithm was proposed for the cardiovascular domain. The current lightweight techniques require a cascade of filters before the detection of R-peaks of an ECG signal can take place. The R-READER is an intuitive technique that takes advantage of the unique shape of ECG signals to accurately detect the R-peaks without a need for the traditional filter approach. It was compared to the widely used Pan-Tompkins algorithm and it gave superior results in terms of accuracy, sensitivity and positive predictivity.

We also proposed a Bio-inspired electroceptive Compressive System (BeCoS) for the lightweight processing of neural signals. BeCoS was inspired by wave-type active

electroreception used by weakly electric fish. It included some key features of the electroreceptive approach and was able to achieve the lightweight sensing, processing, transmission and reconstruction of neural signals. BeCoS was compared to the Block Sparse Bayesian Learning-Bound Optimization (BSBL-BO) technique- a popular approach for lightweight processing of neural signals. Metrics like latency, coherence, level of compression, estimated power and structural similarity were used to compare both approaches. BeCoS gave superior results for most of the metrics.

B. Future Work

For future work we plan to develop algorithms for other PHM domains as well as algorithms that emphasize a need for adaptation to the unique characteristics of the patient, in addition to the current requirements for lightweight processing and system dependability. We intend to further profile and refine the R-READER by running it on embedded systems used for Holter-based long term monitoring of ECG signals.

The BeCoS approach has been used for the monitoring of neural signals in this thesis. However, the technique can be used telemetry of other biosignals as well, especially for signals that are difficult or expensive to sparsify. The signature signal also has the potential to be used as an EEG-based biometric and we plan to explore this possibility in the near future. By using an appropriate disease signature signal, this approach has the potential to be used for the screening of blood for diseases based on the computed values for resistance and capacitance.

Personalized health monitoring is still in its infancy and it has elicited a lot of interest. However, it is yet to be accorded the same level of priority and importance as the health monitoring based on medical instruments located at the hospital. The design of algorithms and techniques that support lightweight signal processing, system dependability and adaptation to

the patient's personal profile will improve the utility and importance of PHM systems.

References

- [1] Bhuiyan, M.Z.A. ; Guojun Wang ; Jiannong Cao ; Jie Wu. Deploying Wireless Sensor Networks with Fault-Tolerance for Structural Health Monitoring. *IEEE Transactions on Computers* 2015; 64(2): 382 – 395.
- [2] Clifton, D.A. ; Pimentel, M.A.F. ; Watkinson, P.J. ; Tarassenko, L. Gaussian Processes for Personalized e-Health Monitoring With Wearable Sensors. *IEEE Transactions on Biomedical Engineering* 2012; 60(1): 193 - 197.
- [3] Splinter, R.. Electroreception. Splinter, R. (ed). *Handbook of Physics in Medicine and Biology*, 1st ed. : CRC Press; 2010.
- [4] Pärkkä, J.. *Analysis of Personal Health Monitoring Data for Physical Activity Recognition and Assessment of Energy Expenditure, Mental Load and Stress*. PhD Thesis, Tampere University of Technology, Finland, 2011.
- [5] Marvasti, F.F. and Stafford, R.S. From Sick Care to Health Care — Reengineering Prevention into the U.S. System. *The New England Journal of Medicine* 2012; 367: 889 - 891.
- [6] Rozenblum, R. and Bates, D.W.. Patient-centred healthcare, social media and the internet: the perfect storm?. *BMJ Quality & Safety* 2012; 001744.
- [7] Misra, A. *Technology Challenges for Health Monitoring and Automated Stream Analysis*; Wayne State University Graduate Research Seminar 2008. http://www.cs.wayne.edu/graduateseminars/gradsem_w08/slides/s03_Misra.pdf (accessed 1 May 2015).
- [8] OECD. *Health at a Glance 2013: OECD Indicators Health at a Glance 2013: OECD Indicators*, OECD Publishing, Paris. http://dx.doi.org/10.1787/health_glance-2013-en (accessed 1 May 2015).
- [9] Shi, L. The Impact of Primary Care: A Focused Review. *Scientifica* 2012
- [10] OECD . *Health at a Glance 2011: OECD Indicators*, OECD Publishing, Paris. http://dx.doi.org/10.1787/health_glance-2011-en (accessed 1 May 2015).
- [11] Lafond, S. *Current NHS spending in England*. http://www.health.org.uk/media_manager/public/75/publications_pdfs/Funding%20overview_Current%20NHS%20spending%20in%20England.pdf (accessed 1 May 2015).
- [12] Gottlieb, S. and Makower, J. A Role for Entrepreneurs: An Observation on Lowering Healthcare Costs via Technology Innovation. *American Journal of Preventive Medicine* 2013; 44(1): S43 – S47.
- [13] Pawar, P., Jones, V. , van Beijnum , B-J.F. and Hermens, H. A framework for the comparison of mobile patient monitoring systems. *Journal of Biomedical Informatics* 2012; 45(3): 544 - 556.

- [14] Alumona T.L., Idigo V.E., and Nnoli K.P. Remote Monitoring of Patients Health using Wireless Sensor Networks (WSNs). *International Journal of Electronics & Communication* 2014; 2(9).
- [15] Islam, S.K., Fathy, A., Wang, Y., Kuhn, M. and Mahfouz, M. Hassle-Free Vitals: BioWireleSS for a Patient- Centric Health-Care Paradigm. *IEEE Microwave Magazine* 2014; 15(7): S25 - S33.
- [16] Estrin, D., Girod, L., Pottie, G. and Srivastava, M. Instrumenting the world with wireless sensor networks. *Proceedings of 2001 IEEE International Conference on Acoustics, Speech, and Signal Processing, Salt Lake City, USA* 2001; 4(): 2033 - 2036.
- [17] Patel S., Park, H., Bonato, P., Chan, L. and Rodgers, M. A review of wearable sensors and systems with application in rehabilitation. *Journal of NeuroEngineering and Rehabilitation* 2012; 9(21).
- [18] Clifton, L., Clifton, D.A., Pimentel, M.A.F., Watkinson, P.J. and Tarassenko, L. Gaussian Processes for Personalized e-Health Monitoring With Wearable Sensors. *IEEE Transactions on Biomedical Engineering* 2012; 60(1): 193 - 197.
- [19] Deloitte 2013 Survey of U.S. Physicians Physician perspectives about health care reform and the future of the medical profession. <http://www2.deloitte.com/content/dam/Deloitte/us/Documents/life-sciences-health-care/us-lshc-deloitte-2013-physician-survey-10012014.pdf> (accessed 1 May 2015).
- [20] Salem, O., Liu, Y., Mehaoua, A, and Boutaba, R. Online Anomaly Detection in Wireless Body Area Networks for Reliable Healthcare Monitoring. *IEEE Journal of Biomedical and Health Informatics* 2014; 18(5): 1541 - 1551.
- [21] Ordóñez, F.J., Toledo, P. and Sanchis, A. Sensor-based Bayesian detection of anomalous living patterns in a home setting. *Personal and Ubiquitous Computing archive* 2015; 19(2): 259 - 270.
- [22] Ko, J-G., Lu, C., Srivastava, M.B., Stankovic, J.A., Terzis, A. and Welsh, M.. Wireless Sensor Networks for Healthcare. *Proceedings of the IEEE* 2010; 98(11): 1947 - 1960.
- [23] Lam, S.C.K., Wong, K.L., Wong, K.O., Wong, W. and Mow, W.H. A smartphone-centric platform for personal health monitoring using wireless wearable biosensors. *7th International Conference on Information, Communications and Signal Processing, 2009. ICICS 2009; Macau.*
- [24] Nikita, K.S. *Handbook of Biomedical Telemetry*, 1st ed. : Wiley- Blackwell; 2014.
- [25] Malik, A.S., Khairuddin, R.N.H.R., Amin, H.U., Smith, M.L., Kamel, N., Abdullah, J.M., Fawzy, S.M. and Shim, S. EEG based evaluation of stereoscopic 3D displays for viewer discomfort. *BioMedical Engineering OnLine* 2015; 14(21).
- [26] *Interdisciplinary Assessment of Personal Health Monitoring*. Schmidt, S. and Rienhof, O. (Eds). IOS Press 2013.
- [27] Trajkovic, V., Vlahu-Gjorgievska, E., Kulev, I. and Koceski, S. Providing Collaborative Algorithms Support for Personal Health Care. *American Journal of*

- Bioinformatics* 2012; 1(1): 41 - 49.
- [28] A Survey of Electronics Obsolescence and Reliability; <http://www.dtic.mil/dtic/tr/fulltext/u2/a531873.pdf>
- [29] Avizienis, A., Laprie, J-C., Randell, B. and Landwehr, C. Basic concepts and taxonomy of dependable and secure computing. *IEEE Transactions on Dependable and Secure Computing* 2004; 1(1): 11 - 33.
- [30] *Cardiovascular diseases (CVDs) Fact sheet.* <http://www.who.int/mediacentre/factsheets/fs317/en/> (accessed 3 May 2015).
- [31] *Brain Disorders: By the Numbers.* <http://mcgovern.mit.edu/brain-disorders/by-the-numbers> (accessed 2 May 2015).
- [32] Olesen, J., Gustavsson, A., Svensson, M., Wittchen, H.U., Jönsson, B., CDBE2010 study group et al. The economic cost of brain disorders in Europe. *European Journal of Neurology* 2012; 19: 155 - 162.
- [33] *European Commission Human Brain Project.* https://www.humanbrainproject.eu/en_GB (accessed 29 April 2015).
- [34] *The Brain Research through Advancing Innovative Neurotechnologies (BRAIN) Initiative.* <http://braininitiative.nih.gov> (accessed 3 May 2015).
- [35] Koehler, F., Winkler, S., Schieber, M., Sechtem, U., Stangl, K., Böhm, M., Boll, H., Baumann, G., Honold, M., Koehler, K., Gelbrich, G., Kirwan, B.A. and Anker, S.D. Impact of remote telemedical management on mortality and hospitalizations in ambulatory patients with chronic heart failure: the telemedical interventional monitoring in heart failure study. *Circulation* 2011. 123(17)
- [36] Ricci, R.P., Morichelli, L. and Santini, M. Remote control of implanted devices through Home Monitoring technology improves detection and clinical management of atrial fibrillation. *Europace* 2009. 11(1):54-61.
- [37] Guerri JC, Antón AB, Pajares A, Monfort M and Sánchez D. A mobile device application applied to low back disorders. *Multimedia Tools and Applications*. 2009; 42(3): 317-340
- [38] Kang JM, Yoo T and Kim H-C. A Wrist-Worn Integrated Health Monitoring Instrument with a Tele-Reporting Device for Telemedicine and Telecare. *IEEE Transactions on Instrumentation and Measurement* 2006; 55(5): 1655-1662
- [39] Tsanas A, Little MA, McSharry PE and Ramig LO. Accurate telemonitoring of Parkinson's disease progression by noninvasive speech tests. *IEEE Transactions on Biomedical Engineering*. 2010;57(4):884-893.
- [40] Dellacà RL, Gobbi A, Pastena M, Pedotti A and Celli B. . Home monitoring of within-breath respiratory mechanics by a simple and automatic forced oscillation technique device. *Physiological Measurements*. 2010;31(4):N11-24.
- [41] Alves de Mesquita J Jr, Bouskela E, Wajnsberg E and Lopes de Melo P. Improved instrumentation for blood flow velocity measurements in the microcirculation of small animals *Review of Scientific Instruments* 2007; 78(2):024303

- [42] Madria S, Kumar V and Dalvi R. Sensor Cloud: A Cloud of Virtual Sensors. *IEEE Software* 2014; 31(2): 70-77.
- [43] Sticherling C, Kühne M, Schaer B, Altmann D and Osswald S. Remote monitoring of cardiovascular implantable electronic devices: prerequisite or luxury? *Swiss Med Wkly.* 2009;139(41-42):596-601.
- [44] Wang H, Peng D, Wang W, Sharif H, Chen H-H and Khoynezhad A. A. Resource-aware secure ECG healthcare monitoring through body sensor networks; *IEEE Wireless Communications* 2010; 17(1): 12-19.
- [45] Fanucci L, Saponara S, Bacchillone T, Donati M, Barba P, Sánchez-Tato I and Carmona C. Sensing Devices and Sensor Signal Processing for Remote Monitoring of Vital Signs in CHF Patients. *IEEE Transactions on Instrumentation and Measurement* 2013. 62(3): 553 – 569
- [46] Lee S-J, Kim J and Lee M. The Design of the m-Health Service Application Using a Nintendo DS Game Console. *Telemedicine and e-Health* 2011; 17(2):124-130.
- [47] Dilmaghani RS, Bobarshad H, Ghavami M, Choobkar S and Wolfe C. Wireless sensor networks for monitoring physiological signals of multiple patients. *IEEE Transactions on Biomedical Circuits and Systems* 2011; 5(4):347-56.
- [48] Hii P-C and Chung W-Y. A Comprehensive Ubiquitous Healthcare Solution on an Android™ Mobile Device. *Sensors (Basel)* 2011; 11(7): 6799–6815.
- [49] Cleven NJ, Müntjes JA, Fassbender H, Urban U, Görtz M, Vogt H, Gräfe M, Göttsche T, Penzkofer T, Schmitz-Rode T and Mokwa W. A novel fully implantable wireless sensor system for monitoring hypertension patients. *IEEE Transactions on Biomedical Engineering* 2012; 59(11):3124-30.
- [50] Pitts DG, Patel MK, Lang PO, Sinclair AJ and Aspinall R. A respiratory monitoring device based on clavicular motion. *Physiological Measurements* 2013;34(8):N51-61.
- [51] Anliker U, Ward JA, Lukowicz P, Tröster G, Dolveck F, Baer M, Keita F, Schenker EB, Catarsi F, Coluccini L, Belardinelli A, Shklarski D, Alon M, Hirt E, Schmid R and Vuskovic M. AMON: a wearable multiparameter medical monitoring and alert system. *IEEE Transactions on Information Technology in Biomedicine* 2004;8(4):415-27
- [52] Cheng CM, Hsu YL, Young CM and Wu CH. Development of a portable device for telemonitoring of snoring and obstructive sleep apnea syndrome symptoms. *Telemedicine and e-Health* 2008;14(1):55-68.
- [53] Chun H, Kang J, Kim KJ, Park KS and Kim HC. IT-based diagnostic instrumentation systems for personalized healthcare services. *Studies in Health Technology and Informatics* 2005;117:180-190.
- [54] Yu Y, Li J and Liu J. M-HELP: a miniaturized total health examination system launched on a mobile phone platform. *Telemedicine and e-Health* 2013;19(11):857-65.
- [55] Fong E-M and Chung W-Y. Mobile Cloud-Computing-Based Healthcare Service by Noncontact ECG Monitoring. *Sensors (Basel)* 2013, 13(12), 16451-16473.

- [56] Giansanti D, Morelli S, Maccioni G and Grigioni M. Portable kit for the assessment of gait parameters in daily telerehabilitation. *Telemedicine and e-Health* 2013;19(3):224-32.
- [57] Gómez EJ, Hernando Pérez ME, Vering T, Rigla Cros M, Bott O, García-Sáez G, Pretschner P, Brugués E, Schnell O, Patte C, Bergmann J, Dudde R and de Leiva. A. The INCA system: a further step towards a telemedical artificial pancreas. *IEEE Transactions on Information Technology in Biomedicine* 2008;12(4):470-479.
- [58] D'Arcy RC, Hajra SG, Liu C, Sculthorpe LD and Weaver DF. Towards brain first-aid: a diagnostic device for conscious awareness. *IEEE Transactions on Biomedical Engineering* 2011;58(3):750-4.
- [59] Chen W, Zhu X, Nemoto T, Kitamura K, Sugitani K and Wei D. Unconstrained monitoring of long-term heart and breath rates during sleep. *Physiological Measurements* 2008;29(2):N1-10.
- [60] Nemiroski A, Christodouleas DC, Hennek JW, Kumar AA, Maxwell EJ, Fernández-Abedul MT and Whitesides GM. Universal mobile electrochemical detector designed for use in resource-limited applications;; *Proceedings of the National Academy of Sciences of the United States of America* 2014;111(33):11984–11989.
- [61] Lee Y, Lee B and Lee M. Wearable sensor glove based on conducting fabric using electrodermal activity and pulse-wave sensors for e-health application. *Telemedicine and e-Health* 2010;16(2):209-17. doi: 10.1089/tmj.2009.0039
- [62] Olansen JB and Rosow E. *Virtual Bio-Instrumentation: Biomedical, Clinical, and Healthcare Applications in LabVIEW*. Prentice Hall PTR. December 2001
- [63] *Managing Performance Measurement Data in Health Care Second Edition*; Joint Commission Resources; Jaclyn Graham (Executive Editor), 2008 by Joint Commission on Accreditation of Healthcare Organizations
- [64] Malathi P and Kirthika B. Performance Analysis of Hybrid (SVM+ICA) Method for two class dataset. *International Journal of Advance Research in Computer Science and Management Studies* 2014; 2(1): 656-661.
- [65] Esmaeeli S and Gholampour I. Reduced memory requirement in hardware implementation of SVM classifiers. *Proceedings of the 20th Iranian Conference on Electrical Engineering (ICEE), 2012* May 15-17; p. 46-50. Tehran, Iran
- [66] Harikumar R, Vijayakumar T and Sreejith MG. Performance Analysis of Support Vector Machine (SVM) for Optimization of Fuzzy Based Epilepsy Risk Level, Classifications from EEG Signal Parameters. *Proceedings of Recent Advances in Intelligent Computational Systems (RAICS), Trivandrum, India, 2011* September 22-24: 351-354.
- [67] Sivanandam SN and Deepa SN. *Introduction to Genetic Algorithms*; Springer Berlin, Heidelberg, Germany; 2008
- [68] Jabbar MA, Deekshatulu BL and Chandra P. Heart Disease Prediction System using Associative Classification and Genetic Algorithm. *Proceedings of International*

- Conference on Emerging Trends in Electrical, Electronics and Communication Technologies (ICECIT), 2012 December 21-23: 183-192
- [69] Kew HP and Jeong DU. Variable threshold method for ECG R-peak detection. *J Med Syst.* 2011;35(5):1085-1094
- [70] Wang J, Zhang Z, Li B, Lee S and Sherratt RS. An enhanced fall detection system for elderly person monitoring using consumer home networks. *IEEE Transactions on Consumer Electronics* 2014; 60(1): 23 – 29
- [71] Nandy S, Das A and Sarkar PP. An Improved Gauss-Newtons Method based Back-propagation Algorithm for Fast Convergence. *International Journal of Computer Applications* 2012; 39(8):1-7.
- [72] Jin Z, Oresko J, Huang S and Cheng AC. HeartToGo: a personalized medicine technology for cardiovascular disease prevention and detection. *Proceedings of IEEE/NIH Workshop on Life Science Systems and Applications, Bethesda, USA., 2009 April 9-10: 80-83.*
- [73] Strohmer T. Measure What Should be Measured: Progress and Challenges in Compressive Sensing. *IEEE Signal Processing Letters*; 19(12): 887 - 893.
- [74] Craven D, McGinley B, Kilmartin L, Glavin M, Jones E. Compressed Sensing for Bioelectric Signals: A Review. *IEEE Journal of Biomedical and Health Informatics*; 19(2): 529-540
- [75] Gama J. *Knowledge Discovery from Data Streams.* Chapman and Hall/CRC . 2010
- [76] Zhu W, Zeng N and Wang N. Sensitivity, Specificity, Accuracy, Associated Confidence Interval and ROC Analysis with Practical SAS Implementations. 2010. [Accessed 14 April , 2015]; <http://www.nesug.org/Proceedings/nesug10/hl/hl07.pdf>.
- [77] Codagnone C. *Reconstructing the Whole: Present and Future of Personal Health Systems.* 2009. [Accessed 5 May 2015]. http://www.evia.imasdtic.es/cli_aetic/ftpportalweb/documentos/phs2020-book-rev16082009.pdf
- [78] Hood L. and Rowen, L. The Human Genome Project: big science transforms biology and medicine; *Genome Medicine* 2013, 5(9).
- [79] Deighton, B. Personal health data clouds to give early warning for cancer, other diseases. http://horizon-magazine.eu/article/personal-health-data-clouds-give-early-warning-cancer-other-diseases_en.html [Accessed 5 May 2015].
- [80] *Genomic Medicine: Principles and Practice* (2nd edition). Kumar, D. Eng, C. (Eds). 2014. Oxford University Press; 2 edition
- [81] McDaid, D. *Countering the stigmatisation and discrimination of people with mental health problems in Europe* European Commission, Luxembourg. 2008.
- [82] Islam SK., Fathy A, Wang Y, Kuhn M and Mahfouz M. Hassle-Free Vitals: BioWireleSS for a Patient-Centric Health-Care Paradigm. *IEEE Microwave Magazine*: 15(7): S25 – S33.

- [83] Heurtefeux K., Mohsin N, Hamida EB and Menouar H. Dynamic and Energy Efficient Wireless BAN Platform for Remote Health Monitoring; 2014 IEEE 10th International Conference on Wireless and Mobile Computing, Networking and Communications (WiMob) Larnaca, Cyprus: 548-555.
- [84] Salem O, Liu Y, Mehaoua A and Boutaba R. Online Anomaly Detection in Wireless Body Area Networks for Reliable Healthcare Monitoring. *IEEE Journal of Biomedical and Health Informatics*. 2014. 18(5): 1541-1551
- [85] Gao T, Massey T, Selavo L, Crawford D, Chen, B-r. ,Lorincz K., Shnayder V, Hauenstein L, Dabiri F, Jeng J, Chanmugam A., White D, Sarrafzadeh M and Welsh M. The Advanced Health and Disaster Aid Network: A Light-Weight Wireless Medical System for Triage. *IEEE Transactions on Biomedical Circuits and Systems*. 2011. 1(3): 203 – 216.
- [86] Chi YM, Jung T-P and Cauwenberghs G. Dry-Contact and Noncontact Biopotential Electrodes: Methodological Review. *IEEE Reviews in Biomedical Engineering*, 2010. 3:106-119.
- [87] Chi YM, Wang Y-T, Wang Y, Maier C, Jung T-P and Cauwenberghs G. Dry and Noncontact EEG Sensors for Mobile Brain–Computer Interfaces. *IEEE Transactions on Neural Systems and Rehabilitation Engineering*, 2012. 20(2): 228-235
- [88] Bernacchia N, Scalise L, Casacanditella L, Ercoli I, Marchionni P and Tomasini EP. Non contact measurement of heart and respiration rates based on Kinect™. 2014 IEEE International Symposium on Medical Measurements and Applications (MeMeA). June 2014; Lisbon, Portugal: 1-5.
- [89] Probing Experience; From Assessment of User Emotions and Behaviour to Development of Products. 2008. Westerink, J., Ouwkerk, M., Overbeek, T.J.M., Pasveer, W.F. (Eds.). Springer Netherlands.
- [90] Meddins R. Introduction to Digital Signal Processing (1st edition). Newnes; 2000.
- [91] Davenport MA, Boufounos PT, Wakin MB and Baraniuk RG. Signal Processing With Compressive Measurements. *IEEE J Selected Topics in Sign Processing*. 2010: 4(2): 445-460
- [92] Zhang Z and Rao BD. Extension of SBL Algorithms for the Recovery of Block Sparse Signals With Intra-Block. *IEEE Transactions on Signal Processing*. 2013. 61(8): 2009-2015
- [93] Zhang Z, Jung T-P, Makeig S and Rao BD. Compressed Sensing of EEG for Wireless Telemonitoring with Low Energy Consumption and Inexpensive Hardware. *IEEE Transactions on Biomedical Engineering* 2013. 60(1): 221-224.
- [94] Map of Life - "Electroreception in fish, amphibians and monotremes" http://www.mapoflife.org/topics/topic_41_Electroreception-in-fish-amphibians-and-monotremes/ (Accessed on February 02, 2015)
- [95] Splinter R (Ed). *Handbook of Physics in Medicine and Biology*; CRC Press; Taylor and Francis Group, USA, 2010.

- [96] Electric Organ Discharge.
http://classic.sidwell.edu/us/science/21bio/new/wef_eod.html
- [97] Snyder JB, Nelson ME, Burdick JW and Maciver MA. Omnidirectional sensory and motor volumes in electric fish. *PLoS Biol* 2007; 11 (e301): 2009-2015
- [98] Scheich H and Bullock TH. The detection of electric fields from electric organs. In *Handbook of Sensory Physiology*, vol. III/3 (ed. A. Fessard). 1974: 201–256. New York: Springer
- [99] von der Emde G and Ronacher B. Perception of electric properties of objects in weakly electric fish: two-dimensional similarity scaling reveals a City-Block metric. 1994. *Journal of Comparative Physiology A*. 175(6): 801-812
- [100] Kramer B. Electric communication and electrolocation. In M. D. Binder, N. Hirokawa & U. Windhorst (Eds) *Encyclopedia of Neuroscience*. 2009: 1038-1045. Berlin Heidelberg: Springer Verlag.
- [101] The energetics of electric organ discharge generation in gymnotiform weakly electric fish; <http://jeb.biologists.org/content/216/13/2459/F1.expansion.html> (Accessed on April 13, 2015)
- [102] Hanika S and Kramer B. Plasticity of electric organ discharge waveform in the South African Bulldog fish, *Marcusenius pongolensis*: tradeoff between male attractiveness and predator avoidance? 2008. *Frontiers in Zoology* 5:7
- [103] Kramer B. Electoreception and communication in fishes. *Progress in Zoology*, 42. Rathmayer W (Ed). 1996. Gustav Fischer, Stuttgart.
- [104] Kramer B and Kuhn B. Electric signalling and impedance matching; The Electric Organ of Mormyrid Fish Actively Adapts to Changes in Water Conductivity. 1993. *Naturwissenschaften* 80: 43-46. Springer-Verlag
- [105] The Physionet Database <http://www.physionet.org/> (Accessed on May 08, 2015)
- [106] Lachaux JP, Rodriguez E, Martinerie J and Varela FJ . Measuring phase synchrony in brain signals. *Human Brain Mapping*, 1999. 8(4): 194-208
- [107] La Rocca D, Campisi P, Vegso B, Cserti P, Kozmann G, Babiloni F, and De Vico Fallani F. Human Brain Distinctiveness Based on EEG Spectral Coherence Connectivity. *IEEE Transactions on Biomedical Engineering*. 2014: 61 (9):2406-2412
- [108] Golinska AK. Coherence function in biomedical signal processing: a short review of applications in Neurology, Cardiology and Gynecology; *Studies in Logic, Grammar and Rhetoric*, 2011. 25(38): 73-82.
- [109] Welch PD. The Use of Fast Fourier Transform for the Estimation of Power Spectra: A Method Based on Time Averaging Over Short, Modified Periodograms. *IEEE Transactions on Audio and Electroacoustics*. 1967. AU-15:70–73.
- [110] Zeng M, Lee J-G, Choi G-S and Lee J-A. Intelligent sensor node based on a low power ECG monitoring system. *IEICE ELEX* 2009: 6(9): 560-565
- [111] Köhler BU, Hennig C and Orglmeister R. *The Principles of Software QRS*

- Detection.; IEEE Engineering in Medicine and Biology Magazine 2002: 21(1):42-57.
- [112] Wang Z and Bovik AC. Mean squared error: Love it or leave it? A new look at Signal Fidelity Measures. Signal Processing Mag. 2009: 26(1):98 - 117.
- [113] Kudeki E. Analog Signals and Systems. 2008. Publisher: Prentice Hall, New Jersey, USA.
- [114] Haliday D. Fundamentals of Physics. 2010. 9th Edition. Wiley, New Jersey, USA.
- [115] Bedard C and Destexhe A. A generalized theory for current-source density analysis in brain tissue 2011. Physical Review E, 84: 041909
- [116] Andrea M, Ettore R, Paolo G, Riccardo B and. Kimimila IL. A New Model to Classify NGS Short Reads by their Allele Origin. 2014 IEEE International Conference on Healthcare Informatics (ICHI), Verona, Italy: 340-342.
- [117] Numez PL and Srinivasan R. Electric Fields of the Brain: The Neurophysics of EEG, Oxford University Press, Oxford, United Kingdom, 2006.
- [118] Xiang Y and Liu S. Coherent high-order harmonic generation by sawtooth-like laser fields. 2013. Optics Express 21(9):11270-11275.
- [119] Berkhout J and Walter DO. Temporal stability and individual differences in the human EEG: An analysis of variance of spectral values. 1968. IEEE Transactions on Biomedical Engineering. 15(3): 165– 168.
- [120] Vogel F and Schalt E. The electroencephalogram (EEG) as a research tool in human behavior genetics: Psychological examinations in healthy males with various inherited EEG variants. 1979. Human Genetics. 47: 81–111
- [121] Campisi P and La Rocca D, Brain waves for automatic biometric based user recognition, IEEE Transactions in Information Forensics and Security. 2014. 9(5): 782 – 800
- [122] Simple Bus Architecture; <http://sba.accesus.com/> (Accessed on May 06, 2015)
- [123] The WISHBONE System-on-Chip (SoC) Interconnect Architecture for Portable IP Cores; <http://opencores.org/opencores,wishbone> (Accessed on May 13, 2015)
- [124] Yang H, Kan C, Liu G and Chen Y. Spatiotemporal Differentiation of Myocardial Infarctions. IEEE Transactions on Automation Science and Engineering, 2013: 938-947
- [125] Nemati E, Deen, MJ and Mondal T. A wireless wearable ECG sensor for long-term applications. IEEE Communications Magazine, 2012. 50(1): 36 - 43,
- [126] Tello JP, Manjarres O, Quijano M, Blanco A, Varona F and Manrique M. Remote Monitoring System of ECG and Human Body Temperature Signals. IEEE (Revista IEEE America Latina) Latin America Transactions. 2013. 11(1): 314 - 318;
- [127] Dong J, Zhang J-w, Zhu H-h., Wang L-p, Liu X. and Li Z-j. A Remote Diagnosis Service Platform for Wearable ECG Monitors. 2012. IEEE Intelligent Systems. 6(27): 36 – 43
- [128] Liu X, Yang J, Zhu X, Zhou S, Wang H and Zhang H. A Novel R-peak

- Detection Method Combining Energy and Wavelet Transformation in Electrocardiogram Signal. Biomedical Engineering: Applications, Basis and Communications. 2014. 26(1)
- [129] What the heart can tell us about the mind: Heart rate variability and PTSD; http://www.research.va.gov/currents/summer2014/summer_2014-25.cfm (Accessed on April 2, 2015)
- [130] Minassian A, Geyer MA, Baker DG, Nievergelt CM, O'Connor DT and Risbrough VB. Heart rate variability characteristics in a large group of active-duty marines and relationship to posttraumatic stress. Psychosomatic Medicine 2014 . 76(4):292-301.
- [131] Freeman R. HRV in Diabetes and Other Disorders; HRV 2006: Techniques, Applications and Future Direction; Boston, USA, April 2006.
- [132] Stein PK. HRV and Risk Stratification:Post-MI; HRV 2006: Techniques, Applications and Future Direction; Boston, USA, April 20, 2006.
- [133] Griffin P and Moorman R. Heart rate characteristics Heart rate characteristics monitoring monitoring to detect neonatal sepsis ; HRV 2006: Techniques, Applications and Future Direction; Boston, USA, April 20, 2006.
- [134] Hossein R, Mahjoob MP, Farahabadi E and Farahabadi A. R Peak Detection in Electrocardiogram Signal Based on an Optimal Combination of Wavelet Transform, Hilbert Transform, and Adaptive Thresholding. 2011. Journal of Medical Systems and Sensors. May-Aug; 1(2): 91–98.
- [135] Jeong CI., Vai MI and Mak PU. QRS Recognition with Programmable Hardware. 2nd International Conference on Bioinformatics and Biomedical Engineering, Shanghai, China, May, 2008: 2028 – 2031.
- [136] Pan J and Tompkins WJ. A Real-Time QRS Detection Algorithm. IEEE Transactions on Biomedical Engineering. 1985. 32(3): 230 - 236;
- [137] Álvarez RA, Penín AJM and Sobrino XAV. A Comparison of Three QRS Detection Algorithms Over a Public Database. 2013. Procedia Technology. 9: 1159–1165
- [138] Citations for "A Real-Time QRS Detection Algorithm";<http://ieeexplore.ieee.org/xpl/abstractCitations.jsp?arnumber=4122029>
- [139] Elgendi M. Fast QRS Detection with an Optimized Knowledge-Based Method: Evaluation on Standard ECG Databases. 2013. PLoS ONE 8(9): e73557.
- [140] Noise Stress Testing. <http://www.physionet.org/physiotools/wag/evnode14.htm> (Accessed on April 6, 2015)
- [141] Afonso VX. ECG QRS detection In: Biomedical digital signal processing 1993: 236-264). Prentice-Hall, Inc.Tompkins, W.J. (Ed)
- [142] Shukla A. and Macchiarulo L. A Fast and Accurate FPGA based QRS detection System. IEEE Engineering in Medicine & Biology Society Conference 2008. Vancouver, Canada: 4828~4831.

- [143] Massachusetts Institute of Technology- Beth Israel Hospital (MIT-BIH) Arrhythmia database ; www.physionet.org/physiobank/database/mitdb/ (Accessed on April 11, 2015)
- [144] Clifford GD, Azuaje F and McSharry P. Advanced Methods and Tools for ECG Data Analysis. Artech House Publishers, 2006
- [145] Cassiano KK and Nadal J. Software Library for Real-Time Cardiac Beat Detection. 17th International Conference on Systems, Signals and Image Processing. Rio de Janeiro, Brazil, June 2009: 546-549.

Appendix A

APPENDIX A. Summary of Studies included in the Review								
S/N	AUTH-ORS	YEAR	JOURNAL	ARCHITECTURE	APPLICATION	ADAPTATION/PERSONALIZATION	STUDY DESIGN	OUTCOME/ RESULTS
1.	Koehler et al. 2-1	2011	Circulation (Journal of the American Heart Association)	12-lead ECG, BP, Weight; Dynamic encryption on cell phone; PDA (Central Device), Bluetooth (Communication)	Impact of remote monitoring on Chronic Heart Failure		710 stable chronic heart failure patients; 17-month (duration); Low statistical power (limitation); Study evaluated effect of remote telemonitoring on mortality.	Primary outcome: Rate of all cause mortality (death) was reduced to 8.4% as compared with 8.7% for normal care; Secondary outcome: Cardiovascular death and hospitalization per 100 person years of follow up reduced to 14.7% as compared to 16.5% for normal care.
2.	Ricci et al 2-2	2009	Eurospace (Europe Society for Cardiology)	Home monitoring, long distance telemetry, automatic transmission of pacemaker data on a daily basis; Implanted cardio device (ICD) with wireless telemetry via a GSM phone as encrypted sms; Data transmitted every night and critical conditions are reported to service center within 3 minutes; Error detection to distinguish between true arrhythmias and R-wave far field oversensing.	Impact of home monitoring on Atrial Fibrillation (AF)	Pacemaker and ICD programming was tailored to patient's individual clinical profile	166 patients for 2 years	Remote monitoring led to AF detection and alert that occurred an average of 148days before scheduled follow up visit Limitation: It was an observational study with no clinical outcome Open issue: how to select appropriate alerts
3.	Guerri et al 2-3	2009	Multimedia Tools and Applications	8-channel Surface EMG, Portable handheld prototype (Platform), connected to phone/PDA via WiFi; PDA: HP IPAQ HX4700, phone: Nokia E41; Includes online telemetry mode and offline mode (with storage on CF card)	Use of mobile devices and wireless networking for assessment of muscular conditions	Configured via a mobile device; Configuration was based on patient's profile or system parameters like duration of exercise, sampling frequency and monitored muscle Config modes: Offline and online	Duration: 55 seconds Phase 1: Feasibility and Reliability: 12 volunteers Phase 2: Usability Assessment: Questionnaires completed by 7 users	Design of a portable device capable of advanced EMG measurements Can be used by both expert and non-expert users
4.	Kang	2006	IEEE	Wrist worn device with 6 biosensors for: (i) Fall detection [2-axis	Wrist-worn		Limitation: Low fidelity	Error Range and Detection

	et al. ²⁻⁴		Transactions on Instrumentation and Measurement	<p>accelerometer, gyroscope and in-house posture sensor] (ii) 1-channel ECG textile electrode (iii) Noninvasive BP [based on a wrist cuff] (iv) SPO2 (v) Respiratory Rate [based on Virtual sensing of r-r intervals of ECG] and (vi) Body Surface Temperature</p> <p>A cellular phone was used as the connection gateway; wireless connection used between wrist worn device and phone; CDMA was used for connection between the phone and medical service center</p> <p>Main algorithms were based on thresholding</p>	<p>device for general health monitoring</p> <p>Anomalies were reported via sms</p>		<p>of biosignals since most measurements were based on readings from the skin. Tests were based on simulated signals and human trials</p>	<p>Rates: ± 5mmHg (NIBP), 2%(SPO2), 1%(ECG), 1.8% (Respiration Rate), 1.5% (Temperature), 91.3% detection rate for 150 simulated falls</p>
5.	Tsanas et al ²⁻⁵	2010	IEEE Transactions on Biomedical Engineering	<p>Virtual sensing based on speech tests from a microphone headset on an Intel AHTD Telemonitoring System for predicting Parkinson's Disease (PD)</p> <p>Algorithm was based on thresholding.</p> <p>Speech signal processing was based on 16 dysphonia measures applied to 5923 sustained phonations.</p>	<p>Accurate system for tracking the progression of Parkinson's Disease Rating Scale (UPDRS).</p> <p>Statistical mapping of a subset of speech features to UPDRS.</p> <p>It showed the potential of sustained vowel phonations in predicting average PD progression.</p>		<p>It was based on 6,000 database recordings from 42 PD patients.</p> <p>Based on objective (rather than subjective) assessment.</p> <p>Human trial was based on a 6 month study of 42 idiopathic PD patients.</p>	<p>This virtual sensing approach can estimate the result within about 7.5. UPDRS points difference from the clinicians' estimates using a simple, self administered non-invasive test.</p>
6.	Dellaca et al ²⁻⁶	2010	Physiological Measurement	<p>Pressure and flow sensors.</p> <p>Respiratory input impedance (Zrs) was measured after a 5Hz pressure stimulus from a loudspeaker was transmitted to the patient through a self-made mesh-type Pneumotachograph (PNT).</p> <p>Zrs was computed using the Least squares algorithm and transmitted over the Internet.</p> <p>Communication was based on GPRS, DSL or WiFi (depending on availability).</p> <p>Encryption was based on Public Key Algorithm.</p> <p>Realtime or scheduled transmission options were available.</p> <p>Reliable and standardized TCP/IP connection was established by using SSH.</p>	<p>Forced Oscillation Technique (FOT) device for unsupervised monitoring to replace supervised spirometry.</p> <p>Useful for diagnosis and staging of obstructive diseases (like COPD and asthma)</p>		<p>5 healthy subjects, 36 consecutive daily home measurements.</p> <p>Reduces the dimensions of current FOT device</p> <p>36 consecutive daily home measurements.</p> <p>Extensive tests on 7 subjects.</p> <p>Limitation: Only 1 COPD patient was used in the tests.</p>	<p>The portable FOT device can be used for unsupervised assessment of airway obstruction over prolonged periods. The maximum error was 10%.</p>
7.	Mesqu	2007	Review of	<p>Photosensor head and photodiodes (Sensors).</p>	<p>Blood flow</p>		<p>Adding a virtual</p>	<p>In vivo tests for 7-10 week old</p>

	ita J Jr et al ²⁻⁷		Scientific Instruments	It was used to implement a virtual velocimeter based on digital cross correlation techniques.	measurements that are less dependent on operator bias. Samples optical signals from microvessel and gives instant velocity.		instrument module to an existing microcirculation hardware reduces operator bias and allows digital signal processing and storage. The manual system depended on the tuning of the system making it susceptible to operator bias.	golden hamsters Pharmacological intervention: successful and accurate monitoring of blood flow velocity in one arteriole analyzed before and after the administration of phenylphrine.
8.	Stichering et al ²⁻⁹	2009	Swiss Medical Weekly	CIED; based on optivol sensor that measured intrathoracic impedance upon the accumulation of intrapulmonary fluid. GSM was used for remote monitoring.	Remote monitoring of ICDs for early detection of disease and device anomaly. It was also used to number of patient visits to the hospital.		It was a survey.	
9.	Wang et al ²⁻¹⁰	2010	IEEE Wireless Communications	It used a 3-lead ECG sensor with a transmission range of 100m. It used a low delay adaptive encryption scheme dependent on the condition of the wireless channel.	Secure and resource aware body sensor network architecture for real-time health monitoring based on unequal resource allocations It used an on-body healthnode data terminal to process and transmit sensor data.		The system allocated extra energy resources to protect the important portion of the transmitted signal.	The tests were based on simulation and real time tests. This lowered energy consumption and gave better signal quality per energy used. Authors stated that shorter QRS windows can improve real-time encryption.
10.	Fanucci et al ²⁻¹¹	2013	IEEE Transactions on Instrumentation and Measurement	7 Sensors: (i) 3-lead ECG (ii) SPO2 (iii) BP (iv) Weight (v) Chest impedance (vi) Respiration (vii) Posture Local-MVI communication: Bluetooth Remote-MVI communication: ADSL or mobile broadband. HTTPS used for security and encryption. A prototype was built and the Pan-Tompkins algorithm was used	Flexible and highly configurable system for monitoring Chronic Health Failure (CHF). It provided alerts	Configuration parameters: Alarm thresholds, transmission policy, selectable symptoms. It also supported	One or few non-continuous daily measurements were made.	ECG simulators and Physionet Toolkit were used for analysis. Pre-prototype tests: 2 patients, 1 month test Post-prototype tests: 30 patients with Chronic Health Failure disease

				for ECG analysis.	for abnormal heart frequency, atrial fibrillation episodes, QRS complexes exceeding 120ms and signs of myocardial ischemia.	remote configuration.		Results: <3% activity misses (mostly in the 1st days). <5% false positive alarms, 95% patients found the system useful and 99% patients were satisfied with system.
11.	Lee et al ²⁻¹²	2011	Telemedicine and e-Health	<p>The system used a Nintendo DS Game Console as the platform. However, the system can also use a PC or PDA.</p> <p>3-channel ECG, 3-axis accelerometer ($\pm 3g$), Tilting (Sensors)</p> <p>1 ECG packet consists of 64 ECG signals</p> <p>ZigBee was used for the local-MVI communication while WiFi was used for the Remote-MVI communication. The system also included a webserver.</p>	Mobile health ECG and gait monitoring system that obviates distance restrictions.			<p>It used a 1 hour test to ensure appropriate wireless connectivity.</p> <p>The Health monitoring test lasted for over 24 hours without any interruption.</p> <p>Packet Loss: <5% for distances less than 20m, much higher and incremental loss beyond 20m</p> <p>For packet error rate (Pe): When Pe=0, no delay; Pe=0.2, 25s delay and Pe=0.4, 157s delay (due to the need for retransmission)</p>
12.	Dilma ghani et al ²⁻¹³	2011	IEEE Transactions on Biomedical Circuits and Systems	<p>ECG (Sensor).</p> <p>Its Wireless Patient Portable Unit (Platform) had a webserver and connected to a central remote node via Internet access provided by a Wireless Access Point Unit (WAPU).</p>	System to monitor patients with chronic diseases in their homes	WPPU can be configured for a variable gain between 500 and 1000.	<p>The study avoided the use of a PC and PDA (to reduce cost).</p> <p>System objectives: Eliminate the need for a PC, eliminate the need for users to configure the system, support automatic transmission of signals, lower cost, increase ease of use.</p>	Same quality of service as PC based systems at a lower cost.
13.	Hii and Chung ²⁻¹⁴	2011	Sensors (Basel)	<p>ECG, Smartphone camera (Sensors).</p> <p>The system was based on 3 layers, namely: (i) Body Sensor Layer [ECG nodes on body] (ii) Personal Network Layer [Mobile phone] (iii) Global Network Layer</p> <p>Platform: Mobile Phone</p> <p>Local-MVI communication: ZigBee</p>	<p>Mobile phone based real time ECG monitoring.</p> <p>It took advantage of the falling cost and rising complexity of mobile phones.</p>			Successful realtime monitoring on a testbed with a human subject.

				<p>Remote-MVI communication: CDMA, GSM, 3G or WiFi</p> <p>Modes: Real-time (immediately viewable on phone) or Store-and-forward (20 byte ECG data and summary reports transferred to the remote end). One ECG data packet contained 10 ECG signals (phone screen could display 5 packets, equivalent to 5s of data).</p> <p>Algorithm: Pan-Tompkins (The analysis was for QRS peaks, QT and RR intervals)</p> <p>The camera was used for scanning the QR barcodes on medicine packs.</p>	A QR code scanner was used to determine patient adherence.			
14.	Cleven et al ²⁵	2012	IEEE Transactions on Biomedical Engineering	<p>Capacitive pressure and temperature (Sensors). Measured intraarterial pressure using an implant consisting of a sensor tip and transponder communicating with a readout station.</p> <p>Local-MVI communication: Inductive coupling.</p> <p>The pressure sensor was powered using wireless magnetic telemetry.</p>	Wireless BP measurement		A batteryless system that uses an implant into the Femoral artery. The implant consists of a pressure sensor and telemetric unit and was placed under the skin.	The trial used an anesthetized sheep and readings were compared to a reference catheter. The system had an accuracy of $\pm 1.0\text{mmHg}$ and a range of 30-300mmHg.
15.	Pitts et al ²⁻¹⁶	2013	Physiological Measurements	<p>Accelerometer (Sensor).</p> <p>The algorithm was based on peak and edge detection.</p> <p>The system provided virtual sensing of respiratory rate based on the longitudinal (Z) axis reading of the accelerometer placed on the patient's clavicle.</p>	Simple low cost device for measuring respiratory rate and inferring disease if the rate falls outside the 12-20 breadth/minute rate of healthy adults.		<p>Respiratory sensor based on clavicular motion</p> <p>A clavicular sensor was used since it gave signals with a greater amplitude and which were more consistent than thoracic sensors.</p> <p>The system was tested on 8 volunteers.</p>	<p>R2 values mean clavicular respiratory rate: 0.89 (lateral) and 0.98 (longitudinal), compared to 0.49 (thoracic).</p> <p>System was unaffected by bioelectrical or electrode problems.</p> <p>A 4-min breath-by-breadth test period was used.</p>
16.	Anlike r et al ²⁻¹⁷	2004	IEEE Transactions on Information Technology in Biomedicine	<p>Blood pressure, SPO2, 1/12-lead ECG, 2-axis accelerometer, pulse, heart rate, temperature (Sensors).</p> <p>Data was encrypted using techniques inherent in GSM/GPRS.</p> <p>Algorithm: Pan-Tompkins.</p>	Unobtrusive wrist-worn multiparametric monitoring system.	Configuration was based on patient specific values: non aerobic/aerobic state (corresponding to level of user activity), age, gender, fitness and medical history.	<p>The study incorporated the patient's profile in order to reduce false alarms.</p> <p>It measured pulse and SPO2 continuously. BP and 30s of ECG were measured 3 times a day or at request of user.</p> <p>The user's health condition/equipment state was grouped into the following zones based on the results:</p>	<p>33 volunteers participated in a 70mins test.</p> <p>Results: For BP, 85% had a difference of less than 5 beats when compared to standard instruments.</p> <p>The ECG results were poor as a result of noise but other readings were ok.</p> <p>70% of users found the system comfortable.</p>

							(i) Normal (ii) Deviant (iii)Risk (iv) High Risk (v) System error																						
17.	Chung et al ²⁻¹⁸	2008	Telemedicine and e-Health	<p>Microphone- an omnidirectional electrets condenser-type (Sensor). System used the measured signals for the virtual sensing of Obstructive Sleep Apnea Syndrome (OSAS)</p> <p>System supported both monitoring and therapeutic applications. The therapeutic application involved nerve stimulation using a low frequency transcutaneous electrical signal.</p> <p>The system included a local webserver.</p> <p>Algorithm: Absolute difference between input voltage and baseline and moving average filter with a window size of 20.</p>	A portable telemonitoring device to recognize sleep-related breathing disorders in real-time	Configuration was based on the detection of a snoring pattern. The detection triggered a system configuration that stimulated the patient's nerve in order to stop the snoring.	5 regular snorers and 5 OSAS patients tested the system.	<p>There was a positive predictivity of 94% and a snoring sensitivity of 94%.</p> <p>The results indicated an OSAS positive predictivity and sensitivity of 73.3% and 81.1% respectively.</p>																					
18.	Chun et al ²⁻¹⁹	2005	Studies in Health Technology and Informatics	<p>Non-Invasive Blood Pressure [NIBP], SPO2, 1-channel ECG textrode electrode, Respiratory Rate [RR], Heart Rate [HR], Body surface temperature, Accelerometer, Posture (Sensors).</p> <p>RR and HR were virtual sensors based on ECG signals.</p> <p>Local-MVI communication: Wireless Remote-MVI communication: sms, cellular</p> <p>The expanded system (Integrated Home Telecare System) comprised the following sensors: 12-channel ECG, Respiratory function, Blood glucose, NIBP, Body fat meter and Spirometer.</p>	Personal Wearable Wristworn Integrated Health Monitoring Device (WIHMD)	<p>System was configured based on patient's diabetic history and postprandial time.</p> <p>The BP tests also considered the patient's history.</p>	<p>The primary system was based on the WIHMD.</p> <p>The secondary system had a number of non intrusive sensors used on the bed, toilet seat and chair. Capacitive sensors were used for the chair.</p> <p>10 volunteers tested the system and authors also used simulations.</p>	<table border="1"> <thead> <tr> <th>Simulation</th> <th>Tests</th> <th>Results</th> </tr> </thead> <tbody> <tr> <td>NIBP</td> <td>100</td> <td>± 4 mmHg</td> </tr> <tr> <td>SPO2</td> <td>100</td> <td>±2%</td> </tr> <tr> <td>HR</td> <td>100</td> <td>±0.9%</td> </tr> <tr> <td>RR</td> <td>50 people</td> <td>±1.8%</td> </tr> <tr> <td>Temp*</td> <td>20</td> <td>±1.5</td> </tr> <tr> <td>Fall#</td> <td>150</td> <td>91.3% #</td> </tr> </tbody> </table> <p>*: Tested in temperature controlled chamber #: Detection rate for simulated falls</p>	Simulation	Tests	Results	NIBP	100	± 4 mmHg	SPO2	100	±2%	HR	100	±0.9%	RR	50 people	±1.8%	Temp*	20	±1.5	Fall#	150	91.3% #
Simulation	Tests	Results																											
NIBP	100	± 4 mmHg																											
SPO2	100	±2%																											
HR	100	±0.9%																											
RR	50 people	±1.8%																											
Temp*	20	±1.5																											
Fall#	150	91.3% #																											
19.	Yu et al ²⁻²⁰	2013	Telemedicine and e-Health	<p>Temperature, mobile phone camera and microphone (Sensors)</p> <p>System used a mobile phone as a miniaturized health exam toolkit.</p> <p>Electronic health records were sent to remote server as e-mails or mms messages.</p> <p>Local-MVI communication: Wireless Remote-MVI communication: Cellular</p> <p>Algorithms: Machine learning</p> <p>System carried out tests for about 12 parameters used in annual physical exams</p>	Mobile phone based system for convenient "annual physical exam".		<p>Eye tests were based on image sizes on phone and feedback from users.</p> <p>The system was trained as follows: 3 deep breaths (for breadth sound), 1 minute data (for heart sound, temperature and ECG).</p> <p>There were 11 volunteers for the test.</p>	The entire test took just about 28 minutes.																					
20.	Fong	2013	Sensors	Platform: Android based phone	Cloud-based Non-	The system	The measurements	The results measured the																					

	and Chung ²⁻²¹		(Basel)	<p>ECG, Heart Rate, Camera (Sensors)</p> <p>Data was shared over the Internet instantaneously using the embedded webserver.</p> <p>Local-MVI communication: Bluetooth communication between capacitive coupled ECG sensor and phone.</p> <p>Inter-MVI communication: WiFi</p> <p>HR was calculated using a virtual sensor based on ECG.</p>	contact ECG monitoring and a QR code based patient adherence scheme.	supported a minimal level of adaptation based on QR code.	required the patient to seat on a chair with capacitive sensors.	website loading times as follows: 1st view load time (2.833ms), repeat view time (0.124ms), the Document Complete parameter, which occurs after all the images content have been loaded (2.833s), the Fully Loaded parameter, which includes any activity triggered by the JavaScript (6.452s).
21.	Giansanti et al ²⁻²²	2013	Telemedicine and e-Health	<p>Sensors: Gastrocnemius Expansion Measurement Unit (GEMU), gyroscope, accelerometer, SECOSP (a step counter)</p> <p>Platform: Custom portable device</p>	Real-time simple portable kit for home-based gait analysis.		<p>The portable kit works with a cascade of Instrumented Walkways (IWs). It also uses walking aids.</p> <p>16 subjects tested the system.</p>	System has a high level of accuracy and costs 948EUR.
22.	Gomez et al ²⁻²³	2008	IEEE Transactions on Information Technology in Biomedicine	<p>Realtime Continuous Glucose Monitoring (CGM) sensor.</p> <p>Platform: PDA (iPAQ hp2210)</p> <p>Local MVI: Bluetooth, Infrared or serial communication</p> <p>Remote MVI: Mobile GPRS for communication to the Telemedicine Central Server (TMCS).</p> <p>The system supports a therapeutic application- the control of an insulin pump.</p>		The PDA was remotely programmed by the TCMS under the doctor's supervision. The insulin pump was configured and controlled remotely in response to the measured CGM values	<p>CGM with real-time programmable insulin pumps.</p> <p>4 system control strategies: (i) Patient control: Manual change supervised by doctor (ii) Doctor control: Come as suggestions that the patient should download and approve (iii) Remote loop control: Programmed by the TCMS under the doctor's supervision. (iv) Personal loop control: Real-time control of the insulin pump based on glucose sensor data</p> <p>The patient has to issue e-consents (digitally signed certificates) before personal data can be accessed.</p>	<p>Only control strategies #1 and #2 were tested and the measured HbA1c values confirmed the effectiveness of the strategy</p> <p>System cost: 7,348 EUR (compared to 5,907 EUR for a CGM system based on a manual approach).</p>

							Feasibility testing phase: 4 Type 1 diabetic patients for 6 months.	
							Clinical testing phase: 10 Type 1 patients for 8 weeks.	
23.	D'Arcy et al 2-24	2011	IEEE Transactions on Biomedical Engineering	EEG sensor. A headset for auditory stimulation. Local-MVI Communication: Bluetooth The algorithm was known as called Halifax Consciousness Scan (HCS). It was based on preprocessing, peak detection and score generation	An approach for replacing the behavioral brain tests with one based on EEG signals. The test provides indicators for 5 identifiable levels of neural processing: sensation, perception, attention, memory and language	The specific parameters of the patient are compared to a normative database.	The portable EEG device for scanning for consciousness awareness addressed 5 challenges/areas: (i) Portability and noise resistance (ii) It has no need for advanced expertise or system training (iii) Addressed the spectrum of EEG-cortical responses (iv) Compared results to a normative database (v) The range of results covered diagnosis, reliability, validity and progression	The authors attempted to provide a solution at the interface between biomedical engineering and neuroscience.
24.	Chen et al 2-25	2008	Physiological Measurements	A pressure sensor was embedded in a pillow for static and dynamic pressure measurements. Wavelet based algorithms were used. Virtual sensing of the pressure was used to reconstruct pulse related waveform information from D4 & D5 components of wavelet transformation. Also, breadth related waveform was reconstructed from the A6 component.	Web-based long term heart and breath rate monitoring during sleep using a single sensor.		The raw pressure was measured under the neck-neck occiput region. The system measures static pressure (based on weight of head) and dynamic pressure (based on fluctuations caused by breathing). Analysis was based on the dynamic pressure. 1 patient was used to test the system over a period of 6 months	The system detected 82.3% of sleep time. The system provided a cheap 1 sensor alternative to replace the traditional \$1,000 11-sensor polysomnography equipment
25.	Nemir oskia et al 2-26	2014	Proceedings of the National Academy of Sciences, USA	A portable system that includes a vibration meter and an audio jack. This system interfaces with a low end mobile phone (Nokia 1100 series model 1112) and can also support 2G, 3G and 4G systems. The system uses a webserver to "geographically decouple" the measurement.	It is an inexpensive device that couples most forms of electrochemical	The system can switch between the following modes: (i) 2 or 3 electrode system.	The system supports cyclic voltammetry, differential phase voltammetry, square wave voltammetry and potentiometry	The system cost just \$25. It is a simple system, much unlike complex microfluidic based system. Latency (transmit and receive) for the blood glucose application was just 2.2s.

				<p>Local-MVI communication: Standard audio cable.</p> <p>Remote-MVI communication: Cellular (based on a live voice link through VoIP Skype between the phone and remote system).</p> <p>The remote server decodes the Frequency Shift Keying (FSK) data and sends an acknowledgement to the phone as an sms to verify the measured value.</p>	<p>analysis directly to the cloud.</p> <p>It uses a handheld device that works in a resource-constrained environment.</p>	<p>(ii) Amperometric (iii) Potentiometric</p> <p>The system can also be configured to accommodate new assays, sequences and standards</p>	<p>It supports low-end phones and does not require apps that are usually required for Smartphone based systems.</p> <p>The proof of concept was demonstrated in 4 application domains: (i) Blood glucose (ii) Trace heavy metals (iii) Sodium in urine and (iv) Test for malaria antigens</p>	<p>The system results for the 4 application domains were compared to results from a commercial bench-top analyzer and the following results were obtained:</p> <p>(i) No difference with respect to performance of the electronics. (ii) Blood glucose standard deviation: 5% (which is much better than most commercial glucometers). (iii) Heavy metals in water: Detection limit of 4μg/L, better than the recommended WHO level of 10μg/L (iii) Sodium in urine: Systematic error of 8%, which is within the certified range of \pm14% (iv) Malaria: Limit of detection was 20ng/mL.</p>
26.	Lee et al ²⁻²⁷	2010	Telemedicine and e-Health	<p>Sensors: Electrodermal Activity [EDA], Pulsewave [Condenser microphone].</p> <p>The EDA sensor was made of conducting fabric lines (instead of AgCl).</p> <p>Platform: Portable arm-band computer</p> <p>Realtime processing supported by a webserver.</p> <p>Local-MVI communication: Serial (RS-232).</p> <p>The algorithm was based on Fast Fourier Transform (FFT).</p>	<p>A system to detect drowsiness based on a correlation between EDA signals and drowsiness.</p>		<p>The system investigated the correlation between skin impedance and drowsiness.</p> <p>The EDA signal was decomposed into 2 signals: (i) Skin Impedance Level (SIL) and (ii) Skin Impedance Response (SIR)</p> <p>The experiment lasted for 30mins.</p>	<p>The detected states: - Aroused condition - Drowsiness - Sleeping</p> <p>The device was able to detect drowsiness before its onset.</p>

저작물 이용 허락서					
학 과	컴퓨터공학과	학 번	20097789	과 정	박사
성 명	아델루이 올루페미 올루월이 ADELUYI OLUFEMI OLUWOLE				
주 소	Chosun University Priv Dorm				
연락처	e-mail : femiadeluyi@yahoo.com				
논문제목	<p style="text-align: center;">한글 : 신뢰할 수 있는 개인 건강 모니터링을 위한 경량 알고리즘의 설계</p> <p style="text-align: center;">영문 : Lightweight Algorithms for Reliable Personalized Health Monitoring</p>				
<p>본인이 저작한 위의 저작물에 대하여 다음과 같은 조건 아래 조선대학교가 저작물을 이용할 수 있도록 허락하고 동의합니다.</p> <p style="text-align: center;">- 다 음 -</p> <ol style="list-style-type: none"> 1. 저작물의 DB구축 및 인터넷을 포함한 정보통신망에의 공개를 위한 저작물의 복제, 기억장치에의 저장, 전송 등을 허락함 2. 위의 목적을 위하여 필요한 범위 내에서의 편집과 형식상의 변경을 허락함(다만, 저작물의 내용변경은 금지함) 3. 배포·전송된 저작물의 영리적 목적을 위한 복제, 저장, 전송 등은 금지함 4. 저작물에 대한 이용기간은 5년으로 하고, 기간종료 3개월 이내에 별도의 의사 표시가 없을 경우에는 저작물의 이용기간을 계속 연장함 5. 해당 저작물의 저작권을 타인에게 양도하거나 출판을 허락을 하였을 경우에는 1개월 이내에 대학에 이를 통보함 6. 조선대학교는 저작물 이용의 허락 이후 해당 저작물로 인하여 발생하는 타인에 의한 권리 침해에 대하여 일체의 법적 책임을 지지 않음 7. 소속 대학의 협정기관에 저작물의 제공 및 인터넷 등 정보통신망을 이용한 저작물의 전송·출력을 허락함 <p style="text-align: center;">동의여부 : 동의(0) 반대()</p> <p style="text-align: center;">2015 년 8 월 24</p> <p style="text-align: center;">저작자 : Adeluyi Olufemi Oluwole (인)</p> <p style="text-align: center;">조선대학교 총장 귀하</p>					



저작자표시-비영리-변경금지 2.0 대한민국

이용자는 아래의 조건을 따르는 경우에 한하여 자유롭게

- 이 저작물을 복제, 배포, 전송, 전시, 공연 및 방송할 수 있습니다.

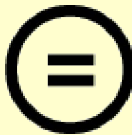
다음과 같은 조건을 따라야 합니다:



저작자표시. 귀하는 원저작자를 표시하여야 합니다.



비영리. 귀하는 이 저작물을 영리 목적으로 이용할 수 없습니다.



변경금지. 귀하는 이 저작물을 개작, 변형 또는 가공할 수 없습니다.

- 귀하는, 이 저작물의 재이용이나 배포의 경우, 이 저작물에 적용된 이용허락조건을 명확하게 나타내어야 합니다.
- 저작권자로부터 별도의 허가를 받으면 이러한 조건들은 적용되지 않습니다.

저작권법에 따른 이용자의 권리는 위의 내용에 의하여 영향을 받지 않습니다.

이것은 [이용허락규약\(Legal Code\)](#)을 이해하기 쉽게 요약한 것입니다.

[Disclaimer](#)

August 2015

PhD Thesis

Lightweight Algorithms for Reliable Personalized Health Monitoring

Graduate School of Chosun University

Department of Computer Engineering

Olufemi Oluwole Adeluyi

신뢰할 수있는 개인 건강
모니터링을위한 경량 알고리즘의
설계

2015 년 8 월 25 일

조선대학교 대학원

컴퓨터학과

아델루이 올루페미 올루월이

Lightweight Algorithms for Reliable Personalized Health Monitoring

Advisor: Prof Jeong-A Lee

**This Thesis is submitted to the Graduate School of Chosun
University in partial fulfillment of the requirements for
the award of a PhD degree**


2015 년 4 월


Graduate School of Chosun University


Department of Computer Engineering


Olufemi Oluwole Adeluyi

Olufemi Oluwole Adeluyi 의 박사학위논문을 인준함

위원장 조선대학교 교수 모상만 

위 원 조선대학교 교수 이지은 

위 원 조선대학교 교수 문인규 

위 원 전남대학교 교수 김철홍 

위 원 조선대학교 교수 이정아 

2015년 6월

조선대학교 대학원

Dedication

*I dedicate this thesis to my darling wife- Ese and
wonderful children- Daniel and Gabrielle. Your
unflinching support and sacrifice gave me strength
for the journey. Thank you very much.*

Acknowledgements

I will start by acknowledging the role of my Advisor- Prof. Jeong-A Lee. Her mentorship, support and belief played an important role in my research journey. I deeply appreciate all her help.

I am grateful to my professors and the members of my thesis committee (professors Sangman Moh, Inkyu Moon, Jieun Lee and Cheol-Hong Kim) for their guidance and support. I also wish to thank Prof. Kiseon Kim of the Gwangju Institute of Science and Technology (GIST) for his great support in my EEG research.

I thank my labmates for their camaraderie. My family and I made many friends during my PhD program and this made Korea a home away from home. I am also grateful to the management team of the National Information Technology Development Agency (NITDA) for their support.

On a personal note, I would like to thank my parents, parents-in-law and siblings for their immense support and encouragement. I am also grateful for the encouragement that I received from my relatives and friends that reside outside Korea.

I am very grateful to my wife- Ese and children- Daniel and Gabrielle. Their love, sacrifice and presence enabled me to endure the challenging seasons.

I wish to conclude by giving great thanks to God for his wisdom and wonderful support.

Table of Contents

Dedication	i
Acknowledgements	ii
Table of Contents	iii
List of Tables	v
List of Figures	vi
Abbreviations	vii
Abstract	x
요 약	xii
I. Introduction	1
A. Overview	1
B. Motivation	5
C. Contributions	7
D. Thesis Outline.....	7
II. Related Work	8
A. Medical Instrumentation.....	8
B. Analysis of Search Results	10
C. PHM: Key Issues and Prospects.....	23
D. Application of the Information to this Thesis.....	25

III. A Bioinspired Algorithm for Lightweight Neural Telemetry	26
A. Telemonitoring of Neural Signals	29
B. The Basics of Electroception.....	29
C. Bio-inspired electroreceptive Compressive System (BeCoS).....	31
D. System Model and Performance Metrics	33
E. Porting Key Electroceptive Features into BeCoS	37
F. Results	43
IV. R-READER: An Algorithm for Lightweight Detection of Fiducial	
Points in the Cardiovascular Domain	59
A. Detection of R-peaks in ECG Signals	59
B. The R-READER Process.....	65
C. Performance.....	71
V. Conclusion and Future Work.....	76
A. Conclusion.....	78
B. Future Work.....	79
Refernces.....	80
Appendix A	91

List of Tables

(Table 1) Sensors used for PHM.....	11
(Table 2) Examples of Virtual Sensing in PHM	13
(Table 3) Monitoring Scenarios for the Cardiovascular Disease Domain	17
(Table 4) Common Algorithms used in MVIs	21
(Table 5) Comparison of BSBL-BO and BeCoS Coherence Values.....	44
(Table 6) Comparison of BSBL-BO and BeCoS Compression Ratios	46
(Table 7) Comparison of the Power and FPGA Resource Utilization for the BO and BeCoS Core Engines	48
(Table 8) Comparison of BSBL-BO and BeCoS CW-SSIM	51
(Table 9) Effect of Numerical Methods on Signal Reconstruction.....	53
(Table 10) R-peak Points in R-READER and Annotation for Record #100.....	73
(Table 11) R-peak Points in R-READER and Annotation for Record #108.....	74
(Table 12) Accuracy of the R-READER Algorithm	75

List of Figures

(Figure 1) A Typical PHM System.....	1
(Figure 2) Location of PHM Systems on Healthcare Delivery Research Space.....	2
(Figure 3) OECD ALE at Birth (1970-2011).....	3
(Figure 4) Healthcare Cost as a % of GDP.....	4
(Figure 5) Search Strategy.....	9
(Figure 6) Platforms used in MVIs.....	13
(Figure 7) Communication Protocols used for PHM at the Patient-end.....	15
(Figure 8) Remote-PHM Communication Protocols.....	16
(Figure 9) Disease Domains.....	16
(Figure 10) Examples of Signature Signals used for Electroreception.....	Error! Bookmark not defined.
(Figure 11) BeCoS Sensing Approach.....	31
(Figure 12) Conceptual Diagram of the BeCoS System Model.....	33
(Figure 13) System Diagram for Testing Models: (a)BSBL-BO and (b) BeCoS.....	35
(Figure 14) Steps for generating an optimized signature signal.....	Error! Bookmark not defined.
(Figure 15) Coherence across the frequency spectrum.....	45
(Figure 16) Top level block diagram of the BeCoS compression engine.....	47
(Figure 17) Top level block diagram of the BSBL-BO compression engine.....	48
(Figure 18) CW-SSIM for Ch7 [1:700].....	52
(Figure 19) CW-SSIM for Ch1 [3000:3650].....	52
(Figure 20) CW-SSIM for Ch4 [6300:6900].....	53
(Figure 21) Effect of Numerical Methods on Signal Reconstruction.....	55
(Figure 22) A Model of the Variatio Generated by Numerical Methods.....	56

(Figure 23) The Effect of Variation on SSIM	57
(Figure 24) The Effect of Variation on CW-SSIM.....	57
(Figure 25) A Typical ECG Signal Showing the Fiducial Points.....	60
(Figure 26) Steps in the Pan & Tompkins Algorithm	62
(Figure 27) R-READER's Selection of Fiducial and R-peak points for Record #100	66
(Figure 28) Flowchart of Steps in the R-READER Process	69
(Figure 29) Accuracy Comparison for the 2 Algorithms	76
(Figure 30) +P Comparison for the 2 Algorithms	76
(Figure 31) Se Comparison for the 2 Algorithms	77

Abbreviations

AAL: Ambient Assisted Living
 AC: Alternating Current
 ADC: Analog to Digital Converter
 ADL: Activities of Daily Life
 BAN: Body Area Network
 BeCoS: Bioinspired electroceptive Compressive System
 BP: Blood Pressure
 BRAM: Block Random Access Memory
 BSBL-BO: Block Sparse Bayesian Learning-Bound Optimization
 BT: Bluetooth
 CLB: Configurable Logic Block
 CPU: Central Processing Unit
 CS: Compressive Sensing
 CVD: Cardiovascular diseases
 CW-SSIM: Complex Wavelet Structural Similarity Index
 DAC: Digital to Analog Converter
 DCT: Discrete Cosine Transform
 DICOM: Digital Imaging and Communications in Medicine
 ECG: Electrocardiography
 EEG: Electroencephalography
 FF: Flip Flop
 FN: False Negatives
 FP: False Positives
 FPGA: Field Programable Gate Arrays
 GA: Genetic Algorithm
 GSM: Global System for Mobile Communications
 HR: Heart Rate
 I/O: Input/Output
 IOB: Input Output Blocks
 ICU: Intensive Care Unit
 LRV: Linear Regression Variation
 LUT: Look Up Table
 MVI: Medical Virtual Instrument
 NN: Neural Networks
 OECD: Organisation for Economic Co-operation and Development
 p-a-i-d: peak-adjacency-interval-detector
 PAN: Personal Area Network
 PHM: Personalized Health Monitoring
 P-T: Pan-Tompkins
 RAM: Random Access Memory
 R-READER: Rapid-Ramp Effective Algorithm for Detection of ECG R-peaks
 ROM: Read Only Memory

SBA: Simple Bus Architecture
SOC: System On Chip
SpO₂: Saturation of Peripheral Oxygen
SVM: Support Vector Machine
TN: True Negatives
TP: True Positives
VCD: Value Change Dump
WAN: Wide Area Network
WT: Wavelet Transform

Abstract

Lightweight Algorithms for Reliable Personalized Health Monitoring

By: Olufemi Oluwole Adeluyi

Advisor : Prof Jeong-A Lee, Ph. D

Department of Computer Engineering

Graduate School of Chosun University

Patient monitoring techniques are fast evolving from the traditional curative, doctor-centered approach to one that is preventive and patient-centered. A number of factors have influenced this transition; notable among these are the spiraling costs of healthcare management, the ageing of society and the advances in sensor technology. Personalized Health Monitoring Healthcare (PHM) systems play an important role in this new approach.

PHM systems are usually implemented in resource constrained environments such as embedded systems running on limited battery power. As such, any algorithm used for diagnosing and classifying diseases should be lightweight and reliable.

The cardiovascular and neurologic domains were used for the analysis in this thesis. For the neurologic domain we proposed an algorithm known as Bio-inspired electroceptive Compressive System (BeCoS). BeCoS was inspired by wave-type active electroreception used by weakly electric fish. It was used for the sensing, processing, telemetry and reconstruction of neural signals. BeCoS was compared with the well regarded Block Sparse Bayesian Learning-Bound Optimization (BSBL-BO) and it gave higher quality results. BeCoS resulted in coherence, average latency, compression ratio and estimated per epoch power values that were 35.38%, 62.85%, 53.26% and 13mW better than BSBL-BO, respectively, while structural-similarity was only 6.295% worse. The original and reconstructed signals still remain visually similar.

The identification of the R-peaks of electrocardiograms (ECG) represents one of the most important steps for the successful monitoring of cardiovascular health. The Pan-Tompkins (P-T) algorithm has been used as a key reference in the design and testing of algorithms used for the detection of R-peaks. The P-T algorithm uses a cascade of filters to process the ECG signals prior to the identification of the R-peaks. This filtration process results in a large overhead. A Rapid-Ramp Effective Algorithm for Detection of ECG R-peaks (R-READER) has been proposed as an alternative to P-T. It is an intuitive algorithm that uses ECG slopes and inflexion points as a basis for the identification of R-peaks without the need to pass the signals through the filters used in traditional approaches. R-READER gave average accuracy, positive predictivity and sensitivity values of 97.79%, 98.23% and 99.54% when compared to values of 87.47%, 88.57% and 98.59% for the P-T algorithm.

In this dissertation we demonstrate that the BeCoS and R-READER algorithms provide reliable and lightweight alternative for health monitoring in the neurologic and cardiovascular domains respectively. Experimental results also demonstrate a potential for significant performance enhancements when compared to the main algorithms used in the domains.

[KEYWORDS]: personalized health monitoring, reliable computing, lightweight processing, electrocardiogram, encephalogram

요 약

신뢰할 수 있는 개인 건강 모니터링을 위한 경량 알고리즘

아델루이 올루페미 올루월이

지도교수 : 이정아

컴퓨터공학과

조선대학교 대학원

환자 모니터링 기술은, 의사 중심적인 치료 위주의 전통적 접근법에서, 환자 중심적인 예방 위주의 새로운 접근법으로 빠르게 진화하고 있다. 헬스케어 관리 비용의 증가, 사회의 노령화와 센서 기술의 발달 등이 이러한 변화에 영향을 미치는 요소들이다. 개인 맞춤형 건강 모니터링 헬스케어 (PHM) 시스템은 이러한 새로운 접근법에서 중요한 역할을 하고 있다.

제한된 배터리 전력으로 작동하는 embedded 시스템과 유사하게, PHM 시스템은 통상적으로 자원이 제한된 환경에서 구현 되기 때문에, 질병을 진단하고 분류하는 알고리즘은 신뢰성은 물론이고, 연산처리량이 가벼워야 한다.

본 논문에서는 신경계 및 심혈관 영역에서 신뢰성을 유지하면서도 연산처리량을 가볍게 하는 알고리즘을 제안한다. 신경계 영역에서는 Bio-inspired electroceptive Compressive System (BeCoS)라는 알고리즘을 제안한다. BeCoS의 개념은 약한 전기를 사용하는 어류의 파동형(wave-type) 활성 전기인식(electroreception)에서 착안하였다. 이 알고리즘은 신경 신호의 감지, 처리, 원격 측정 그리고 신호 복원을 위해 사용되었다. BeCoS 알고리즘은 잘 알려진 Block Sparse Bayesian Learning-Bound Optimization (BSBL-BO)와 비교했을 때 보다 높은 품질의 결과를 제공하였다. BeCoS는 BSBL-BO보다 62.85% 증가한 일관성, 35.38% 감소한 평균 처리시간, 53.26% 증가한 압축비, 13mW 감소한 추정 epoch 당 전력값을 보였고, 구조적 유사성에서는 6.295% 감소하였지만, 원래 신호와 복원된 신호는 시각적 유사성을 유지했다.

심혈관 영역에서는, 심혈관 건강의 성공적 모니터링에 가장 중요한 단계들 중 하나인, 심전도 R-peaks의 검출에 중점을 두었다. 주요 비교대상으로 Pan-Tompkins (P-T) 알고리즘을 활용하면서, R-peaks을 찾기 위한 경량 알고리즘을 설계하고 실험하였다. P-T 알고리즘은 R-peaks의 확인 이전에 ECG 신호를 처리하기 위해 연속적인 필터를 사용하는데, 이 과정이 큰 오버헤드(overhead)를 초래한다. 본

논문에서는 P-T 알고리즘의 대안으로 ECG R-peaks 의 발견을 위한 Rapid-Ramp Effective 알고리즘, R-READER 를 제안한다. R-READER 는 R-peaks 검출 기반으로, 전통적 접근법이 사용하는 필터가 아닌, ECG 의 기울기와 만곡점(inflexion point)을 사용하는 직관적 알고리즘이다. R-READER 는, P-T 알고리즘이 보인 각각 87.47%, 88.57%, 그리고 98.59%의 평균 정확성, 긍정적 예측도 그리고 감도 값과 비교할 때, 각각 97.79%, 98.23% 그리고 99.54% 값을 제공했다.

본 논문에서는, 신경계 및 심혈관 영역에서의 건강 모니터링을 위하여, 신뢰성을 유지하면서도 연산처리량이 가벼운 대안으로 BeCoS 와 R-READER 알고리즘을 제시하였으며, 이 영역들에서 사용된 기존의 주요 알고리즘과 비교해 보았을 때, 제시된 BeCoS 와 R-READER 알고리즘의 성능이 향상됨을 실험 결과를 통하여 보였다.

[KEYWORDS]: 개인 맞춤형 건강 모니터링(PHM), 신뢰할 수 있는 계산, 경량 프로세싱, 심전도, 뇌파기록

I. Introduction

A. Overview

Health monitoring refers to a systematic approach for keeping track of the health status of any given entity. It can refer to both animate and inanimate objects. For example, the process of monitoring the degradation of infrastructure like bridges and buildings falls under this category, as does the process of monitoring the health of a human being. The former is usually referred to as structural health monitoring (SHM) [1], while the latter is called personalized health monitoring (PHM) [2].

In this thesis, PHM refers to the process of using wearable sensors to monitor a patient's biosignals over an extended period in order to track, predict and maintain their health. PHM usually takes place in uncontrolled environments outside the confines of a hospital [3, 4]. It is more useful for monitoring signals that change over time rather than those that rarely change or those that do not change such as a patient's genotype. Fig 1 shows the common parts of a PHM system.

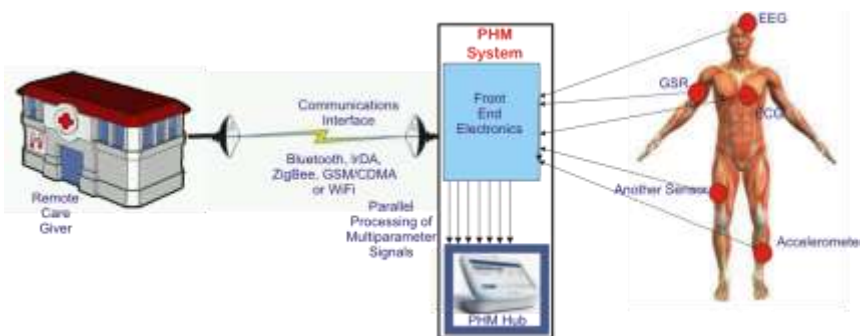


Figure 1: A Typical PHM System

The global healthcare industry has evolved from one that places an emphasis on a curative, doctor-centered healthcare approach to a patient-centered approach that focuses on prevention [5, 6]. This paradigm shift has increased the importance of diagnostic health monitoring and has played a role in making PHM a core part of today’s healthcare delivery system. Fig 2 shows the approximate location of PHM systems in the healthcare delivery research space; toward the top ends of preventive and automated medicine.

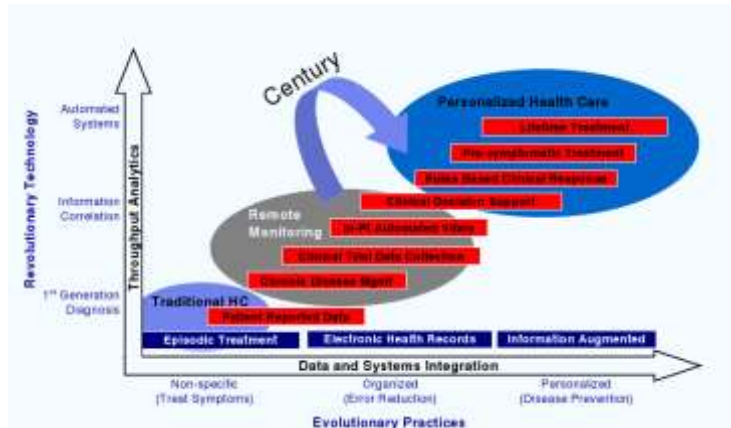


Figure 2: Location of PHM Systems on the Healthcare Delivery Research Space [7]

In addition to the effect of the paradigm shift, three (3) main developments have led to the popularity of PHM:

1. The Rapid Ageing of Society
2. The Rising Cost of Healthcare and the Dwindling Budgets
3. The Availability of Cost-effective Enabling Technologies

The Rapid Ageing of Society

Recent demographic studies have indicated an increase in the Average Life Expectancy (ALE) in many developed countries. As shown in Fig 3, the 2011 ALE at birth for countries in the Organisation for Economic Co-operation and Development (OECD) is now 80.1 years [8]. This represents an average increase of 10.1 years from 1970, with the Republic of Korea and

Turkey having the largest individual increase of 19.0 and 20.4 years respectively.

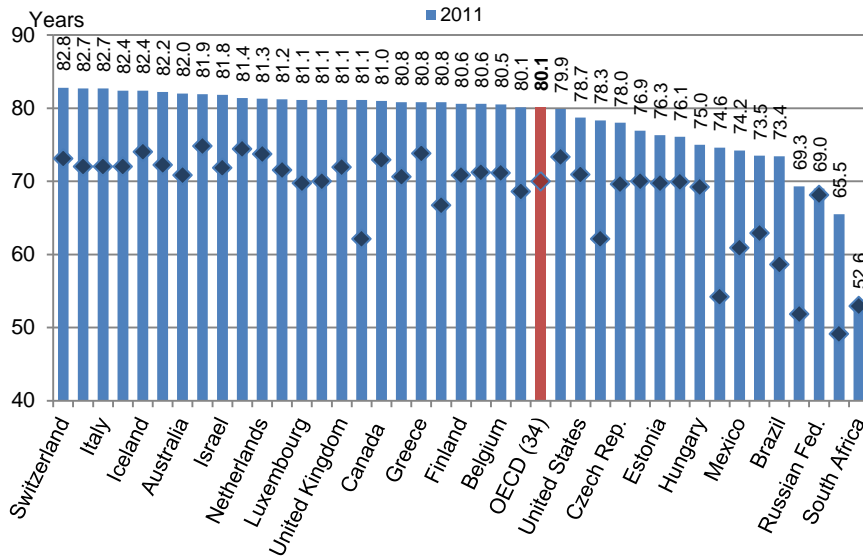


Figure 3: OECD ALE at Birth (1970-2011) [8]

The Rising Cost of Healthcare and the Dwindling Budgets

Healthcare is traditionally perceived as a key determinant of the general quality of life of people and it usually forms a significant part of a country's economy [9]. As shown in Fig 4, there has been a steady increase in the amount of healthcare costs as a percentage of GDP. In 2009, the average share of the total healthcare expenditure as a part of GDP in OECD countries was 9.6%. The United States, Netherlands, Italian and Korean GDP shares were 17.7%, 11.9%, 9.2% and 7.4% respectively [8].

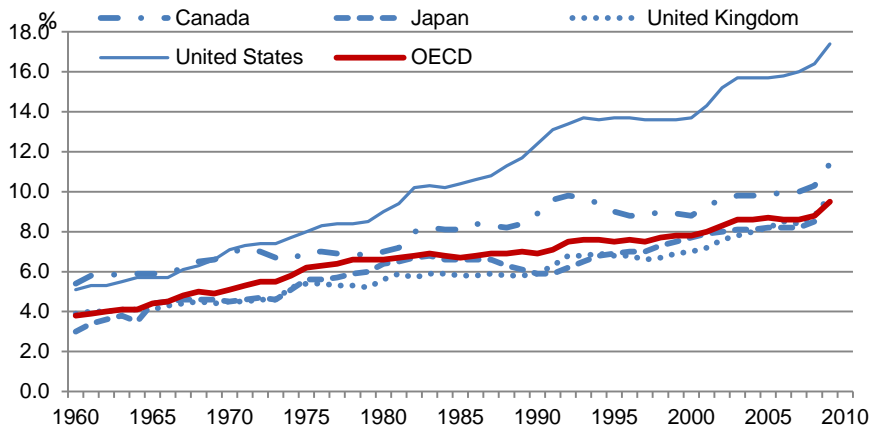


Figure 4: Healthcare Cost as a % of GDP [10]

This increase has not led to a rise in healthcare budgets as many governments have adopted a more frugal approach to government spending in virtually every sector of the economy, including the healthcare sector. For example, in the United Kingdom there was a shortfall of 630million GBP in the 2013/2014 budget for the National Health Scheme (NHS) [11]. Many governments now view the use of technology as a viable option for reducing healthcare costs [12].

The Availability of Cost-effective Enabling Technologies

Recent technological advances in areas such as the sensors, memory, wireless communication and digital signal processing have aided the deployment of PHM systems [13, 14]. Semiconductor technologies like Micro-Electro-Mechanical Systems (MEMS) and Nano-Electro-Mechanical-Systems (NEMS) have also enabled the design of devices with high levels of functionality and miniaturization [15]. As a result of these advances, sensors and actuators have become smaller, cheaper, more sensitive and less power hungry [16].

B. Motivation

Current PHM systems have been generally limited to fitness applications and do not play a significant role in clinical decision making [17, 18]. This is because a number of the systems do not provide the level of reliability required of standard medical systems [19]. Current PHM systems also focus on intermittent monitoring and detection of abnormal signals rather than on the continuous long term monitoring of the entire signals as is common in standard devices at the hospital [20, 21].

PHM systems, unlike their hospital-based equivalents, have to operate under a number of resource constraints [22]. Many PHM systems use batteries to meet their energy requirements [23] and these batteries would be easily depleted when the systems are designed to support long term monitoring and more reliable analysis.

In addition to pattern recognition and disease classification, PHM systems need to support the telemetry of the signals to the physician [24]. These wireless systems usually have limited bandwidths and may experience interference. This would increase the amount of *latency* required to transmit the signals and would restrict the system's ability to support real time monitoring.

PHM systems have a limited storage capacity but they process biosignals, many of which have a high temporal resolution [25]. This leads to very big datasets which require a large amount for storage sometimes beyond the storage capacity of the systems. These challenges have led to research efforts that are aimed at developing PHM systems whose computational requirements are more sensitive to the resource constraints. Such systems should be lightweight in terms of their power, storage and latency profiles.

The algorithms for processing and classifying the signals play an important role in determining the level of complexity of the PHM systems [26, 27]. As such, a proper design of the algorithms is a suitable approach for ensuring that the systems are lightweight. Physicians base their decisions on inferences drawn from the biosignals of the patients. For PHM systems to be reliable they must provide results that are similar to the results obtained by using standard medical devices. Reliability refers to the ability of a system to deliver a service that can justifiably be trusted and the ability to avoid failures that are more frequent and more severe than is acceptable [28, 29].

As a result of the sensitive nature of healthcare, the ultimate decision of the medical choices that are made lies with the physicians. However, a lot will depend on the reliability of the data that is made available to them by the PHM systems.

Ideally PHM systems can be used to monitor signals from any part of the human body. However, this research will focus on two key domains- cardiovascular and neurologic. The cardiovascular domain was selected because it is the leading cause of global deaths. In 2012, it accounted for 17.5 million deaths- 31% of the total number of global deaths [30].

Neurologic disorders now constitute a significant global disease burden [31] and they account for 35% of the global disease burden. An estimated cost of 798 billion EUR was spent on this burden in Europe in 2010 [32]. As a result of its growing importance a number of research efforts around the world now focus on reducing this burden [33, 34].

The research presented in this thesis deals with issues involving lightweight processing and reliability of PHM systems in general, with a greater emphasis on PHM systems in the cardiovascular and neurologic domains.

C. Contributions

In this thesis, we have described a suite of lightweight algorithms for reliable personalized health monitoring. The main contributions are as follows:

- A systematic analysis of the present state, inhibiting challenges and future outlook of medical instrumentation in personalized health monitoring
- Identification of key requirements for lightweight and reliable personalized health monitoring
- Design of a bioinspired lightweight and reliable multichannel algorithms for continuous long term monitoring of neural signals
- Design of an intuitive lightweight and reliable algorithm for continuous long term monitoring of the main fiducial point in cardiovascular signals

D. Thesis Outline

The rest of this thesis is organized as follows: A systematic review of the current body of work on PHM is given in Chapter 2. It identifies the key disease domains, sensors, platforms, algorithms, communication protocols and challenges of PHM systems.

Chapter 3 describes BeCoS- an algorithm for the lightweight sensing, processing, transmission and reconstruction of neural signals. The R-READER algorithm is described in Chapter 4. It is a lightweight approach for identifying the R-peaks of an ECG signal without a need for the noise filtering used in traditional techniques. The conclusions and proposed future work are given in Chapter 6.

II. Related Work

A. Medical Instrumentation for PHM

PHM systems aim to attain a level of reliability comparable to the reliability of medical instruments based at the hospital. Insights on the key requirements for these PHM systems was gained from a systematic literature search that focused on the present state, inhibiting challenges and future outlook of medical instrumentation used for personalized health monitoring.

A total of 915 main articles were reviewed from a search on instrumentation and health monitoring that covered the following databases- Cochrane Library (1992 – August 2014: 40 articles were selected), Web of Science (1973 – August 2014: 233 articles were selected) and MEDLINE (1996 – August 2014: 642 articles were selected). The objective of this systematic review is to give an overview of the current body of work covering instrumentation used for personalized health monitoring.

The emphasis is on the identification of key architectures used for such systems in terms of the type of sensors, modality, type of communication interface and network model. Second, it describes the important application domains of PHM, its level of adaptation and the common algorithms utilized. Third, it outlines the key outcomes of PHM systems, as well as the current challenges and the anticipated future research directions for the field.

Selection Process

The 915 articles generated from the search were further narrowed using a selection process based on the following 5-stage strategy:

1. Deletion of doubles
2. Title scan
3. Abstract scan
4. Cursory full text scan
5. Detailed full text scan

The search strategy is shown in Fig. 5.

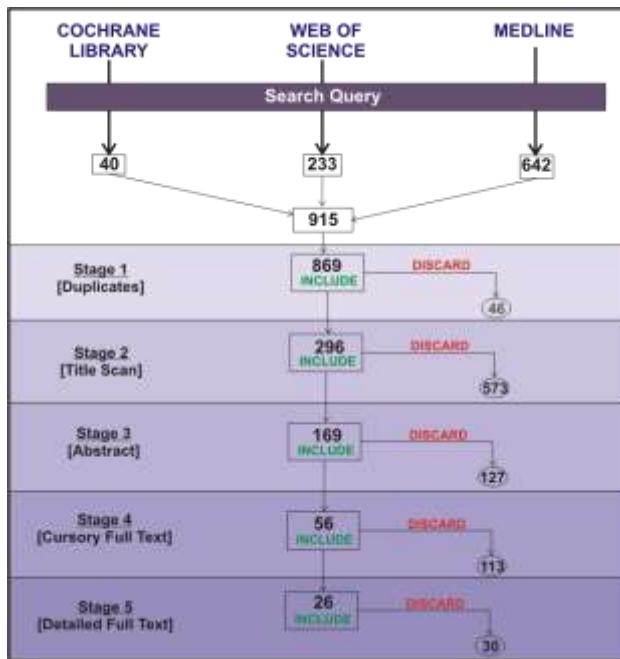


Figure 5: Search Strategy

There were 46 articles that were duplicated and these were deleted before the articles were screened based on their titles. Titles that indicated contents very different from research related to PHM were discarded. There were 573 articles discarded at this stage, leaving a total of 296 articles for the abstract-scan stage. During the abstract scan we eliminated articles that did not align with the theme of medical instrumentation in PHM; 127 articles were filtered out at this stage.

The remaining 169 articles were subjected to a cursory scan of the full text which essentially involved identifying the sections, as well as reading the introduction, discussion and conclusion sections. Articles that did not give sufficient details on the items relating to the theme were discarded. After this stage there were 56 articles that were subjected to a detailed full text scan out of which a further 39 articles were discarded. The criteria included the ones listed in the previous stage and for articles that contained similar ideas we chose the one that outlined the idea with the greatest level of detail. A preference was also given to articles that covered multiple domains, those that addressed unique applications and those which described the instrumentation process in some detail. After these stages we retained 26 core articles for the review. A description of each of these articles is given in Appendix A.

B. Analysis of Search Results

From the analysis of the 26 research articles included in this review, we identified a number of key features that characterize the use of instrumentation for PHM. These features will be discussed in the subsequent sections under the following groupings:

- Architecture
- Application
- Outcomes

Architecture of PHM Systems

The architecture describes the hardware portion of the PHM system and the communication interface. It comprises the sensors, system platform and the communication interface utilized for both the local and remote ends of the MVI.

Sensors and Sensing

The sensors capture the analog biosignals from the patient and condition it for further

processing. The sensing technology plays an important role in the utility of PHM systems. The sensors used in PHM systems can be categorized based on the level of invasiveness.

Table 1: Sensors used for PHM

S/No.	Sensor	Cases	%
1	Electrocardiogram [35, 39, 44, 45, 46, 47, 48, 51, 54, 55]	10	38.50%
2	Blood Pressure [35, 39, 45, 49, 51, 53]	6	23.10%
3	Accelerometer [38, 46, 50, 51, 53, 56]	6	23.10%
4	Oxygen Saturation [38, 45, 51, 53]	4	15.40%
5	Temperature [38, 49, 53, 54]	4	15.40%
6	Microphone [39, 52, 54, 61]	4	15.40%
7	Posture [38, 45, 53]	3	11.50%
8	Pressure [40, 49, 59]	3	11.50%
9	Weight [35, 45]	2	7.70%
10	Cardiac Implantable Electronic Device [36, 43]	2	7.70%
11	Gyroscope [38, 56]	2	7.70%
12	Blood Glucose [57, 60]	2	7.70%
13	Photodiode [41, 53]	2	7.70%
14	Surface Electromyography [37]	1	3.80%
15	Electroencephalography [58]	1	3.80%
16	Tilt [46]	1	3.80%
17	Camera [54]	1	3.80%
18	Pedometer [56]	1	3.80%
19	Gastrocnemius Expansion [56]	1	3.80%
21	Electro Dermal Activity [61]	1	3.80%
22	Chest Impedance [45]	1	3.80%

Invasiveness refers to a need for a puncture of a patient's skin or the introduction of a foreign

body into a patient in order to monitor some signal. Thus, the sensors can be classified as non-invasive or invasive. Tab. 1 shows the type of sensors used in the selected articles and the percentage of the 26 studies where they were used.

At 38.5%, Electrocardiogram (ECG) sensors represent the most extensively used sensors for PHM and when one includes the Cardiac Implantable Electronic Device (CIED) sensors this rises to 46.2%, implying that close to half of PHM systems monitor heart signals. Blood pressure (BP) sensors and accelerometers are the next most prevalent at 23.1% each. It is interesting to note that a number of some of these sensors measure signals as a proxy for another signal of interest and are thus known as virtual sensors.

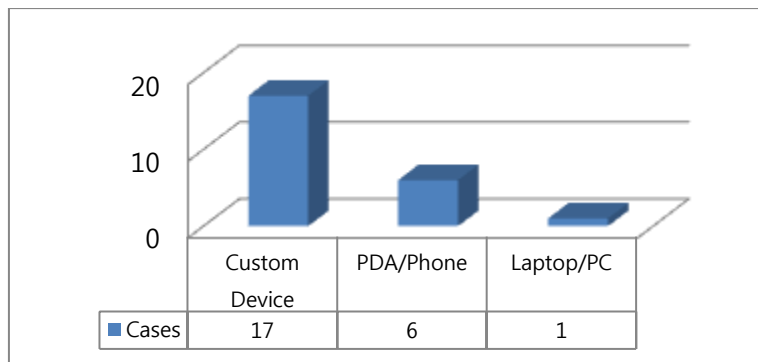
Virtual sensors [42] are fast becoming an important part of the PHM architecture. They refer to sensors that are based on software rather than hardware and they infer their readings from the relevant hardware sensor(s). These virtual sensors enable patients to monitor biosignals for which it is either impractical to have access to the signal of interest or for which the sensors or related equipment may be too expensive. From the reviewed articles, there were 13 cases (or half) that used virtual sensing. The actual sensors used for this process are listed in Tab 2.

Platform

Many PHM systems do not use a personal computer (PC) as their platform (only one uses the PC [41]). Most of them use a custom device [38, 39, 40, 44, 45, 46, 47, 49, 50, 51, 52, 53, 56, 58, 59, 60, 61] or a mobile phone/personal digital assistant (PDA) [35, 37, 48, 54, 55, 57] as their platform of choice as shown in Fig. 6. The 2 cases of Cardiac Implantable Electronic Devices (CIEDs) [36, 43] were not included since they only use mobile phones for communicating with a remote system.

Table 2: Examples of Virtual Sensing in PHM

S/No.	Virtual Sensor	Actual Sensor	No of Cases
1	Respiratory Rate [38, 50, 53, 59]	ECG, Accelerometer, Pressure	4
2	Heart Rate [53, 55]	ECG	2
3	Respiratory Input Impedance [40]	Pressure	1
4	Blood Flow Velocity [41]	Optical	1
5	Drowsiness Analysis [61]	EDA	1
6	Gait Analysis [56]	Gastrocnemius Expansion Measurement Unit (GEMU)	1
7	Parkinson's Disease Progression [39]	Microphone	1
8	Obstructive Sleep Apnea Syndrome (OSAS) [52]	Microphone	1
9	Consciousness Awareness [58]	EEG	1
	Total		13


Figure 6: Platforms used in MVIs

Network Models and Communication System

All the PHM systems in the reviewed articles were based on a client-server network model. In most of the systems, the sensed signals were forwarded from the local (or patient) end to an access point device in close proximity to the sensors for onward transmission to a remote server at the remote (or physician) end. In many cases the platforms described in the previous section were used as the access points.

One trend worth noting about PHM network models involves the direct connection between the output of the biosignals and a remote webserver or cloud service, rather than a connection to a specific remote server at the physician's end. Five (5) of the reviewed articles [46, 52, 55, 60, 61] used such a model. A number of advantages can be derived from this approach. One such advantage is the potential of “geographically decoupling” the biosignals [60]. In other words, it reduces the mobility restrictions on the patients since their signals can be streamed to the webserver while they move around freely. The platforms need to be configured as a webserver and should have access to the Internet. Another advantage of this approach is that the signals can be simultaneously viewed by different authorized people (such as the physician and the care giver). The approach can also exploit the memory and processing capabilities of a web or cloud service while reducing the computational complexity of the PHM system at the patient end.

Communication in PHM systems can either be within the modules at the local (patient) end or between the instruments at the patient end and those at the remote (physician) end. As shown in Fig. 7, the wireless protocol was the most common for local-PHM communication and was used in 73.9% of the cases. This included 26.1% for Bluetooth [35, 45, 54, 55, 57, 58], 8.7% for ZigBee [46, 48] and 39.1% of wireless protocols that were not specified [36, 43, 44, 47, 49, 52, 53, 56, 57]. There were 8.7% of the cases that used RS-232 protocols [38, 61] and another

17.4% that used other methods [39, 40, 44, 50]. Some articles did not specify the communication protocol [41, 51, 59].

The cellular networks were the most common approach of for communication in PHM systems between the patient-end and the physician-end. They were used in 56% of the cases [35, 36, 37, 38, 43, 44, 45, 48, 51, 52, 53, 54, 57, 60]. It was followed by the wireless approach (36%, of which 28% were for WiFi [37, 40, 44, 46, 50, 55, 56] and another 8% for unspecified wireless techniques [40, 47]). Digital Subscriber Lines (DSL) were used in 8% of the references [40, 45]. The details are shown in Fig. 8. Some articles used multiple techniques for remote communication and others did not specify the communication protocol [41, 49, 50, 51, 58, 59, 61].

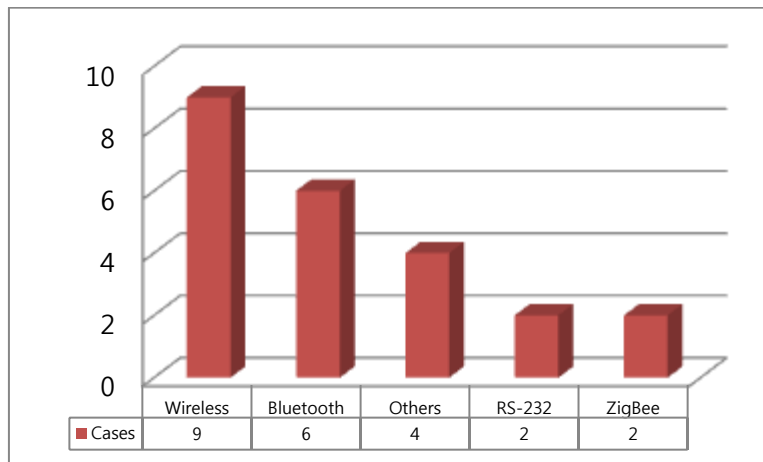


Figure 7: Communication Protocols used for PHM at the Patient-end

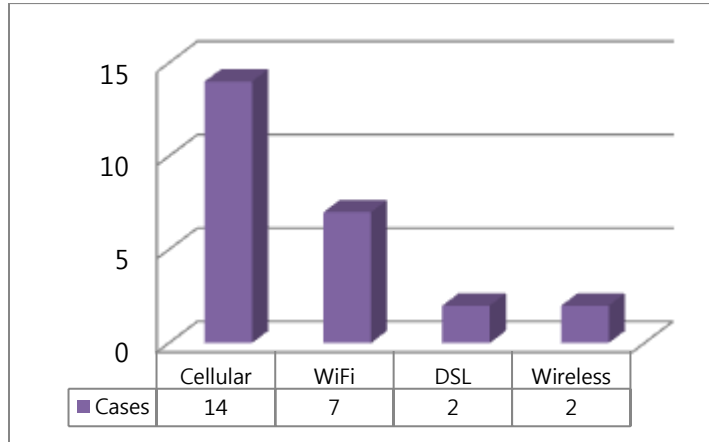


Figure 8: Remote-PHM Communication Protocols

Applications

PHM applications refer to the disease domains, adopted modality, level of system adaptability and algorithms that govern the operation of the instrument.

Disease Domains

PHM systems can be used for medical research applications, clinical applications, healthcare information management systems and mathematical modeling of physiologic systems [63], to name but a few domains of application. However, an analysis of the research articles in this review showed that PHM systems focus on some specific disease domains (Fig 9).

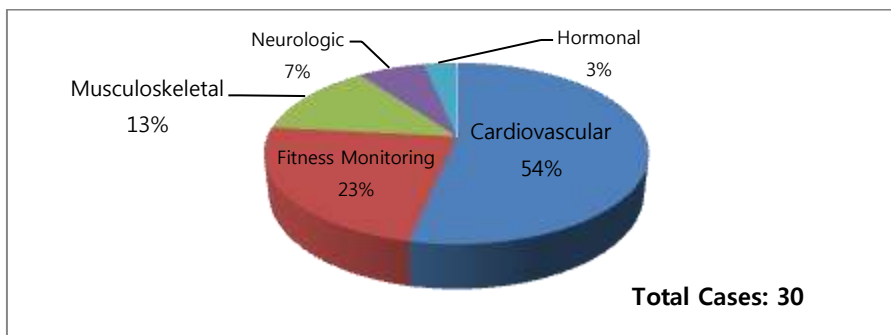


Figure 9 Disease Domains

The Cardiovascular Disease (CVD) domain accounts for over half of the cases. This is understandable since CVDs are the largest single contributor to global mortality. This domain covers the monitoring of biosignals that give an insight into the state of the patient’s heart.

Fitness monitoring refers to cases where the PHM did not target a specific domain. These cases were basically for monitoring general health and fitness. They accounted for about a quarter of the cases. The musculoskeletal domain addressed areas like fall detection, gait analysis and back pain.

Table 3: Monitoring Scenarios for the Cardiovascular Disease Domain

S/No.	Monitoring Scenario	No of Cases
1	Heart Monitoring [35, 43, 44, 47, 48, 55, 58]	7
2	Chronic Heart Failure [35, 45]	2
3	Spirometry [40, 53]	2
4	Hypertension [49]	2
5	Blood Flow Velocity [42]	1
6	Snoring [59]	1
7	Obstructive Sleep Apnea [52]	1
	Total	16

The cases under the neurologic domain focused on mental health monitoring using EEG sensors in one case [48] and using an EDA sensor [51] as a virtual sensor for monitoring drowsiness in the second case. The hormonal disease domain involved a case where blood glucose levels were monitored for the management of diabetes [47].

The constituent monitoring scenarios classified under the cardiovascular domain are shown in Tab 3.

Modality

The modality refers to the expected effect on the state of health of the patient. An overwhelming number of the cases reviewed (24 cases or 92.3%) focused solely on extracting, analyzing and reporting a patient's biosignals. Only 2 PHM systems (7.7%) triggered some form of therapeutic activity in response to the results of the analysis. The first case controlled the delivery of insulin to the diabetic patient [47] and the second case involved a stimulation to help the sleeping patient to stop snoring [52].

System Adaptability

The theme 'personalized health monitoring' presupposes a need to have systems that are personalized to suit the individual needs of a patient. This requires that the systems support some level of adaptability. In the literature review there were 11 (or 42.3%) of the articles that supported some level of adaptation [36, 37, 45, 47, 51, 52, 53, 55, 57, 58, 60]. Most of these were based on adaptation at the communication and architectural levels rather than at the patient level. Five of the six cases with adaptation at the patient level [36, 52, 53, 57, 58] were based on the patient's clinical profile while the sixth was based on the activity state of the patient [61].

Algorithms

The algorithms used in PHM systems refer to a step-by-step procedure for diagnosing and classifying a disease using a finite number of steps [63]. They help patients and physicians to make sense of the biosignals generated by the patient. The choice of the algorithm depends on

the type of diseases to be diagnosed, type of input parameters available for the process and the available resources for the computation.

Several algorithms can be used with PHM systems. A number of the main algorithms used across the various disease domains are either a subset or a combination of the following categories: Derivative-based, Support Vector Machine (SVM), Genetic Algorithm (GA), Threshold-based, Wavelet-based, Neural Networks and Compressive Sensing.

An SVM is a supervised learning model that uses data points (support vectors) closest to the decision surface (hyperplane) of the expected diagnosis to classify new data [64]. It provides a deterministic approach for obtaining an accurate classification that is unique and global. However, the algorithm can tend to be complex and it has high memory requirements [65]. In [66], SVM is used for classify the risk of epilepsy in patients based on their EEG signals.

A GA is a bio-inspired approach that is based on adaptive heuristics. It mimics the process of natural selection in nature and implements the classification using a fitness function. This algorithm is conceptually simple and useful for scenarios where there are several input parameters. The inductive nature of GA means that it can work with internal rules and does not need to know or work with the problem-specific rules. As a result, GAs can be used for several types of problems. It also has the advantage of being robust to dynamic changes in the system environment but cannot integrate problem specific information [67]. GA was used to predict the presence of heart disease in [68].

For many of the biosignals it is possible to predict the presence or absence of a disease based on a given level in the signal and this level is known as the threshold. Algorithms based on the thresholds classify the disease based on some pre-specified or adaptive threshold. These types

of algorithms provide a heuristic approach that is straight forward and generally simpler to implement than the other types of algorithms. Threshold based algorithms were used with ECG signals in [69] and for fall detection in [70].

The NN is a nondeterministic algorithm that was inspired by the interconnection of the neurons in the brain. Its classification is based on simple but highly connected processing elements whose weights are dynamically modified in response to incoming signals based on some learning rule. It is an accurate, robust and highly parallel technique. However, it is comparatively slower than other algorithms and tends to be resource intensive for systems with large input data sets [71]. It was used to screen for heart diseases in [72].

Compressive sensing (CS) is an emerging paradigm for energy efficient sensing, data compression and transmission of biosignals [73, 74]. The CS approach involves the transformation of the sensed data into a domain where the data is sparse in order to reduce the signal processing requirements. It is quite useful for applications where data capture is expensive in terms of time and power. Compressive sensing is discussed in more detail in the next chapter.

Tab 4 shows a list of the algorithms that were explicitly stated by the authors of the reviewed articles. The Pan-Tompkins algorithm featured in the most number of cases (3) and was used for systems targeting the cardiovascular domain. It was proposed in the late 1980s but has remained relevant today because of its suitability for real-time and resource-light processing of ECG signals. It is a first-derivative method that detects the R-peaks of the ECG signals using thresholding techniques following a series of filter stages. This algorithm is described in greater detail in Chapter IV. Peak detection algorithms also were also used in 3 of the systems.

Evaluation Metrics

The choice of the algorithm to use for a given disease domain depends on the following metrics- accuracy, precision, training time, speed, robustness, scalability, specificity and selectivity [75, 76].

The *accuracy* refers to the proximity of the measured value to the actual value. In the field of medicine the accuracy of the measurement has a greater level of importance as it may well be the difference between life and death for the patient. The accuracy is a ratio of the correct readings (true positives and true negatives) to all the readings taken as shown in Eq 1.

Table 4: Common Algorithms used for PHM

Algorithm	Cases
Pan-Tompkins [45, 48, 51]	3
Peak detection [38, 50, 58]	3
Thresholding [38, 39]	2
Wavelet transform [55, 59]	2
Correlation [41, 43]	2
Fuzzy-based [44]	1
Machine learning [54]	1
Least squares [40]	1
Edge detection [50]	1

$$\text{Accuracy} = \frac{\text{Number of correct assessments}}{\text{Number of total assessments}} = \frac{\text{TN}+\text{TP}}{\text{TN}+\text{TP}+\text{FN}+\text{FP}} \quad (1)$$

Precision refers to the consistency of the results under unchanged conditions. It is the ratio of the true positives to the total number of positives (true and false). The true positives refer to the number of positive outcomes that were correctly identified while the true negatives refer to the number of negative outcomes that were correctly identified. Conversely, the false positives (FP) and the false negatives (FN) refer to those incorrectly identified as positive and negative respectively.

Speed refers to the duration it takes to complete the classification process and this includes the time used in the training process for the classifier algorithm. For many medical signals this training process is needed to ensure proper analysis and classification. The *robustness* of an algorithm describes how much the performance is independent of the type and distribution of the input signals.

Scalability refers to the ability of the system to maintain its level of performance as the size of the input signal increases. In medical diagnosis, the specificity is the proportion negative classifications that are correctly made while the sensitivity refers to the proportion of positive classifications that are correctly made. As such specificity focuses on correct exclusions while sensitivity focuses on correct detections. The specificity and sensitivity can be calculated using Eq 2 and Eq 3 respectively.

$$\text{Specificity} = \frac{\text{Number of true negative assessments}}{\text{Number of all negative assessments}} = \frac{\text{TN}}{\text{TN}+\text{FP}} \quad (2)$$

$$\text{Sensitivity} = \frac{\text{Number of correct assessments}}{\text{Number of all positive assessments}} = \frac{\text{TN}+\text{TP}}{\text{TP}+\text{FN}} \quad (3)$$

C. PHM: Key Issues and Prospects

There are five (5) themes that were identified from the review as the key issues in the design and development of PHM systems, namely:

1. The need for personalization based on the profile of the patient
2. The need for more diverse PHM systems
3. The need for resource-light systems that support reliable long-term monitoring
4. The need for more non-invasive and non-intrusive PHM systems
5. The need for a greater degree of system miniaturization, virtualization and for more cloud based applications

Personalization for PHM Systems

Personalization is one of the main motivations for PHM [77]. It is a trend away from the sometimes ineffective “one-size-fits-all” approach used in standard medicine to a more effective approach that is customized for the specific needs of a given patient. The conclusion of The Human Genome Project [78] in 2001 has significantly increased interest in the area of personalized medicine, where diagnostic routines are used to determine the best treatment approach that can suit a specific patient. Many research efforts are exploring approaches that would enable PHM systems to adapt themselves to the unique profile of the patient in areas such as the patient’s genetic information or other biomedical data unique to the patient [79, 80].

Diversity for PHM Systems

More research effort is needed to increase the variety of PHM systems, away from devices that mainly focus on cardiovascular health and general fitness monitoring. For example, mental health is becoming a big global healthcare concern. It has been reported that one in four people now experience a mental health problem in their lifetime [81]. EEG sensors provide a low cost option for monitoring brain signals and researchers need to take advantage of this.

Reduced Processing Complexity and Long Term Monitoring

The requirement for mobility in PHM systems comes with a need for flexible and less power hungry applications since many of these systems use batteries as their power sources. The current need for continuous biosignal monitoring puts an additional strain on the limited resources of the PHM systems [82, 83, 84, 85]. As such, lightweight algorithms are required to ensure reliable health monitoring within the constraints imposed by these systems. Such algorithms must be lightweight with regard to the following metrics:

- (i) Power
- (ii) Memory
- (iii) Bandwidth
- (iv) Latency

Non-invasiveness and Non-intrusiveness

Non-invasive and non-intrusive are two words that describe the desired type of sensors for PHM systems [86]. It is desirable to provide comfortable sensors for the patients since the PHM systems are expected to support long term monitoring. Many PHM systems are non-invasive and these include systems that use ECG, EEG and accelerometer based sensors. In addition to a need to support non-invasive sensing, recent PHM systems go a step further by supporting non-intrusive sensors. The goal of a non-intrusive PHM system is to sense biosignals without intruding into the activities of daily living of the patient. A common approach involves the use of non-contact and capacitive sensors that are embedded into clothing, furniture, watches or jewelry [87, 88, 89].

Another approach involves the use of proxy or virtual sensors. For example, [59] uses a virtual sensor based on a pressure sensor embedded in a pillow. By using this approach, the

authors avoided the need for expensive, complex and intrusive polysomnography equipment by inferring its readings from the virtual sensor.

D. Application of the Information to this Thesis

In this thesis we will focus on the third key issue of PHM- the need resource-light systems that support reliable long-term monitoring. The thesis addresses two main domains- the dominant domain for PHM systems (the cardiovascular domain) and one of the fastest growing domains of interest (the neurologic domain).

The approach involved studying these two domains and identifying the unique features of the relevant biosignals that can be exploited to develop an intuitive approach for reducing the complexity of signal processing. we identified the main lightweight approaches used for long term monitoring of biosignals in these domains, located the most computationally intensive portions of the algorithms and devised a way around them without sacrificing the reliability of the system. Algorithms have been developed for the two domains and compared with the current leading lightweight algorithms.

III. A Bioinspired Algorithm for Lightweight Neural Telemetry

A. Telemonitoring of Neural Signals

Neural signals usually result in a very large dataset, the processing and transmission of which require much energy, storage and processing time. In this chapter we present a Bio-inspired electroceptive Compressive System (BeCoS) as an approach for minimizing these penalties. It is a lightweight and dependable system for the compression, transmission and reconstruction of neural signals inspired by active electroceptive sensing used by weakly-electric fish. It uses a signature-signal and a sensed pseudo-sparse differential signal to transmit and reconstruct the neural signals remotely.

Some signals from a 64-channel EEG dataset have been used to compare BeCoS with the Block Sparse Bayesian Learning-Bound Optimization (BSBL-BO) technique - a popular compressive sensing technique used for low energy and reliable wireless telemonitoring of EEG signals. This research explores the possibility of using BeCoS as a lightweight and dependable approach for the compression and recovery of non-sparse EEG signals.

Compressive Sensing

Traditional sensing techniques are based on the Nyquist theorem [90] and this requires signals to be sampled at a frequency equal to at least double their bandwidth in order to perfectly capture the signal. Compressive sensing (CS) techniques approach the challenge of sensing in a much different way.

In CS, the goal is to find a base, γ , to transform a high dimensional analogue data, \mathbf{x} , of dimension N , into a k -sparse analogue data set, \mathbf{x}^* using the Eq (4).

$$\mathbf{x} = \boldsymbol{\gamma} \mathbf{x}^* \quad (4)$$

The next step in CS involves the use of a user defined sensing matrix, Φ , to generate \mathbf{y} , a compressively sensed representation of \mathbf{x} using Eq (4) and (5).

$$\mathbf{y} = \Phi \mathbf{x} \quad (5)$$

The original signal, \mathbf{x} , is then reconstructed at the remote receiver using \mathbf{y} and Φ . \mathbf{y} is a compressively sensed representation of \mathbf{x} when $\boldsymbol{\gamma}$ and Φ are incoherent. This condition is met when Φ is chosen as a random matrix. The CS approach is effective when there is a sparse representation of the original signal. In this approach, the greater the level of sparsity of the sensing matrix, Φ , the greater the potential compression ratio and the lower the energy requirements.

CS [91] provides a good option for the lightweight sensing, processing, transmission and reconstruction of signals. However, CS systems need to use signals that are sparse in the time or transformed domains in order to reconstruct the signals with a high level of fidelity. EEG signals are neither sparse in the time nor the transformed domains and this makes the traditional CS- based EEG telemonitoring approach inadequate for clinical applications.

For non-sparse signals, it is necessary to use a sparsifying dictionary matrix, \mathbf{D} , to obtain a sparsified form of \mathbf{x} (\mathbf{x}^d) as shown in Eq (6). Eq (5) can thus be replaced by Eq (7).

$$\mathbf{x} = \mathbf{D} \mathbf{x}^d \quad (6)$$

$$\mathbf{y} = \Phi \mathbf{D} \mathbf{x}^d \quad (7)$$

Again, the success of the approach depends on the system's ability to find a sparse representation of \mathbf{x} . This underscores the importance of finding an appropriate user defined dictionary matrix, \mathbf{D} . This process can be challenging for arbitrary signals like EEG since general dictionary matrices are unable to sparsify them sufficiently.

Block Sparse Bayesian Learning Bound Optimization (BSBL-BO)

The Block Sparse Bayesian Learning (BSBL) framework has recently been proposed as a lightweight approach for processing biosignals in a way that avoids the requirement of an optimal dictionary matrix. It is based on the premise that most natural signals have a rich structure and can be represented as a concatenation of blocks [92] as shown in Eq(8). It uses user defined block partitions and assumes that most of these blocks are sparse.

$$\mathbf{s} = [\underbrace{s_1, \dots, s_{l_1}}_{s_1^T}, \dots, \underbrace{s_{l_{g-1}+1}, \dots, s_{l_g}}_{s_g^T}]^T \quad (8)$$

where s_i describes the block interval i of length l .

BSBL-BO is a fast learning BSBL based on the bound-optimization method [92]. It has been effectively applied as a lightweight solution for the reconstruction of temporally correlated EEG signals [93]. The authors' empirical results showed that non-sparse EEG signals can be reconstructed with a high level of fidelity by using BSBL-BO with standard dictionary matrices.

In [93], the solution was based on the use of a sparse binary matrix as the sensing matrix, Φ , and an inverse Discrete Cosine Transform (DCT) as the dictionary matrix, \mathbf{D} . The use of this type of dictionary matrix created a system that was 2.58 times faster than a system which did not use the dictionary matrix [93]. BSBL-BO has been used as the reference technique for

comparing BeCoS.

B. The Basics of Electroreception

Electroreception, also known as electroreception, refers to the ability to perceive natural electrical stimuli. Lampreys, bees, sharks, cockroaches and rays are examples of species that use electroreception either for communication or location of objects [94]. Some of these species are highly sensitive to changes in the electric field around them. For example, the shark can detect changes as low as $1 \times 10^{-10} \text{V/m}$ [95].

Electroreception can either be active or passive. In passive electroreception the sensing species detects a field originating from another species while in active electroreception the specie senses its environment by generating an electric field and detecting the distortions made to it by the field of another animal or object. The biological sensors used for the detection are known as the “Ampullae of Lorenzini”[94]. The generated electric field, also known as its signature signal, may be modulated to make it unique to the sending species. It can give information of the fish’s individual identity, sex, social and non-social behavior [96].

The weakly electric fish is a good example of an animal that uses active electroreception [95, 97]. This approach can either be based on small pulses (pulse-type) or a quasi-sinusoidal discharge (wave-type) and it allows the specie to identify the properties of the sensed object. For example, a weakly electric fish can detect and discriminate objects based on their ohmic and capacitive properties [94, 95, 98, 99]. The signature signal of the fish has *very large intraspecific waveform variability and usually has a triangular or sawtooth pattern* [100]. Fig 10 shows some examples of signature signals.

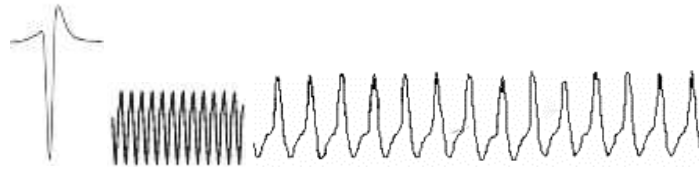


Figure 10: Examples of Signature Signals used for Electroreception [96, 102, 103]

Similar electrolocation techniques are used by bats and in radar technology. In those approaches there is a Doppler shift as a result of a relative motion between the source and the target. However, in electroreception there is *no frequency shift* due to the movement of electric signals [103].

The fish makes the process of sensing more efficient by *matching the impedance* between itself and its sensing environment. This way it can use a minimal amount of energy to sense its environment. The impedance, Z , is a combination of the resistance, R , and the capacitive reactance, X_C as shown in Eq (9). All living organisms have considerable capacitive properties that filter the signature signal in a way that *maintains the phase* [104].

$$Z = R + X_C \quad (9)$$

The resistance is independent of frequency while the capacitive reactance is inversely proportional to the product of the frequency and capacitance. The fish detects the distortions to the electric field that reflect the conductivity of the sensed object. The change is measured as a change in the *transepidermal voltage gradient* in the area next to the skin of the prey [103]. It was also noted that good conductors increase the transepidermal voltage while insulators have a decreasing effect. Also, *the detection of object waveforms relies on a purely temporal (and not spectral frequency) analysis.* [100].

A description of the key features of electroreception used in BeCoS is given in the section on ‘Porting Key Electroceptive Features into BeCoS’.

C. Bio-inspired electroreceptive Compressive System (BeCoS)

The BeCoS approach utilizes the electroreceptive approach for the sensing, compression and transmission of physiological signals as shown in Fig. 11. The approach is based on the wave-type active electroreception option. The modulated vector derived from this approach contains a high proportion of elements whose amplitude is close to zero. The Results section of this chapter provides further details about this.

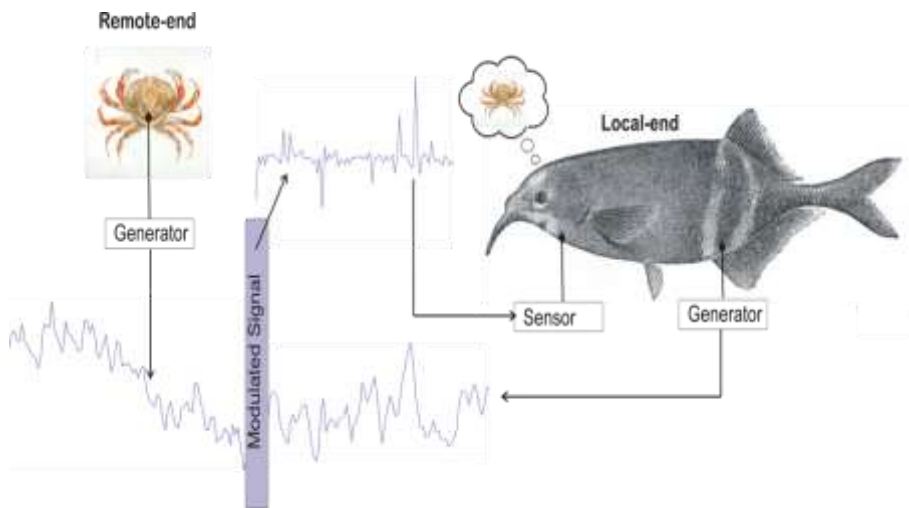


Figure 11. BeCoS Sensing Approach

BeCoS assumes that the *signature signal* vector (of length, E), originates from H , analogous to the local-end of the weakly electric fish. The \mathbf{h} vector is transmitted in the direction of R , analogous to the position of the object to be sensed, which generates an \mathbf{r} vector (of length, Z). $Z \gg E$ and $Z = wE$ (where w is a positive integer).

A modulated vector, \mathbf{p} , is generated when the \mathbf{h} and \mathbf{r} vector waves interact. The vector, \mathbf{p} , is given by Eq (10):

$$\mathbf{p} = [p_1, p_2, \dots, p_w] = \left[\frac{d\mathbf{r}_{jE+1, jE+2, \dots, E(1+j)}}{d\mathbf{h}} \right]_{j=0,1,2, \dots} \quad (10)$$

where each vector \mathbf{p}_w has a length, E which is the size of each epoch of the neural signals.

In this approach, $\frac{d\beta}{d\alpha}$ is a numerical differentiation given as the gradient between two adjacent points and defined as shown in Eq. (11).

$$\frac{df(\alpha)}{d\alpha} = \frac{f(\alpha+\Delta\alpha) - f(\alpha)}{(\alpha+\Delta\alpha) - (\alpha)} \quad (11)$$

The neural signals of interest are usually measured and stored as time series data. As such, there is a need to compute modulated signal, $p = \frac{dr}{dh}$ by using the differentiation-by-part as shown in Eq (12):

$$\mathbf{p} = \frac{d\mathbf{r}}{d\mathbf{h}} = \frac{d\mathbf{r}}{d\mathbf{t}} \div \left[\frac{d\mathbf{h}}{d\mathbf{t}} + \delta \right] = \dot{\mathbf{r}} / (\dot{\mathbf{h}} + \delta); \quad \delta = \begin{cases} 1 \times 10^{-6}, & \dot{\mathbf{h}} = 0 \\ 0, & \dot{\mathbf{h}} \neq 0 \end{cases} \quad (12)$$

where δ is a small positive stabilizer that prevents numerical instability when $\dot{\mathbf{h}} = 0$

Similarly, \mathbf{r} is reconstructed by integration as shown in Eq (13). The cumulative trapezoidal numerical integration method was used.

$$\mathbf{r}_{\text{recon}} = \int \mathbf{p} d\mathbf{h} = \int \mathbf{p} \mathbf{h} d\mathbf{t} \quad (13)$$

D. System Model and Performance Metrics

The BeCoS model is shown in Fig. 12. The multi-channel physiological signals are captured in real-time using appropriate sensors at the patient’s end- the local end of the Medical Virtual Instrument (MVI). A sparse differential signal is then generated in quasi real time. For each channel, a vector (\mathbf{h}) of length E is selected as the signature signal and all subsequent signals are differentiated with respect to the appropriate signature signal. This differential signal (\mathbf{p}) is wirelessly transferred to the physician’s end- the remote MVI. Here, the differentiated signal is integrated with respect to $d\mathbf{h}$ in order to reconstruct the original signals. An Additive White Gaussian Noise (AWGN) channel with an SNR of 0dB is assumed. The reconstructed signals ($\mathbf{r}_{\text{recon}}$) are then compared to the original signal using a set of performance metrics.

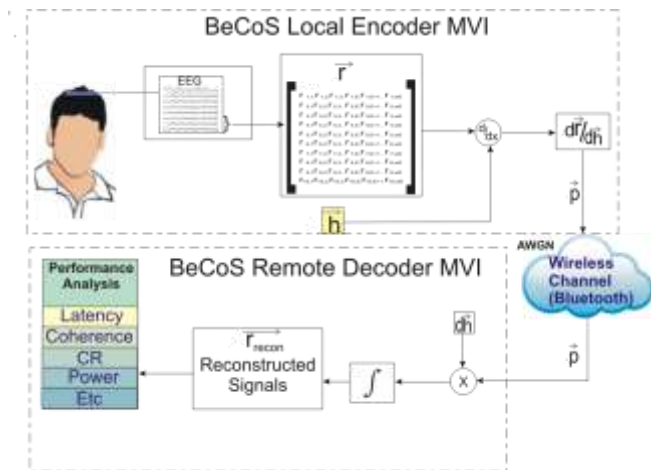


Figure 12: Conceptual Diagram of the BeCoS System Model

The \mathbf{r} vector is segmented into w equal non-overlapping segments, each representing an epoch block, with a length equal to the length of the signature signal vector, \mathbf{h} , as shown in Eq

(14).

$$\mathbf{r} = [\underbrace{u_1, \dots, u_E}_{1\text{st seg}}, \underbrace{u_{E+1}, \dots, u_{2E}}_{2\text{nd seg}}, \dots, \underbrace{u_{E(w-2)+1}, \dots, u_{(w-1)E}}_{(w-1)\text{th seg}}, \underbrace{u_{E(w-1)+1}, \dots, u_{wE}}_{w\text{th seg}}] \quad (14)$$

where u_i is the i^{th} element of \mathbf{r}

Dataset of Physiological Signals

Standard EEG databases have been used for this work. The EEG signals were taken from a 64-channel EEG Motor Movement/Imagery Dataset. It was obtained from an arrangement of sensors based on the international 10-10 system and provided on the Physionet website [105].

The Physionet signals were sampled at 160 samples/s and the following 8 channels were used for the analysis- Fc5, Fc3, Fc1, Fcz, Fc2, Fc4, Fc6 and C5, as channels 1-8 respectively. Each channel had a sequence length of 9,760 data points. An epoch length, E , of 244 was used and this resulted in 40 epochs, (w) .

The signals were used to simulate a typical signal compression, transmission and reconstruction scenario for EEG signals as shown in Fig 13. An Analog to Digital Converter (ADC) is used to emulate the signal acquisition phase. Location A refers to the patient-end of the MVI, where resource-constrained portable and mobile instruments are used. The instruments are usually powered by batteries. By contrast, location B refers to the physician-end of the MVI, where the signals are reconstructed on desktop computers or servers and powered by AC power.

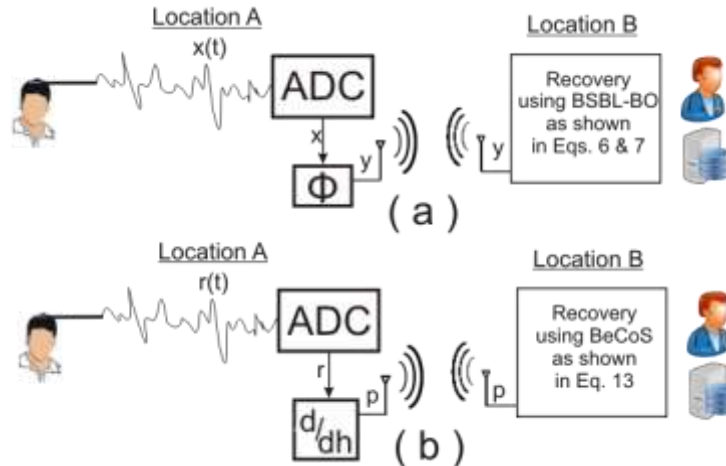


Figure 13: System Diagram for Testing Models: (a) BSBL-BO and (b) BeCoS

Performance Metrics

Five performance metrics have been chosen to evaluate the BeCoS approach. They are coherence, latency, compression ratio (CR), power and structural similarity as described in this section.

Coherence

EEG signal processing techniques are reliant on the frequency content of the signal [106]. As such, it is important to take the frequency content into consideration when comparing the signals at the local and remote ends. Spectral coherence provides this type of comparison. It is a measurement of the linear correlation between two neural electrodes [107] as a function of frequency and it is very useful for comparing EEG signals [108]. It computes the amount of synchrony between 2 stationary signals at a specific frequency [106]. The coherence metric compares the signals sensed at location A of Fig 13 with the signals reconstructed at location B of the same figure. The magnitude squared Coherence, C_{XY} , of two signals X and Y is given by Eq (15).

$$C_{XY}(f) = \frac{|P_{XY}(f)|^2}{P_{XX}(f)P_{YY}(f)} \quad (15)$$

P_{XX} and P_{YY} are the power spectral densities of X and Y respectively. P_{XY} is the cross spectrum of X and Y.

It is calculated based on the standard Welch's averaged periodogram method [109]. A Hamming window size of 125 was used for the computation.

Latency

The latency is calculated as the time between the acquisition of the sensed signal at location A and its reconstruction at location B of Fig 13. A zero delay over the noiseless wireless channel has been assumed. The learning phase of the BSBL-BO algorithm takes place at location B, prior to reconstruction. Many PHM systems require real-time monitoring and it is important to keep the latency at a minimum.

Compression Ratio

The compression ratio, CR, refers to the ratio of the dimensionality of the original signal to that of the sparsified sensed signals. The dimensionalities (non-sparseness) of the sensed and original signals are given as m and n respectively. CR is given in Eq (16). The compression takes place at location A of Fig 13.

$$CR = 1 - \frac{m}{n} \quad (16)$$

Power Consumption

Power consumption is a major consideration for health monitoring systems as they are likely to depend on batteries for their energy requirements [93, 110, 111]. According to [92], low energy

health monitoring systems are lighter and more comfortable for patients since they use smaller, longer lasting batteries. Power is important at the patient-end (location A) due to the use of batteries but it is not an important consideration at location B. The patient side core-engines of BeCoS and BSBL-BO were implemented in a Xilinx Virtex 5 FPGA and used to calculate the power consumption.

Structural Similarity

The frequency content of EEG signals has already been identified as an important feature for neural signal processing. The second important feature is the structural similarity of the reconstructed waveform with respect to the original signal [112]. A Structural Similarity (SSIM) index [93] is the standard metric for quantifying this. However, it has been shown in [112] that even a slight translation, scaling or rotation of the reconstructed signals can greatly affect the SSIM value. [112] went further to propose a Complex-Wavelet SSIM (CW-SSIM) as a more robust metric for comparison. The CW-SSIM index has been chosen as the metric since the BeCoS approach scales and translates the signals. CW-SSIM is calculated using Eq (17).

$$\tilde{A}(s_x, s_y) = \frac{2|\sum_{i=1}^N s_{x,i} s_{y,i}^*| + j}{2\sum_{i=1}^N |s_{x,i} + s_{y,i}^*| + j} \quad (17)$$

where s_x and s_y are the coefficients extracted from the same spatial locations of the same wavelength sub-bands of the two images being compared; s^* is the complex conjugate of s . j is a small positive constant (stabilizer)

E. Porting Key Electroceptive Features into BeCoS

This section shows how BeCoS integrates the most relevant features of the electroception discussed in the section entitled “The Basics of Electroception”. Some of these features were *italized* for emphasis in that section. The features have been identified and discussed below:

1. Same Type: The signature signal should be of the same type as the monitored signal. This requires the following:

- The signal should be of the same length as the signal being monitored. In the case of long term monitored signals, BeCoS requires the biosignal to be monitored in segments equal to the length of the signature signal
- The signal should be a similar biosignal to the biosignal of interest. As such, an EEG signal will be used for monitoring EEG signals
- More importantly, there should be a good level of ‘impedance matching’ between the signature signal and the segments of the biosignal of interest. This feature is further described in feature #4.

2. Signal Sparsification: The signature signal of the electric fish significantly sparsifies the monitored signals. BeCoS also uses a similar signature signal to achieve sparsification without a need for the base or dictionary matrices shown in Eqs (4-7). The level of sparsity can be further increased through the design of a signature signal with very large gradients at specific points as determined by the designer.

As shown in Eq (12), the modulated sparse signal, \mathbf{p} , is computed by dividing the inter-signal gradient of the sensed signal by that of the signature signal. As such, the designer can generate a very sparse signal, by choosing a signature signal, \mathbf{h} , with many large swing gradients (those that are very large compared to the corresponding gradient of the sensed signal, $\dot{\mathbf{r}}$).

3. Support for Sample Rate Conversion: The design of a signature signal described in #2 can also be used for downsampling of the sensing process and for sampling rate conversion without the need for the measurement matrix used in standard CS techniques. By noting the points in

the signature signal where there are very large gradients, the sensing protocol can avoid sampling those points since \mathbf{p} , will always be close to zero at those points.

For example the sampling rate can be halved by ensuring that the signature signal has very large swings at every other point or a third of the sampling rate can be used if two out of every three points have large swings.

4. Impedance Matching: As mentioned previously, the weakly electric fish uses an impedance matching between the local and remote ends in order to ensure an efficient sensing process. As shown in Eq 18, this impedance has both ohmic (R) and reactive components (X_C). In the ‘Basics of Electroception’ section we highlighted the fact that electroreception is not affected by shifts in frequency and it maintains the phase of the signature frequency.

$$Z = R + X_C \quad (18)$$

This suggests that the impedance matching in electroreception aims to maintain the ohmic value, while keeping the frequency dependent reactance at a minimum. The transfer function of a system is a mathematical function relating the output or response of a system to the input or stimulus [113]. For systems that have the same impedance, the transfer function is equal to 1. This appears similar to a scenario where input and output EEG signals are matched. In such a scenario the coherence is also equal to 1. As such, for BeCoS we will use a coherence term to represent the ohmic resistance.

The capacitive reactance, X_C , for capacitance, C , at frequency, f , is computed [114] as shown in Eq (19):

$$X_C = \frac{1}{2\pi fC} \quad (19)$$

The capacitance, C , can be calculated [114] as shown in Eq (20) and Eq (21):

$$C = I / \frac{dV}{dt} \quad (20)$$

$$C = \epsilon_o \epsilon_r \frac{A}{d} \quad (21)$$

Where I is the current in amps, $\frac{dV}{dt}$ is the voltage swing rate in Volts/second, ϵ_r is the dielectric constant, ϵ_o is the permittivity of free space ($\approx 8.854 \times 10^{-12}$ Farad/m). A is the overlap area between the two objects and d is the distance (in meters) between the two objects.

The brain can be modeled as a constant current source [115] and in electroception the overlap area between the fish and the prey is relatively constant. The dielectric constant and the permittivity of free space do not change. As such only d and $\frac{dV}{dt}$ may vary and these are the parameters that can be adjusted to alter the capacitance. Both terms need to be low in order to keep C high. This is logical since the fish would prefer sensing prey located at a close distance to it. The EEG signals do not provide any d parameter but the voltage swing rate can be calculated as shown in Eq 22:

$$Swing = \frac{1}{t} \sum_0^t |x_t - x_{t-1}| \quad (22)$$

where x_t is the EEG signal at time, t

The Swing Ratio (SR) is the ratio of the voltage swing of the system response (EEG signal being sensed) to the voltage swing of the stimulus (signature signal). The impedance equation shown in Eq (18) can be re-written to indicate the parts for coherence and SR as shown in Eq

(23). BeCoS does not work with impedance per se, as such, another term will be used to describe this similarity- *zygosity* (Z_{BeCoS}). The name was inspired by a similar term used to describe the degree of identity in the genome of twins [116].

$$Z_{\text{BeCoS}} = \frac{R}{\propto C_{XY}} + \frac{X_C}{\propto SR} \quad (23)$$

Minimize

Z_{BeCoS} is dependent on the coherence and SR as shown in Eq (24):

$$Z_{\text{BeCoS}} \propto (C_{XY}, SR) \quad (24)$$

From Eqs (23) and (24), an ideal optimized signature signal for BeCoS should have the following properties:

1. Have a high level of coherence to the sensed signal
2. Have a low swing ratio (ie the voltage swing of the signature signal should be high when compared to the voltage swing of the original EEG signal)

The second property can be attained by making using a signature signal that follows a pattern similar to the pattern of the natural signature signal used by weakly electric fish- the sawtooth waveform pattern. However, this signal still needs to be coherent with the sensed signal in order to meet the first requirement.

According to [116] it is possible to maintain a high level of coherence between two signals with different amplitudes and/or phases as long as the phase difference tends to remain constant. In calculating coherence it is necessary to know how stable the phase between two waves is and how quickly it changes with time. In [117], the coherence of a high-order harmonic spectrum was controlled by adjusting the sawtooth shape parameter.

EEG signals reflect the personalized information about the unique anatomical and functional attributes of a patient’s brain, including personality traits and genetic information [118, 119, 120, 121]. The signal coherence of EEG signals was used as a biometric in a recent study [107]. As such, the signature signal should have a high coherence when compared to a signal segment taken from the measured EEG signal.

Based on the foregoing discussions a procedure for designing an ideal optimized signature signal is presented in the next section.

Designing an Optimized Signature Signal

In this section we describe the process for designing an ideal optimized signature signal that satisfies the primary requirement of high coherence and the secondary requirement of a large swing ratio as described in the previous section. The process is shown in Fig 14.

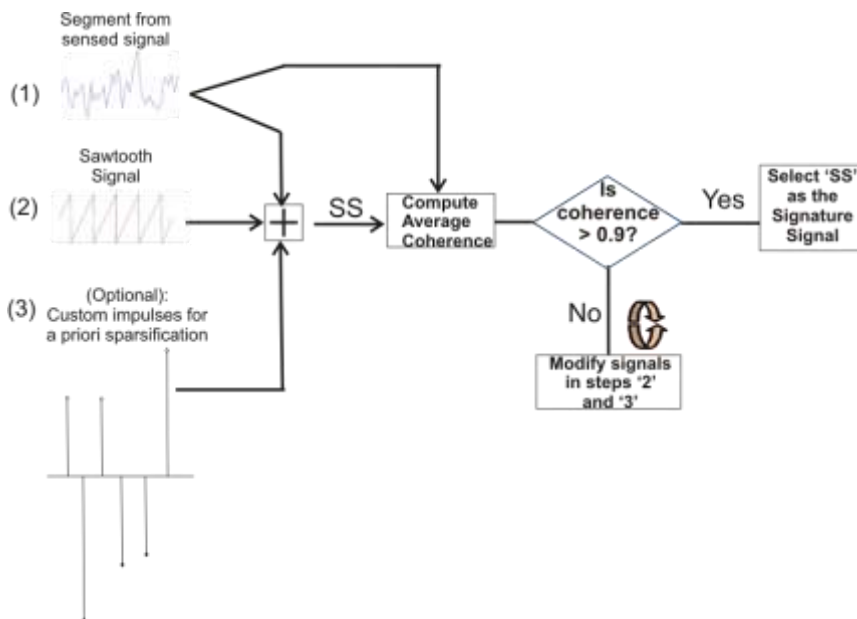


Figure 14 : Steps for generating an optimized signature signal

The following are the steps for generating an ideal optimized signature signal for BeCoS:

1. The first option for getting a non-optimized signature signal involves the selection of a signal that is highly coherent with the signal to be sensed. A segment of the sensed signal can be used as the seed signal. In this study the first epoch is used as the seed signal.
2. The second option for a more optimized signature signal requires the addition of a sawtooth signal with a known voltage swing to the coherent signature signal used in the first option. This composite signal should still be coherent to the measured signal.
3. A third option for an ideal optimized signal requires the addition of high valued input pulses to the summation of the seed signature signal and sawtooth signal. The output of step 3, called 'SS', is then compared with the seed signal to determine the coherence. If the average coherence is high enough (≥ 0.9), then SS is chosen as the signature signal. If the coherence is less than 0.9, steps '2' and '3' are iteratively modified until an 'SS' with the required coherence is attained. This gives an ideal optimized signature signal but the process has extra computational requirements.

F. Results

The EEG datasets were used to compare BSBL-BO and BeCoS based on the 5 metrics described in the previous section. The tests were conducted on a Xilinx Virtex 5 FPGA and an Intel Pentium 4 system, with a 3.0GHz CPU and 2GB RAM. For the BSBL-BO experiments a 122 x 384 sparse binary sensing matrix, Φ , was used and a 244 x 244 inverse DCT matrix as the dictionary matrix, \mathbf{D} .

Coherence

The average coherence value for BeCoS and BSBL-BO were compared (Table 5). The average coherence was also compared across a frequency range of 0-90Hz (Fig. 15). BeCoS had an average coherence of 0.949 across the 8 channels while BSBL-BO had an average of 0.701. Also, BeCoS maintained a near optimum coherence between 2.1Hz and 84.38Hz. On the other hand, BSBL-BO fluctuated across the spectrum with a peak of 0.996 at 0.7Hz and a trough of 0.497 at 90Hz.

Table 5: Comparison of BSBL-BO and BeCoS Coherence Values

BSBL-BO	BeCoS	% Increase
0.701	0.949	35.38%

Overall, BeCoS had 35.38% better average values. BSBL-BO is an adaptive learning approach that exploits the intra-block correlation of the signals. This is less linear than the BeCoS approach and increases the power of the noise in the reconstructed signal. BeCoS generates a reconstructed signal that is linearly dependent on the original signal since the differential and integral operators used have a linear time invariant property in the Fourier domain.

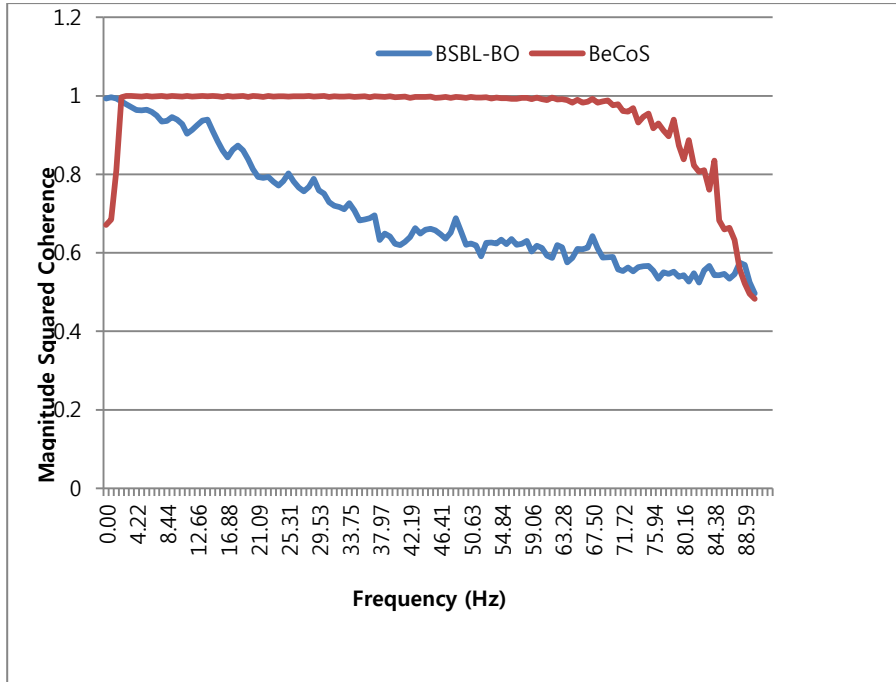


Figure 15: Coherence across the frequency spectrum

Latency

The latency refers to the time taken for sensing, processing, transmitting and reconstructing the neural signals. In BSBL-BO it involves these stages as well as the learning stage as discussed earlier. For BeCoS, it involves the steps shown in Eqs (12-13). The sensing, processing and reconstruction phases of BeCoS basically involve a few additions and multiplications. For the BSBL-BO it involves additions on the accumulators that result from the sparse binary sensing matrix, the multiplications with the inverse DCT dictionary matrix and the learning process.

With BeCoS we had an average of 0.117ms for processing each epoch, compared to 5.869ms that was used by BSBL-BO. As such, BeCoS used just 1.99% of the processing time used by BSBL-BO. The processing time we got was similar to the time reported in the reference BSBL-BO paper [93], where 105ms was used to process an epoch. The epoch length used in

that paper was 384 data points for 32 channels. This results in 0.273ms per data point or 2.085ms per epoch. That paper also used a 192x384 sparse binary matrix to sparsify the signal while we used a 122x244 sparse binary matrix for this work. By factoring in this ratio of 2.477, one can estimate that the process described in the reference paper would have taken about 5.165ms/epoch for the experimental setup used in this paper. Also, the system used in the reference paper had a 2.8GHz CPU and 6GB RAM while a system with a 3GHz CPU and a 2GB RAM was used in this research. This may also explain why the result in the reference paper was slightly faster than the BSBL-BO processing results obtained in this research.

Compression Ratio

By representing the sensed signal with respect to a pre-specified signature signal, the BeCoS approach reduces a large portion of the original values to values that are close to zero. Values of the sensed signal, x , where $|x| < 0.99\text{mV}$ were taken to be sparse. This pseudo-sparsity reduces the dimensionality of the transmitted signal and increases the effective compression ratio (see Eq. 16). The comparison was based on the same optimal configuration for BSBL-BO used to attain a low-cost EEG system in [93] (compression ratio of 50%). As seen in Table 6, BeCoS achieved an average compression ratio of 76.63% or 53.26% better than BSBL-BO, even though the non-optimized signature signal was used for the analysis.

Table 6: Comparison of BSBL-BO and BeCoS Compression Ratios

BSBL-BO	BeCoS	% Increase
50%	76.63%	53.26%

Power and Hardware Resource Consumption

Previous research [95] already shows that weakly electric fish use the electroceptive approach

to maximize the energy efficiency of their sensing process and we have also used it for the efficient sensing, processing and transmission of the neural signals. We implemented the core compression engines of BeCoS and BSBL-BO in hardware in order to get a realistic estimation of the power consumption at the patient-end of the telemonitoring system.

The Simple Bus Architecture (SBA) [122] was used for both designs. The SBA is lightweight computer architecture that implements a minimum essential subset of the open source Wishbone signals interface [123]. It consists of software tools and intellectual property (IP) cores that are interconnected by buses and it enables the implementation of a System on Chip (SoC). The availability of the essential blocks enable the system designer to concentrate on the core design and this helps to speed up the design process and makes it portable across different FPGA platforms. The master core is a special state machine that performs basic dataflow like a microprocessor without the high resource utilization that characterizes soft processor.

The top level block diagrams for the BeCoS and BSBL-BO compression engines are shown in Fig 16 and 17 respectively.

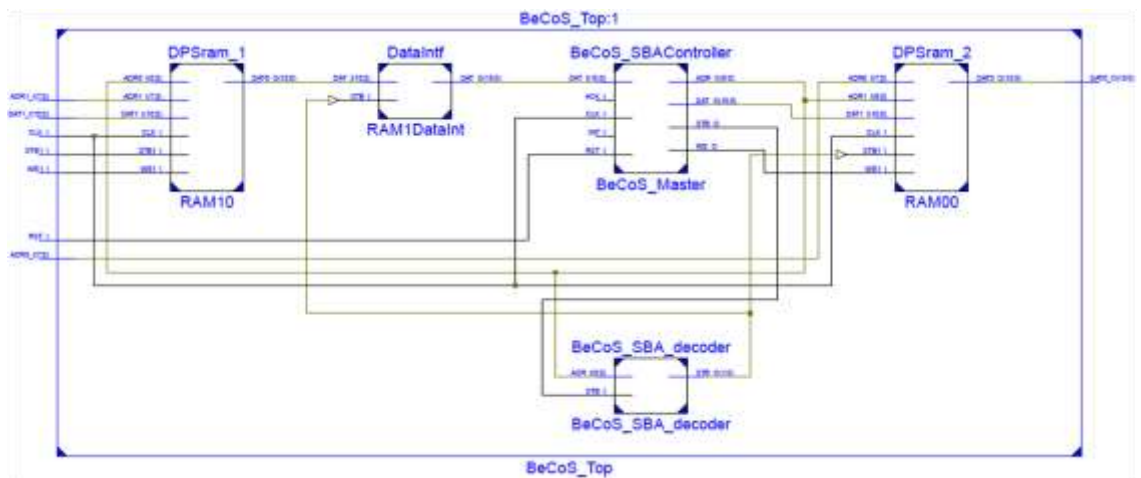


Figure 16: Top level block diagram of the BeCoS compression engine

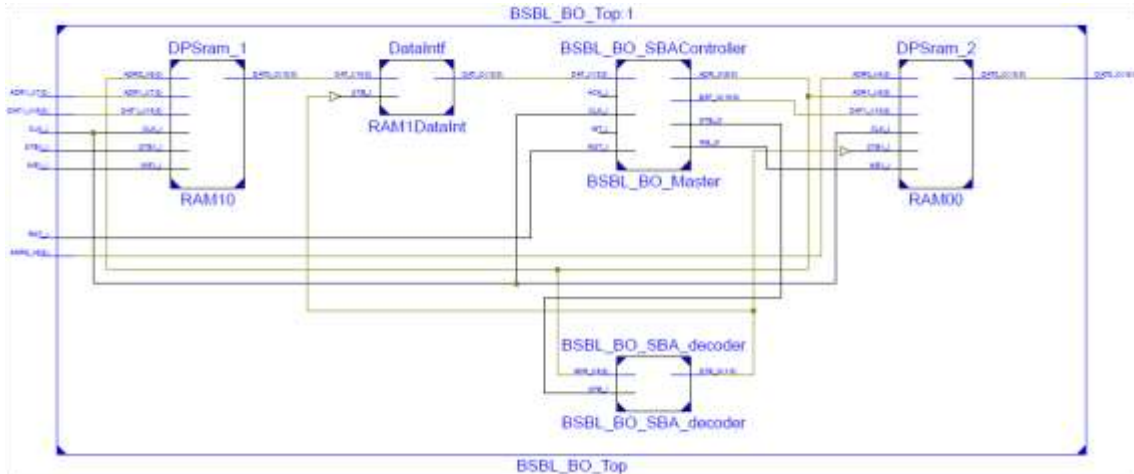


Figure 17: Top level block diagram of the BSBL-BO compression engine

The following blocks and signal names were used for the BeCoS engine (Fig 16):

- SBA Controller: Master System Controller
- SBA Decoder: SBA Address Decoder
- DPSram: Dual Port Single Clock RAM
- DataInf: Data Output Bus Interface
- CLK_I: Main clock (1 bit)
- RST_I: Active high reset (1 bit)
- ADR0_I: Address output bus (8 bit)
- DAT0_O: Data output bus (16 bit)
- WE1_I: Write Enable (16 bit)
- STB1_I: Strobe acknowledgement (1 bit)
- ADR1_I: Address input bus (1 bit)
- DAT1_I: Data input bus (8 bit)
- INT-I: Interrupt (16 bit)
- RAM 10 (0-255, for EEG data values)
- RAM 00 (0-255 for output values)

Similarly, the following blocks and signal names were used for the BSBL-BO engine (Fig 17):

- SBA Controller: Master System Controller
- SBA Decoder: SBA Address Decoder
- DPSram: Dual Port Single Clock RAM
- DataInf: Data Output Bus Interface
- CLK_I: Main clock (1 bit)
- RST_I: Active high reset (1 bit)

- ADR0_I: Address output bus (8 bit)
- DAT0_O: Data output bus (16 bit)
- WE1_I: Write Enable (16 bit)
- STB1_I: Strobe acknowledgement (1 bit)
- ADR1_I: Address input bus (1 bit)
- DAT1_I: Data input bus (8 bit)
- INT-I: Interrupt (16 bit)
- RAM 10 (0-255, for EEG data values)
- RAM 00 (0-127 for output values)

A master clock of 160Hz was used. At each rising edge of the clock one EEG signal was sent as an input to the compression engine. This process mimics the data acquisition process in a live PHM system where an EEG sensor captures signals at a given sampling rate. The epoch EEG data was stored in a RAM (RAM 10) with a resolution of 16bits. The BeCoS engine stores 245 consecutive EEG signals in RAM 10 per epoch while the BSBL-BO engine stores 244 EEG signals. Both systems used two banks of double port memories. The first was for the input data while the second was for the output data.

The BeCoS engine uses 3 internal buffers (IB1, IB2 and IBS). At each rising clock edge, an EEG signal is fed into the first internal buffer (IB1). At the second rising edge, the content of IB1 is transferred to IB2 and the next EEG signal is fed into IB2. On the third cycle, the difference (IB2-IB1) is computed and stored in IBS (see Eq 11). The BSBL-BO engine has 244 internal buffers because all 244 EEG values must be obtained in order to compute the output signals for each epoch.

For BSBL-BO, at each rising edge of the clock a new consecutive EEG signal is stored in the internal buffers consecutively from IB1 to IB244. For BeCoS, only two consecutive signals are required to compute the corresponding output signal. For example, the 1st and 2nd EEG signals are used to compute the 1st output, the 13th and 14th EEG signals are used to compute

the 13th output and the 244th output signal can be computed when the 244th and 245th EEG values are in the internal buffers. The buffers were implemented using Configurable Logic Blocks (CLBs).

To compute the output signal, the BeCoS engine divides the value of the BS buffer with the corresponding signature signal as shown in Eq. 12. The signature signals were stored in a ROM table. The BSBL-BO output signals were computed using a sparse binary sensing matrix (Φ) as shown in Eq. 5. Each column of the sensing matrix contained just two non-zero entries to allow the use of accumulator registers, rather than multipliers. The resulting output signals were then generated based on the sensing matrix. The BeCoS engine has an output of 244 signals while the BSBL-BO has an output of 122. As such, the BeCoS system has 244 output registers (OR) while the BSBL-BO approach has 122 output registers.

Table 7: Comparison of the Power and FPGA Resource Utilization for the BSBL-BO and BeCoS Core Engines

	FFs	LUTs	IOBs	BRAMs	Power
Total No of FPGA Resources	69,120	69,120	640	148	-
BSBL-BO (% Utilization)	3,981 (5.8%)	1,743 (2.52%)	51 (7.97%)	2 (1.35%)	1.204W
BeCoS (% Utilization)	123 (0.18%)	881 (1.27%)	52 (8.13%)	3 (2.03%)	1.191W

The hardware synthesis report is shown in Tab. 7 and it gives the resource utilization for both systems using a Xilinx Virtex 5 FPGA (XUPV5-LX110T). The table shows the amount of

Flip Flops (FF), Look Up Tables (LUTs), Input Output Blocks (IOBs) and Block RAMs (BRAMs) used.

The Value Change Dump (VCD) was used with the Xilinx Power Analyzer to calculate the power consumption of both systems. The results are also shown in Table 7. BeCoS used 13mW less power than BSBL-BO to process one epoch of EEG signals at the patient’s end. To put this figure in better perspective, let us assume the system at the patient’s end is running on a Samsung Galaxy 4 phone with an Li-Ion battery rated at 2100mAh and 3.8V. This battery would serve the BSBL-BO system for 8,837 hours and the BeCoS system for 8,933hours- a difference of 96 hours or 4 days.

Structural Similarity

The average CW-SSIM values for both BSBL-BO and BeCoS are shown in Tab. 8.

Table 8: Comparison of BSBL-BO and BeCoS CW-SSIM

BSBL-BO	BeCoS	% Increase
0.969	0.908	-6.295%

Tab 8 shows that BeCoS has an average CW-SSIM decrease of 6.295%. As noted in the metrics section of structural similarity, the SSIM is highly altered by the scaling of the signal. Similarly, its enhancement (CW-SSIM) still gets affected by scaling and rotation, even though it is more robust than SSIM. There is a degree of scaling in the BeCoS approach as a result of the numerical integration during the reconstruction phase and this invariably lowers the CW-SSIM.

However, as seen in Figs 18-20, regardless of the scaling and translation, the structure of the

reconstructed signal using the BeCoS approach is still strikingly similar to the original EEG signal.

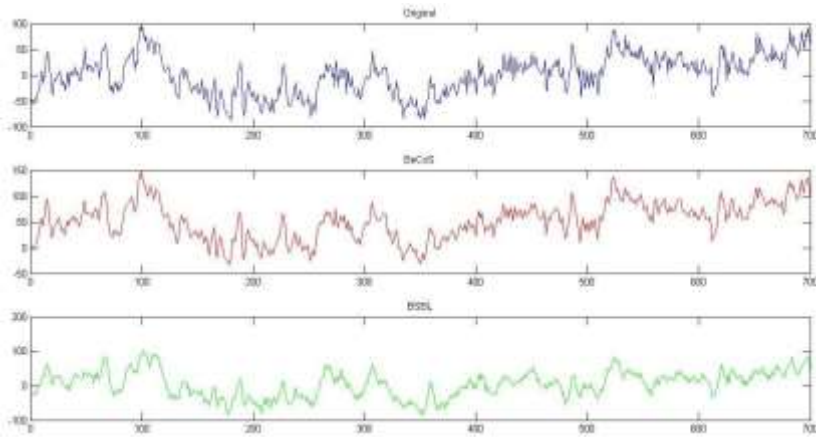


Figure 18: CW-SSIM for Ch7 [1:700]

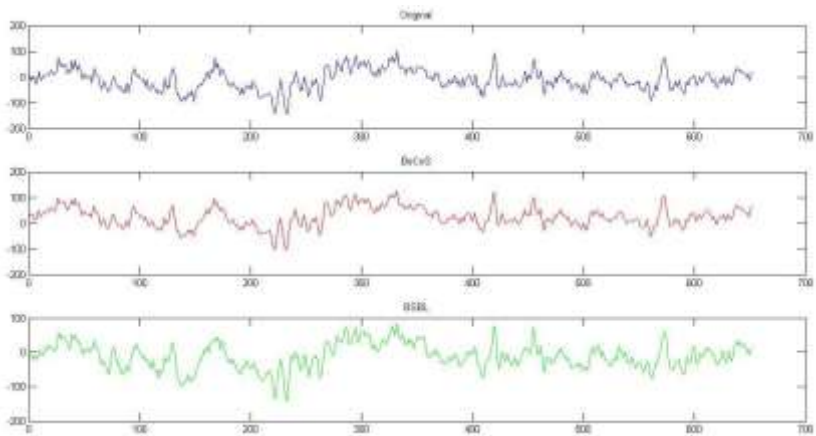


Figure 19: CW-SSIM for Ch1 [3000:3650]

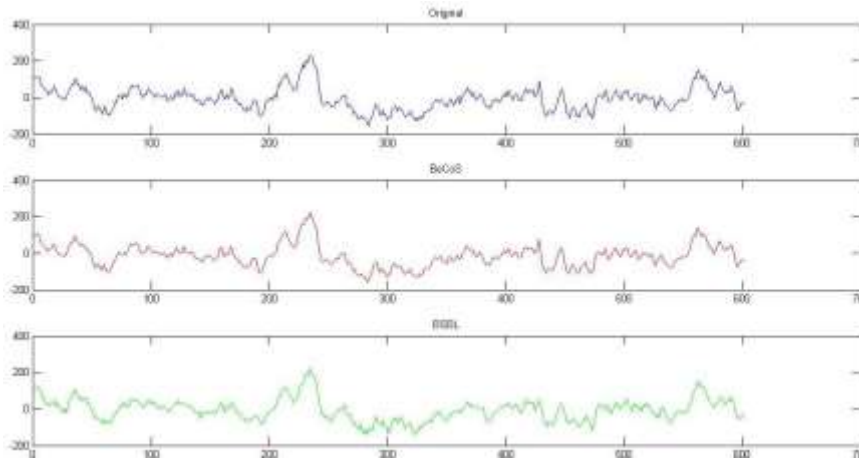


Figure 20: CW-SSIM for Ch4 [6300:6900]

Effects of Variations on SSIM and CW-SSIM

To further explain the lower CW-SSIM value for BeCoS, consider a random sample shown in Tab 9 with columns for the original sample, its numerical differentiation, numerical integration, numerical integration plus the offset value and the variation. Numerical integration, as opposed to analytical integration, uses approximations and introduces a non-uniform variation when compared to the original signals. In order to use analytical approaches the exact equation of the signal must be known in advance and this is not possible for real time physiological signals. As such, a numerical integration method is the most feasible integration approach that can be used for such signals.

Table 9: Effect of Numerical Methods on Signal Reconstruction

Original	Num Diff	Num Int	Num Int + Offset	Variation
40	1.2	0	40	0
41.2	1	1.1	41.1	0.1
42.2	1	2.1	42.1	0.1
43.2	0.8	3	43	0.2

44	0.8	3.8	43.8	0.2
44.8	0.6	4.5	44.5	0.3
45.4	0.6	5.1	45.1	0.3
46	0.5	5.65	45.65	0.35
46.5	0.3	6.05	46.05	0.45
46.8	0.3	6.35	46.35	0.45
47.1	0.2	6.6	46.6	0.5
47.3	0	6.7	46.7	0.6
47.3	0	6.7	46.7	0.6
47.3	-0.1	6.65	46.65	0.65
47.2	-0.2	6.5	46.5	0.7
47	-0.3	6.25	46.25	0.75
46.7	-0.5	5.85	45.85	0.85
46.2	-0.5	5.35	45.35	0.85
45.7	-0.6	4.8	44.8	0.9
45.1	-0.7	4.15	44.15	0.95
44.4	-0.8	3.4	43.4	1
43.6	-0.9	2.55	42.55	1.05
42.7	-1	1.6	41.6	1.1
41.7	-1.1	0.55	40.55	1.15
40.6	-1.2	-0.6	39.4	1.2
39.4	-1.3	-1.85	38.15	1.25
38.1	-1.4	-3.2	36.8	1.3
36.7	-1.5	-4.65	35.35	1.35
35.2	-1.6	-6.2	33.8	1.4
33.6	-1.7	-7.85	32.15	1.45
31.9	-1.8	-9.6	30.4	1.5
30.1	-1.9	-11.45	28.55	1.55
28.2	-2	-13.4	26.6	1.6
26.2	-2	-15.4	24.6	1.6
24.2	-2.2	-17.5	22.5	1.7
22	-2.3	-19.75	20.25	1.75
19.7	-2.4	-22.1	17.9	1.8
17.3	-2.5	-24.55	15.45	1.85
14.8	-2.5	-27.05	12.95	1.85
12.3	-2.7	-29.65	10.35	1.95

9.6	-2.8	-32.4	7.6	2
6.8	-2.8	-35.2	4.8	2
4	-3	-38.1	1.9	2.1
1	-3.1	-41.15	-1.15	2.15
-2.1	-3.1	-44.25	-4.25	2.15
-5.2	-3.3	-47.45	-7.45	2.25
-8.5	-3.3	-50.75	-10.75	2.25
-11.8	-3.5	-54.15	-14.15	2.35
-15.3	-3.5	-57.65	-17.65	2.35
-18.8	-3.7	-61.25	-21.25	2.45

Fig 21 shows the original sample and sample reconstructed by numerical integration as well as this reconstructed sample value plus an addition of the initial offset.

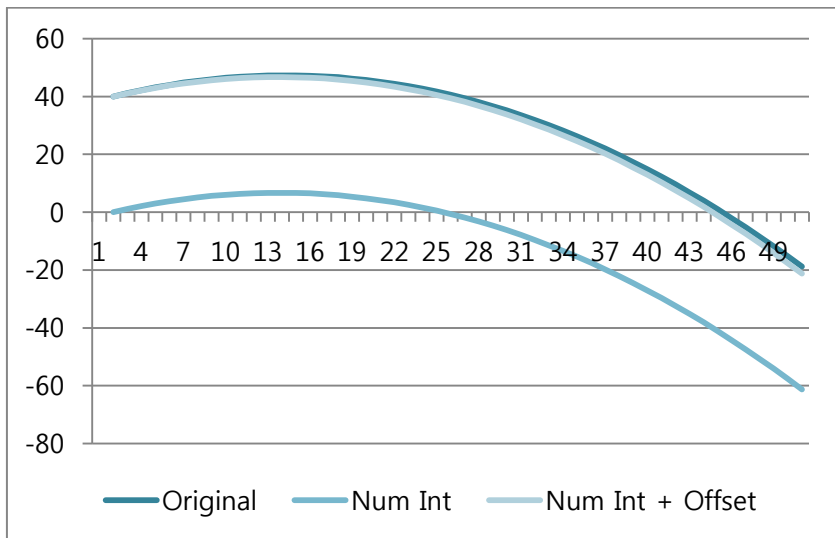


Figure 21: Effect of Numerical Methods on Signal Reconstruction

The figure clearly shows that all three signals have a similar structure. The variation is shown in Fig. 22. A regression analysis was used to generate a Linear Regression Variation (LRV) model in order to estimate the equation of this variation and we obtained the following

equation:

$$y=0.049011x+(-0.02478)$$

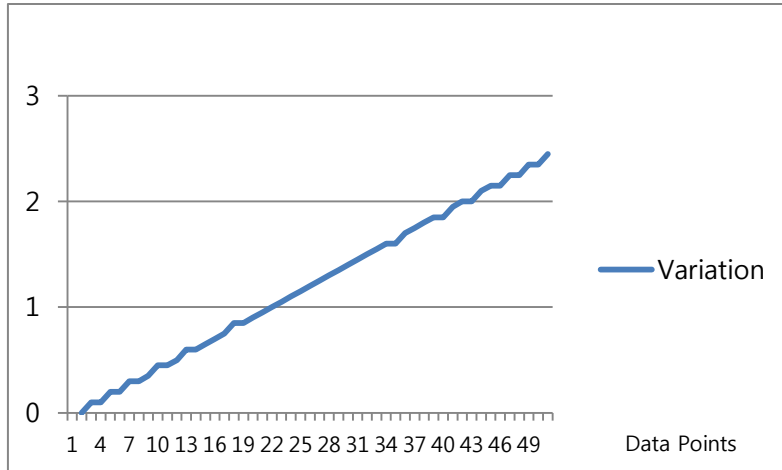


Figure 22: A Model of the Variation Generated by Numerical Methods

We have used the data in channel 1 of the EEG signals used in this research to visualize the effect of variations on the SSIM and CW-SSIM values. The SSIM and CW-SSIM were calculated by comparing the data in channel 1 with the following samples:

- (i) Original sample (comparing it with itself, Or)
- (ii) Original sample minus 1mV (Or-1)
- (iii) Original sample plus 1mV (Or+1)
- (iv) Original sample minus 5mV (Or-5)
- (v) Original sample plus 5mV (Or+5)
- (vi) Original sample plus 10mV (Or+10)
- (vii) Original sample plus 20mV (Or+20)
- (viii) Original sample plus 50mV (Or+50)
- (ix) Original Sample plus Linear Regression Variation model (Or+LRV)
- (x) Original Sample plus Linear Regression Variation model, treating it one epoch at a time (Or+LRV, 1 epoch)

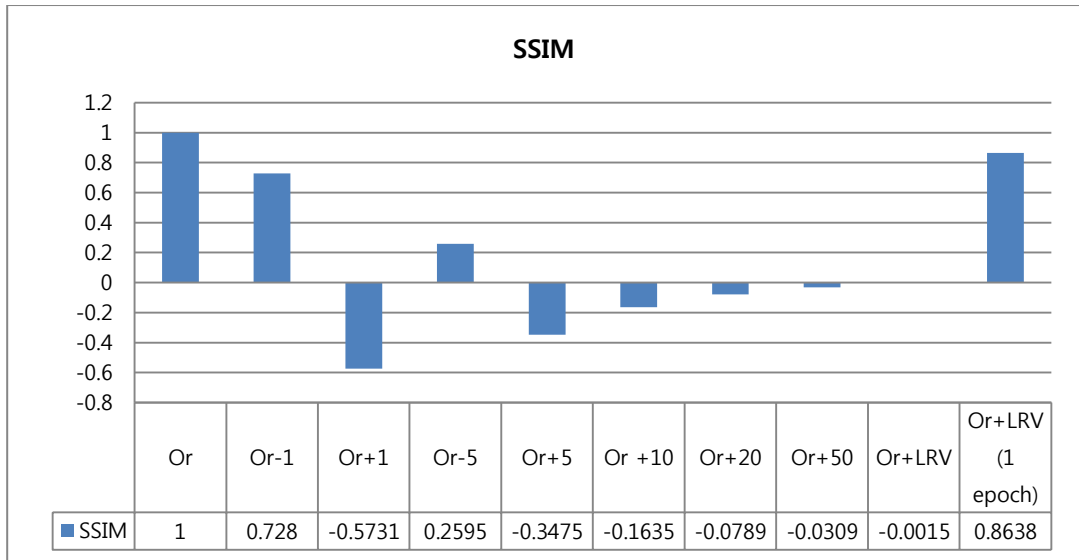


Figure 23: The Effect of Variation on SSIM

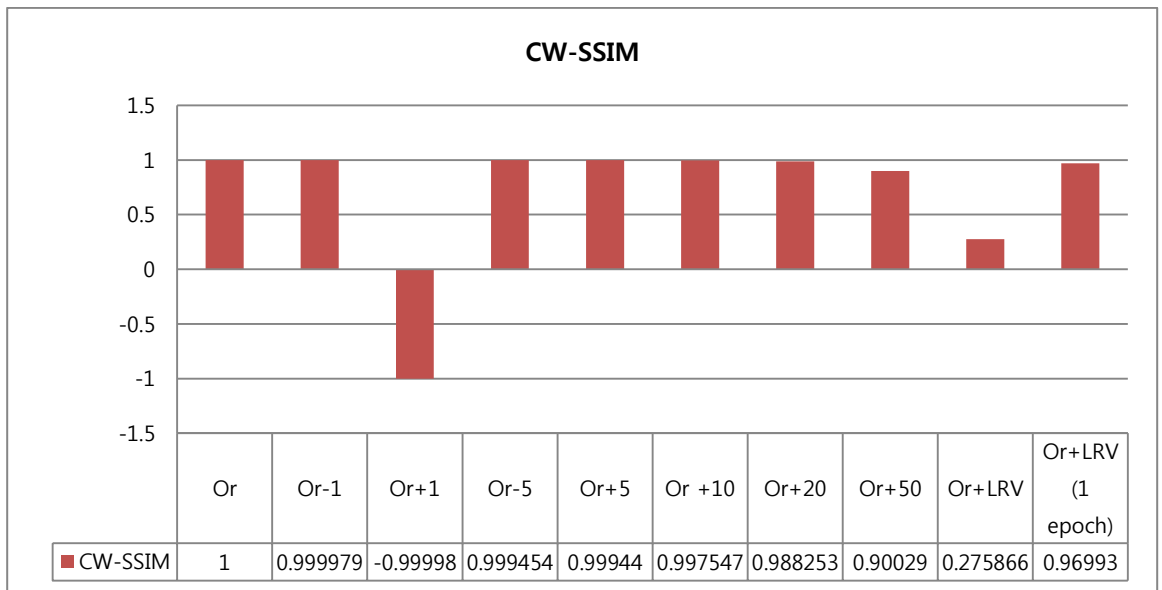


Figure 24: The Effect of Variation on CW-SSIM

As seen from Fig 23, any variation beyond 1mV significantly diminishes the SSIM values. The SSIM value for Or+LRV is almost zero but it gives a better result when it is treated epoch

by epoch.

The CW-SSIM measurements are fairly stable for different variations. The degradation becomes more apparent for higher variations as well as for the model that uses LRV. Such a model is feasible in practice since PHM systems are likely to fall under the LRV model. This is because the noise level experienced by the system can be affected by the location of the patient as well as the condition of the sensors.

The CW-SSIM calculation in the BeCoS approach is similar to the LRV based model and this explains why the values are lower than the CW-SSIM values for the BSBL-BO approach even though the reconstructed signals look similar. The CW-SSIM was used for the analysis in this research because it is currently regarded as one of the most robust approaches for measuring structural similarity. However, in the future it may be necessary for researchers to develop a new type of structural similarity index that is more robust to variations such as LRV.

A Combination of BeCoS and BSBL-BO for Personalized Health Monitoring

The following points succinctly describe how BeCoS relates to traditional CS techniques used for the telemonitoring of biosignals:

1. BeCoS can be used as a lightweight approach for significantly sparsifying an otherwise non-sparse signal. We obtained a compression ratio of at least 75% in each case. After this stage the sparse biosignal can be suited to traditional CS techniques
2. BeCoS can be used as a *stand alone* technique as an alternative to conventional CS techniques used for the telemonitoring of 'costly-to-sparsify' biosignals.

IV. R-READER: An Algorithm for Lightweight Detection of Fiducial Points in the Cardiovascular Domain

A. Detection of R-peaks in ECG Signals

The accurate identification of the R-peak of an electrocardiogram (ECG) cycle is the first step towards automated classification of the cycle. In this chapter we present a lightweight algorithm, known as R-READER: a Rapid-Ramp Effective Algorithm for Detection of ECG R-peaks. It is based on an intuitive and effective identification of inflexion points in the ECG cycle through the calculation of adjacent slopes between the signals. Traditional techniques require a number of expensive filtration stages in order to detect the R-peaks.

The R-READER approach significantly reduces the amount of filters and takes advantage of the unique shape and fiducial features of the ECG signal to accurately identify the R-peaks. It is compared with the Pan-Tompkins (P-T) algorithm - a popular lightweight algorithm used for the detection of R-peaks. The MIT-BIH Arrhythmia database was used for the analysis.

The Fiducial Points of an Electrocardiogram

An ECG signal is a record of the electrical activity of the heart and it is the basic cardiologic test used to analyze the condition of a patient's heart [124, 125]. It gives a graphic representation of the readings obtained from electrodes that are placed on the surface of the human skin and near the heart. [126]. The ECG signal is made up of a number of regions/fiducial points, namely the P-wave, Q-R-S complex and the T-wave as shown in Fig. 25. It traces a morphology identified by P, Q, R, S and T peaks and troughs [127]. The QRS-complex is the most distinguishing feature of the ECG and it serves as the basis for detection

and analysis. The peak of this complex is known and the R-peak and it is the most important point in virtually every ECG algorithm. The ECG signal has the most unique fiducial points when compared to other biosignals and R-READER takes advantage of this attribute.

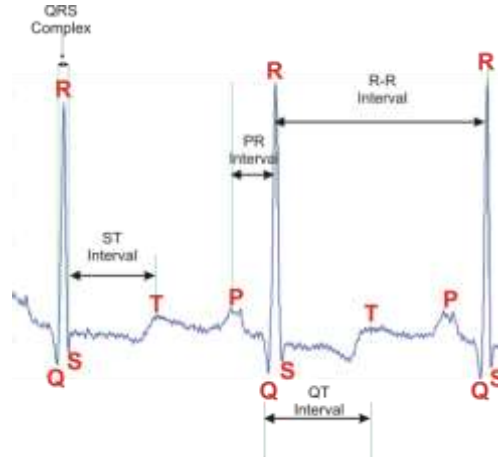


Figure 25: A Typical ECG Signal Showing the Fiducial Points

Automated R-peak Detection

As stated earlier, personalized health monitoring has become an important approach to patient care and ECG monitoring is the most common feature of this approach. The R-peak is the most striking point in the QRS complex. In general, the R-peak of an ECG cycle is that point in the cycle where the highest (or lowest) amplitude occurs. Its detection is the most important step in the diagnosis of cardiac disorders and is the basis for virtually all ECG algorithms [128]. The heart rate variability (HRV) can say a lot about a person's health. For example, diabetes, arrhythmias, sleep apnea, congestive heart failure, neonatal sepsis and even Post-traumatic stress disorder (PTSD) can be inferred from the heart rate and heart rate variability (HRV), all of which can be computed when the locations of the R-peaks are known [129, 130, 131, 132, 133].

There are a number of automated methods for the detection of the R-peaks of the ECG signals already in literature. A common approach for most existing methods involves the use of two stages, namely the preprocessor stage and the decision phase. The preprocessor phase is used to improve the general quality of the ECG signal; a major part of which is the denoising of the signal. After this is complete, the decision phase is activated for the selection of the per-cycle R-peak based on some given algorithm.

A range of techniques currently being used for these phases are based on *Derivatives & Digital Filters*, *Wavelet Transformation*, Neural Networks and Genetic algorithms amongst others [134, 135]. The Derivatives & Digital Filters approaches are the most common. This approach is based on the fact that typical ECG signals have frequency components between the ranges of about 10Hz to 25Hz. A filter stage is thus used to suppress components outside this range. The most well known algorithm in this approach is the algorithm proposed by Pan & Tompkins [136, 137]. Most research papers that focus on algorithms for the real-time detection of R-peaks compare themselves to the Pan-Tompkins algorithm. The paper has been cited 793 times [138].

The P-T algorithm uses a set of filters to extract a noise free ECG signal before the detection of R-peaks and the QRS complex. Prior to the detection phase, the P-T passes the ECG signal through low and high pass filters, followed by a differentiator, a squaring operator and a moving window integrator. These stages are shown in Fig. 26.

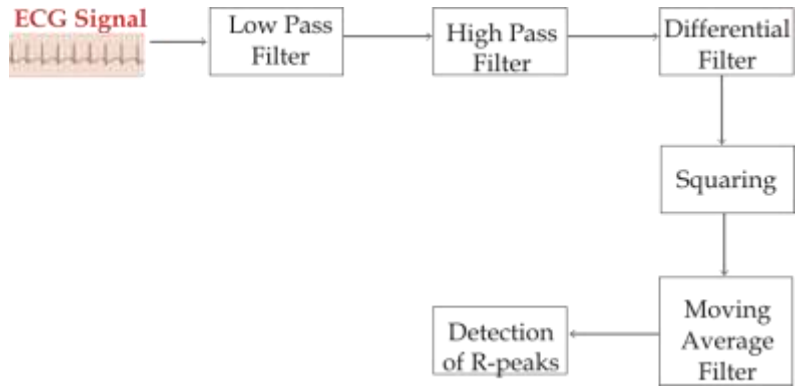


Figure 26: Steps in the Pan & Tompkins Algorithm

It also takes advantage of the fact that there is a steep slope in the region surrounding the QRS complex. The use of thresholds, θ and θ_2 , make up a major part of the P-T algorithm. These thresholds are determined after two learning phases and QRS complexes are only searched for in regions that exceed the thresholds; θ is the primary threshold of interest and θ_2 (which is a fixed fraction of θ) is only used as a backup threshold if no values exceed the primary threshold after a given time interval.

Noise and the ECG Signal

It is common to have ECG records that include noise from many sources [139]. Such noises include noise from sources like muscle movements and powerline interference. Muscle movement noise results from the patient’s movement, while power line interference is the 50/60Hz noise that is due to the presence of power lines around the location of the patient. The fiducial points in a noise-contaminated ECG signal may be obscured to such a point that detection can become difficult. An ECG analyzer performs many tasks, but its task of dealing with the noise has been identified as the major problem faced by system designers [140].

Traditional methods of dealing with noise involve the use of one or more types of filters- high pass low pass filters. However, the use of such methods presents two challenges; the first is that it increases the computational complexity of the system, along with the hardware and software resources required to obtain a reliable result. The second challenge is that the accuracy of the filtering depends on an accurate or near accurate knowledge of the *type(s)* of noise present in the ECG signal. The coloration of the noise can play an important role in the accuracy of the results. The ideal situation is for the system designer to know the type of noise(s) affecting the signal. However this is not always feasible. Also, the growing trend of ambulatory PHM of ECG signals further limits the designer's knowledge of the noise experience by the system in such a situation.

The R-READER approach has been designed to support lightweight and dependable analysis of ECG signals in the presence of different kinds of noise without the need to filter the signal prior to analysis.

Overhead and Complexity of Filtering Techniques

As mentioned earlier, the complexity of the preprocessing stage of the P-T algorithm introduces some overhead in the detection process. These overheads fall under different categories, including overhead in terms of time and memory. A total of four filtration steps are present in the P-T Algorithm, namely the low pass filter, high pass filter, differential filter and moving window integrator filter. The P-T algorithm uses approximate integer filter and this makes it suitable for lightweight real-time R-peak detection. An integer filter is a special type of filter that has only integer coefficients [141].

The P-T algorithm is widely acknowledged to be one of the ECG processing algorithms with the least degree of processing complexity. It uses approximate integer filters. This makes it

suitable for lightweight real-time R-peak detection and for use in PHM systems. However, the overhead incurred in the filtration phases still accounts for a significant amount of processing overhead.

Algorithms can be implemented in either software or hardware (usually with FPGAs), with the FPGAs generally considered to have better performance in terms of speed. By using integer filters the P-T algorithm is suitable for implementation in hardware. However, even with this advantage there is still a considerable penalty.

For example, with a Xilinx Spartan® xc3s5000 FPGA, an average delay of 16 samples is introduced in the low pass filter, 6 samples from the high pass filter, 2 samples from the derivative filter, 7 samples from the squaring and 16 samples from the moving window integrator [142]. This gives a total of 47 sample delays or a 235s delay at a sampling rate of 200Hz. Again, this inhibits the goal of a lightweight real-time PHM system.

Another penalty worth noting is the memory penalty. It depends on the amount of previous samples required to make a decision about a fiducial point. The preprocessor stage of the P-T algorithm requires at least 32 previous samples in order to determine a fiducial point. More often, due to possible delays in the processing stage, memory capacity in excess of this amount is required; [142] used 60 samples. These samples are stored in the system's RAM. These overheads do not even include the additional overhead required to implement the various filters.

MIT-BIH Arrhythmia Database

The Massachusetts Institute of Technology- Beth Israel Hospital (MIT-BIH) Arrhythmia database [143] contains 48 two-channel ambulatory ECG recordings that last for 30minutes each. They were sampled at 360 samples per second and have a resolution of 11 bits over a

10mV range. Each of the records includes a detailed annotation by experts and this provides a vital guide during the analysis of the accuracy of ECG algorithms. Most of the research articles focused on ECG algorithm use this as the test database [144]. The best (least noisy) record- Record #100 and the worst (most noisy) record- Record #108, were used to analyze R-READER and P-T algorithms.

B. The R-READER Process

The design of R-READER has been guided by the objectives of having a light-weight, fault (noise) tolerant, latency reducing and quasi-realtime ECG analyzer for rapid and dependable analysis even in resource constrained environments, such a mobile phones and personal digital assistants (PDAs). Thus, R-READER has been designed to strike a balance between the complexity of the algorithm and the dependability of the analysis. Many previous algorithms expend a lot of overhead on the preprocessor stages, especially the filtering of the signals. As such, a prime motive for this work is the design of a technique that reduces or eliminates the need for signal filtering without sacrificing the accuracy of the results.

R-READER is based on the characteristics of the slopes of adjacent ECG signals and the identification of inflection points in the signal. As shown in Fig 25, the ECG signal is comprised of 3 major parts, the most prominent of which is the QRS complex, with the R-peak being the distinguishing feature of the complex.

A close observation of an ECG signal shows that the absolute values of the ECG signals in the QRS complex have the greatest values when compared to the signals of the other regions. It gives a sloping surface between the interconnection levels, also known as a ramp, and this inspired our choice of the name for the algorithm. Using these varying slopes as a basis, we have developed an algorithm that can rapidly detect the QRS-complex region, especially the

start-of-complex, R-peak and end-of-complex. An example of the selection of fiducial points for one of the cycles in record #100 is shown in Fig. 27.

The slope, s , between any two signals, x , is given by Eq (25):

$$S = \frac{x_n - x_{n-1}}{t_n - t_{n-1}} \quad (25)$$

where x is the signal and t is the corresponding time

The time between samples is given by the sampling period and this is the inverse of the sampling frequency. In effect, every adjacent signal is separated by the same constant interval- the sampling period. This makes it possible to simplify the equation by removing the denominator to get a modified slope, s_m , for use in R-READER as shown in Eq (26). This approach reduces the complexity involved in implementing the algorithm.

$$S_m = x_n - x_{n-1} \quad (26)$$

where x is the signal

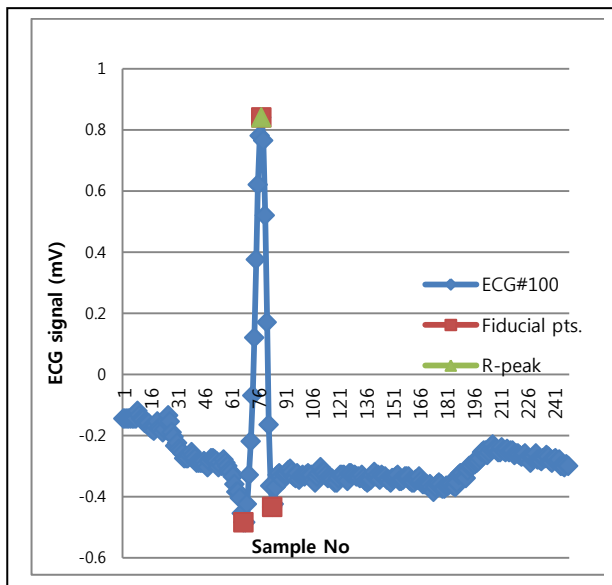


Figure 27: R-READER’s Selection of Fiducial and R-peak points for Record #100

Each of the fiducial points of the ECG signal occurs at an *inflexion* point. An inflexion point is a point on a graph where the slope *changes* sign. This simple point enables us to streamline the algorithm to obtain an efficient and accurate algorithm devoid of unnecessary complexity.

The steps are described below:

- (i) Find the modified slope, s_m , between two adjacent signals x_n and x_{n-1}
- (ii) Detect the presence of inflexion points from the slopes; inflexion points exist if there is a sign change between the adjacent modified slope values, $s_{m,n}$ and $s_{m,n-1}$
- (iii) Store the ECG signal x_n corresponding to the presence of a positive modified slope $s_{m,n+}$ as the candidate cycle-r-peak; also store its associated sample time, t_n
- (iv) Store the average maximum R-peak, R_{pmax} for the cycles 11-20 (the first 10 cycles are omitted to enable us obtain a R_{pmax} that reflects the overall ECG signal rather than the transients at startup)
- (v) Determined the peak-adjacency-interval-detector (p-a-i-d) as the average of the intervals between the first 10 R-peak values analyzed
- (vi) Subject the subsequent analysis to the following conditions:
 - a. the absolute value candidate cycle-r-peak must be greater than the R-peak threshold, R_{p-Th} , where $R_{p-Th} > 0.6 * R_{pmax}$
 - b. adjacency between candidate r-peaks must be at least 0.5 of the p-a-i-d, but not greater than 1.5 of the p-a-i-d
 - c. recompute R_{pmax} and/or p-a-i-d if the preceding 10 detected values fall below 0.8 of the current R_{pmax} and/or p-a-i-d of after 500 detected R-peaks, whichever comes first
- (vii) For multiple inflexion points in the region of interest, the following *4-point sieving criteria* is used:

- a. choose the maximum value closest to the p-a-i-d interval signal from the last selected R-peak
 - b. first priority is given to signals that are ± 5 samples from the p-a-i-d interval signal from the last selected R-peak
 - c. second priority is given to signals that are ± 5 inflexion points from the p-a-i-d interval signal from the last selected R-peak
 - d. third priority is given to signals that are ± 10 inflexion points from the p-a-i-d interval signal from the last selected R-peak
- (viii) Compare the R-peak signal points to the R-peak points in the annotated result
- (ix) Determine the accuracy, sensitivity and positive predictivity

The post-training steps in the R-READER 2.0 algorithm are depicted in the flowchart shown in Fig.28.

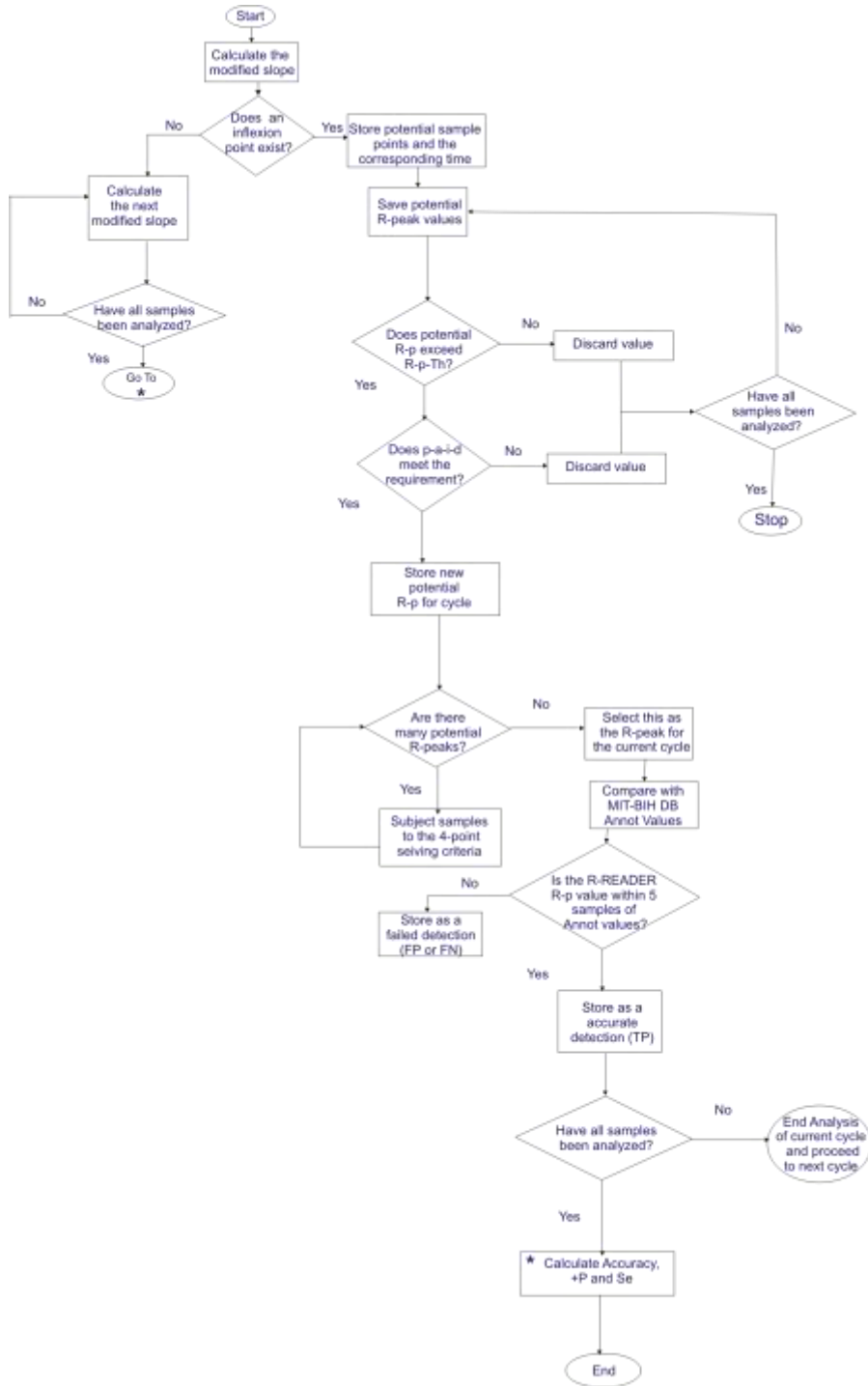


Figure 28: Flowchart of Steps in the R-READER Process

The R-READER Training Process, p-a-i-d and R_{pmax}

A training process, also known as learning phase, is an important requirement in many adaptable algorithms. It allows a designer to obtain an optimized result for any given scenario. The R-READER training process involves the implementation of the algorithm to detect the R-peaks in the first 20 cycles. For this phase, an initial R_{pmax} value of 0.6 is used.

For the R-READER algorithm there are two key parameters upon which the decisions are based- namely the R_{pmax} and the p-a-i-d. The R_{pmax} is the median maximum R-peak for a given set of cycles being reviewed. It gives a good estimate of the expected range of the R-peak in subsequent cycles and enables the selection of a threshold value as a fraction of the R_{pmax} . An initial value is determined at the onset of the execution of the algorithm and is used for the remainder of the analysis. However, R-READER is an adaptable algorithm, as such, a new calculation of R_{pmax} can be initiated by the system designer or automatically if the preceding 10 R-peaks of the current analysis all fall below 0.8 of the current R_{pmax} or after 500 detected peaks, whichever comes first.

The next important parameter is the peak-adjacency-interval-detector (or p-a-i-d). This parameter is also very crucial as it helps the algorithm to eliminate potential R-peaks that occur too soon after a selected R-peak. The basis of using this parameter stems from the fact that is physiologically impossible for a patient to encounter an R-peak within a given time window after a previous R-peak. The p-a-i-d value takes precedence over the R-p-Th in the determination of the R-peak for a given cycle. Again, the p-a-i-d value is obtained after the training process at the onset of the execution of the algorithm and a recalculation can be initiated automatically or by the system designer, similar to the case with R_{pmax} .

In both cases the training values from the first 10 cycles are discarded and the decisions are made based on the values obtained from cycles 11-20. This is to rule out the effect of transient values that are possibly obtained during the start of the ECG readings in preference for values that are likely to better reflect the overall ECG signals.

R-READER and Filtering Process

A key goal of the various filtering steps used in P-T and related algorithms is the accentuation of the fiducial points. Since all these fiducial points occur at inflexion points, R-READER focuses on locating all the existing fiducial points without filtering and these points are used as a basis for decision making in the R-READER process.

At a sampling rate of 200Hz, each ECG sample point occurs 5ms after the preceding sampled point. Noise, regardless of its coloration, occurs for a finite duration of the ECG signal and when it occurs it affects a group of succeeding samples, rather than just an individual sample. As such, it is still possible to accurately determine the relative inflexion points in an ECG signal even in the presence of noise.

C. Performance Evaluation

To assess the performance of R-READER, we have selected some records from the MIT-BIH Arrhythmia Database. In particular, we have chosen the best (least noisy) record- #100 and the worst (most noisy) record- #108. Both records run for approximately 30 minutes and include 650,000 samples, containing an average of over 2,000 cycles each. The #100 is from a 69 year old male patient, while the #108 is from an 87 year old female patient. Record #108 is widely acknowledged as being a very noisy signal [145].

The R-READER is compared with the popular Pan Tompkins algorithm using the following metrics:

- Average Accuracy
- Positive Predictivity and
- Sensitivity

In line with convention, the accuracy has been determined as the proportion of the true positives (TP), which is the number of right R-peak locations detected within ± 5 samples from the peak chosen by the annotators of the database [140]. The failed detections are the false positives (FP) and false negatives (FN). The false positives refer to detections made by R-READER that were not chosen by the annotators while the false negatives are the peaks that were not detected by R-READER but were identified by the annotators. The accuracy can be calculated by Eq (27).

$$\text{Accuracy} = \frac{1 - \text{Failed Detections}}{\text{Total Beats Given in Annotation}} \quad (27)$$

The positive predictivity, +P, is given by Eq (28):

$$+P = \frac{TP}{TP+FP} \quad (28)$$

The sensitivity, Se, is given by Eq (29):

$$S_e = \frac{TP}{TP+FN} \quad (29)$$

Tables 10 and 11 compare the R-peak positions chosen by R-READER for the first 20 cycles and the ones chosen by the annotators for records #100 and #108 respectively. It also gives the deviation between the R-READER detected values and those detected by the annotators.

Table 10. R-Peak Points in R-READER and Annotation for Record #100

Cycle #	R-READER R-peak	Annotated R-peak	Deviation
1	78	77	1
2	371	370	1
3	664	662	2
4	948	946	2
5	1232	1231	1
6	1516	1515	1
7	1810	1809	1
8	2046	2044	2
9	2404	2402	2
10	2707	2706	1
11	2999	2998	1
12	3284	3282	2
13	3561	3560	1
14	3864	3862	2
15	4172	4170	2
16	4467	4466	1
17	4766	4764	2
18	5062	5060	2
19	5348	5346	2
20	5635	5633	2

Table 11. R-Peak Points in R-READER and Annotation for Record #108

Cycle #	R-READER R-peak	Annotated R-peak	Deviation
1	23	23	0
2	88	89	1
3	442	442	0
4	789	791	2
5	1155	1156	1
6	1493	1493	0
7	1821	1822	1
8	2157	2158	1
9	2517	2518	1
10	2889	2890	1
11	3238	3238	0
12	3593	3594	1
13	3924	3926	2
14	4105	4104	1
15	4197	4198	1
16	4602	4604	2
17	4971	4972	1
18	5350	5351	1
19	5715	5716	1
20	6115	6115	0

Table 12 compares the R-READER and P-T algorithms for records #100 and #108 in terms of true positives, false positives, false negatives, accuracy, positive predictivity and sensitivity. Graphical comparisons of the accuracy, positive predictivity and sensitivity are shown in Fig. 27, Fig. 28 and Fig. 29 respectively.

Table 12. Accuracy of the R-READER Algorithm

Record#100							
<i>Algorithm</i>	<i>Total Number of ECG Cycles</i>	<i>TP</i>	<i>FP</i>	<i>FN</i>	<i>Accuracy</i>	<i>+P</i>	<i>S_e</i>
P-T	2273	2273	0	0	100.00%	100.00%	100.00%
R-READER	2273	2273	0	0	100.00%	100.00%	100.00%
Record #108							
<i>Algorithm</i>	<i>Total Number of ECG Cycles</i>	<i>TP</i>	<i>FP</i>	<i>FN</i>	<i>Accuracy</i>	<i>+P</i>	<i>S_e</i>
P-T	1763	1542	199	22	87.47%	88.57%	98.59%
R-READER	1763	1724	31	8	97.79%	98.23%	99.54%
Average Accuracy of Both Records							
<i>Algorithm</i>					<i>Accuracy</i>	<i>+P</i>	<i>S_e</i>
P-T					93.74%	94.29%	99.30%
R-READER					98.90%	99.12%	99.77%

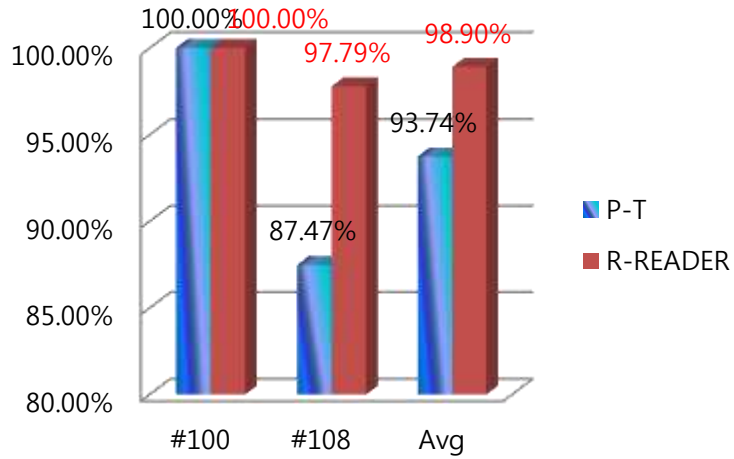


Figure 29: Accuracy Comparison for the 2 Algorithms

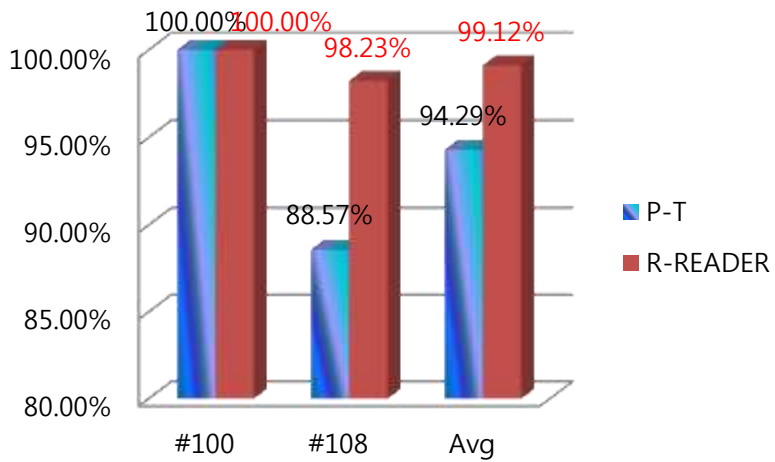


Figure 30: +P Comparison for the 2 Algorithms

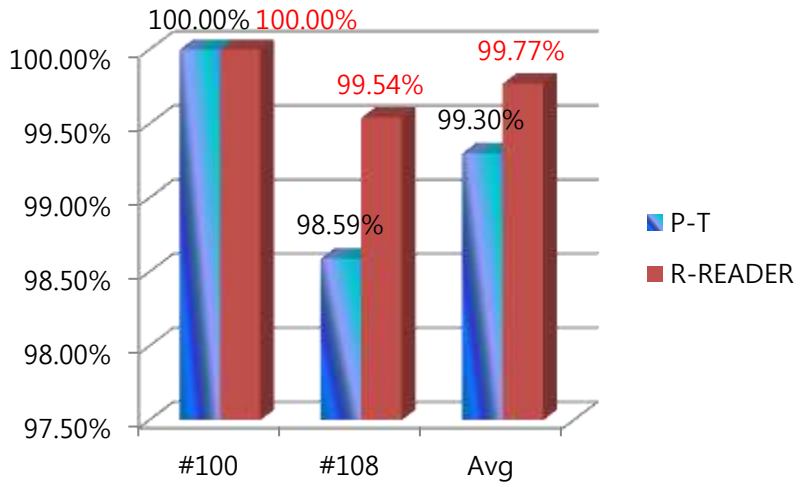


Figure 31: S_e Comparison for the 2 Algorithms

V. Conclusion and Future Work

A. Conclusion

In this thesis we have dealt with the design considerations for developing PHM systems. In particular, we have focused on the need for lightweight processing as a means of reducing the complexity of such systems. We noted the importance of system dependability in PHM systems and proposed some techniques that satisfy the need for lightweight processing as well as the need for system dependability.

The Cardiovascular and Neurologic domains were chosen as the main domains of interest. The former was chosen because it accounts for a large proportion of current PHM systems. The latter was chosen because of the growing interest in the domain as a result of the steep rise in the number of people with neurologic disorders around the world. We proposed a lightweight technique for each of the domains.

The Rapid-Ramp Effective Algorithm for Detection of ECG R-peaks (R-READER) algorithm was proposed for the cardiovascular domain. The current lightweight techniques require a cascade of filters before the detection of R-peaks of an ECG signal can take place. The R-READER is an intuitive technique that takes advantage of the unique shape of ECG signals to accurately detect the R-peaks without a need for the traditional filter approach. It was compared to the widely used Pan-Tompkins algorithm and it gave superior results in terms of accuracy, sensitivity and positive predictivity.

We also proposed a Bio-inspired electroceptive Compressive System (BeCoS) for the lightweight processing of neural signals. BeCoS was inspired by wave-type active

electroreception used by weakly electric fish. It included some key features of the electroreceptive approach and was able to achieve the lightweight sensing, processing, transmission and reconstruction of neural signals. BeCoS was compared to the Block Sparse Bayesian Learning-Bound Optimization (BSBL-BO) technique- a popular approach for lightweight processing of neural signals. Metrics like latency, coherence, level of compression, estimated power and structural similarity were used to compare both approaches. BeCoS gave superior results for most of the metrics.

B. Future Work

For future work we plan to develop algorithms for other PHM domains as well as algorithms that emphasize a need for adaptation to the unique characteristics of the patient, in addition to the current requirements for lightweight processing and system dependability. We intend to further profile and refine the R-READER by running it on embedded systems used for Holter-based long term monitoring of ECG signals.

The BeCoS approach has been used for the monitoring of neural signals in this thesis. However, the technique can be used telemetry of other biosignals as well, especially for signals that are difficult or expensive to sparsify. The signature signal also has the potential to be used as an EEG-based biometric and we plan to explore this possibility in the near future. By using an appropriate disease signature signal, this approach has the potential to be used for the screening of blood for diseases based on the computed values for resistance and capacitance.

Personalized health monitoring is still in its infancy and it has elicited a lot of interest. However, it is yet to be accorded the same level of priority and importance as the health monitoring based on medical instruments located at the hospital. The design of algorithms and techniques that support lightweight signal processing, system dependability and adaptation to

the patient's personal profile will improve the utility and importance of PHM systems.

References

- [1] Bhuiyan, M.Z.A. ; Guojun Wang ; Jiannong Cao ; Jie Wu. Deploying Wireless Sensor Networks with Fault-Tolerance for Structural Health Monitoring. *IEEE Transactions on Computers* 2015; 64(2): 382 – 395.
- [2] Clifton, D.A. ; Pimentel, M.A.F. ; Watkinson, P.J. ; Tarassenko, L. Gaussian Processes for Personalized e-Health Monitoring With Wearable Sensors. *IEEE Transactions on Biomedical Engineering* 2012; 60(1): 193 - 197.
- [3] Splinter, R.. Electroreception. Splinter, R. (ed). *Handbook of Physics in Medicine and Biology*, 1st ed. : CRC Press; 2010.
- [4] Pärkkä, J.. *Analysis of Personal Health Monitoring Data for Physical Activity Recognition and Assessment of Energy Expenditure, Mental Load and Stress*. PhD Thesis, Tampere University of Technology, Finland, 2011.
- [5] Marvasti, F.F. and Stafford, R.S. From Sick Care to Health Care — Reengineering Prevention into the U.S. System. *The New England Journal of Medicine* 2012; 367: 889 - 891.
- [6] Rozenblum, R. and Bates, D.W.. Patient-centred healthcare, social media and the internet: the perfect storm?. *BMJ Quality & Safety* 2012; 001744.
- [7] Misra, A. *Technology Challenges for Health Monitoring and Automated Stream Analysis*; Wayne State University Graduate Research Seminar 2008. http://www.cs.wayne.edu/graduateseminars/gradsem_w08/slides/s03_Misra.pdf (accessed 1 May 2015).
- [8] OECD. *Health at a Glance 2013: OECD Indicators Health at a Glance 2013: OECD Indicators*, OECD Publishing, Paris. http://dx.doi.org/10.1787/health_glance-2013-en (accessed 1 May 2015).
- [9] Shi, L. The Impact of Primary Care: A Focused Review. *Scientifica* 2012
- [10] OECD . *Health at a Glance 2011: OECD Indicators*, OECD Publishing, Paris. http://dx.doi.org/10.1787/health_glance-2011-en (accessed 1 May 2015).
- [11] Lafond, S. *Current NHS spending in England*. http://www.health.org.uk/media_manager/public/75/publications_pdfs/Funding%20overview_Current%20NHS%20spending%20in%20England.pdf (accessed 1 May 2015).
- [12] Gottlieb, S. and Makower, J. A Role for Entrepreneurs: An Observation on Lowering Healthcare Costs via Technology Innovation. *American Journal of Preventive Medicine* 2013; 44(1): S43 – S47.
- [13] Pawar, P., Jones, V. , van Beijnum , B-J.F. and Hermens, H. A framework for the comparison of mobile patient monitoring systems. *Journal of Biomedical Informatics* 2012; 45(3): 544 - 556.

- [14] Alumona T.L., Idigo V.E., and Nnoli K.P. Remote Monitoring of Patients Health using Wireless Sensor Networks (WSNs). *International Journal of Electronics & Communication* 2014; 2(9).
- [15] Islam, S.K., Fathy, A., Wang, Y., Kuhn, M. and Mahfouz, M. Hassle-Free Vitals: BioWireleSS for a Patient- Centric Health-Care Paradigm. *IEEE Microwave Magazine* 2014; 15(7): S25 - S33.
- [16] Estrin, D., Girod, L., Pottie, G. and Srivastava, M. Instrumenting the world with wireless sensor networks. *Proceedings of 2001 IEEE International Conference on Acoustics, Speech, and Signal Processing, Salt Lake City, USA* 2001; 4(): 2033 - 2036.
- [17] Patel S., Park, H., Bonato, P., Chan, L. and Rodgers, M. A review of wearable sensors and systems with application in rehabilitation. *Journal of NeuroEngineering and Rehabilitation* 2012; 9(21).
- [18] Clifton, L., Clifton, D.A., Pimentel, M.A.F., Watkinson, P.J. and Tarassenko, L. Gaussian Processes for Personalized e-Health Monitoring With Wearable Sensors. *IEEE Transactions on Biomedical Engineering* 2012; 60(1): 193 - 197.
- [19] Deloitte 2013 Survey of U.S. Physicians Physician perspectives about health care reform and the future of the medical profession. <http://www2.deloitte.com/content/dam/Deloitte/us/Documents/life-sciences-health-care/us-lshc-deloitte-2013-physician-survey-10012014.pdf> (accessed 1 May 2015).
- [20] Salem, O., Liu, Y., Mehaoua, A, and Boutaba, R. Online Anomaly Detection in Wireless Body Area Networks for Reliable Healthcare Monitoring. *IEEE Journal of Biomedical and Health Informatics* 2014; 18(5): 1541 - 1551.
- [21] Ordóñez, F.J., Toledo, P. and Sanchis, A. Sensor-based Bayesian detection of anomalous living patterns in a home setting. *Personal and Ubiquitous Computing archive* 2015; 19(2): 259 - 270.
- [22] Ko, J-G., Lu, C., Srivastava, M.B., Stankovic, J.A., Terzis, A. and Welsh, M.. Wireless Sensor Networks for Healthcare. *Proceedings of the IEEE* 2010; 98(11): 1947 - 1960.
- [23] Lam, S.C.K., Wong, K.L., Wong, K.O., Wong, W. and Mow, W.H. A smartphone-centric platform for personal health monitoring using wireless wearable biosensors. *7th International Conference on Information, Communications and Signal Processing, 2009. ICICS 2009; Macau.*
- [24] Nikita, K.S. *Handbook of Biomedical Telemetry*, 1st ed. : Wiley- Blackwell; 2014.
- [25] Malik, A.S., Khairuddin, R.N.H.R., Amin, H.U., Smith, M.L., Kamel, N., Abdullah, J.M., Fawzy, S.M. and Shim, S. EEG based evaluation of stereoscopic 3D displays for viewer discomfort. *BioMedical Engineering OnLine* 2015; 14(21).
- [26] *Interdisciplinary Assessment of Personal Health Monitoring*. Schmidt, S. and Rienhof, O. (Eds). IOS Press 2013.
- [27] Trajkovik, V., Vlahu-Gjorgievska, E., Kulev, I. and Koceski, S. Providing Collaborative Algorithms Support for Personal Health Care. *American Journal of*

- Bioinformatics* 2012; 1(1): 41 - 49.
- [28] A Survey of Electronics Obsolescence and Reliability; <http://www.dtic.mil/dtic/tr/fulltext/u2/a531873.pdf>
- [29] Avizienis, A., Laprie, J-C., Randell, B. and Landwehr, C. Basic concepts and taxonomy of dependable and secure computing. *IEEE Transactions on Dependable and Secure Computing* 2004; 1(1): 11 - 33.
- [30] *Cardiovascular diseases (CVDs) Fact sheet.* <http://www.who.int/mediacentre/factsheets/fs317/en/> (accessed 3 May 2015).
- [31] *Brain Disorders: By the Numbers.* <http://mcgovern.mit.edu/brain-disorders/by-the-numbers> (accessed 2 May 2015).
- [32] Olesen, J., Gustavsson, A., Svensson, M., Wittchen, H.U., Jönsson, B., CDBE2010 study group et al. The economic cost of brain disorders in Europe. *European Journal of Neurology* 2012; 19: 155 - 162.
- [33] *European Commission Human Brain Project.* https://www.humanbrainproject.eu/en_GB (accessed 29 April 2015).
- [34] *The Brain Research through Advancing Innovative Neurotechnologies (BRAIN) Initiative.* <http://braininitiative.nih.gov> (accessed 3 May 2015).
- [35] Koehler, F., Winkler, S., Schieber, M., Sechtem, U., Stangl, K., Böhm, M., Boll, H., Baumann, G., Honold, M., Koehler, K., Gelbrich, G., Kirwan, B.A. and Anker, S.D. Impact of remote telemedical management on mortality and hospitalizations in ambulatory patients with chronic heart failure: the telemedical interventional monitoring in heart failure study. *Circulation* 2011. 123(17)
- [36] Ricci, R.P., Morichelli, L. and Santini, M. Remote control of implanted devices through Home Monitoring technology improves detection and clinical management of atrial fibrillation. *Europace* 2009. 11(1):54-61.
- [37] Guerri JC, Antón AB, Pajares A, Monfort M and Sánchez D. A mobile device application applied to low back disorders. *Multimedia Tools and Applications*. 2009; 42(3): 317-340
- [38] Kang JM, Yoo T and Kim H-C. A Wrist-Worn Integrated Health Monitoring Instrument with a Tele-Reporting Device for Telemedicine and Telecare. *IEEE Transactions on Instrumentation and Measurement* 2006; 55(5): 1655-1662
- [39] Tsanas A, Little MA, McSharry PE and Ramig LO. Accurate telemonitoring of Parkinson's disease progression by noninvasive speech tests. *IEEE Transactions on Biomedical Engineering*. 2010;57(4):884-893.
- [40] Dellacà RL, Gobbi A, Pastena M, Pedotti A and Celli B. . Home monitoring of within-breath respiratory mechanics by a simple and automatic forced oscillation technique device. *Physiological Measurements*. 2010;31(4):N11-24.
- [41] Alves de Mesquita J Jr, Bouskela E, Wajnsberg E and Lopes de Melo P. Improved instrumentation for blood flow velocity measurements in the microcirculation of small animals *Review of Scientific Instruments* 2007; 78(2):024303

- [42] Madria S, Kumar V and Dalvi R. Sensor Cloud: A Cloud of Virtual Sensors. *IEEE Software* 2014; 31(2): 70-77.
- [43] Sticherling C, Kühne M, Schaer B, Altmann D and Osswald S. Remote monitoring of cardiovascular implantable electronic devices: prerequisite or luxury? *Swiss Med Wkly.* 2009;139(41-42):596-601.
- [44] Wang H, Peng D, Wang W, Sharif H, Chen H-H and Khoynezhad A. A. Resource-aware secure ECG healthcare monitoring through body sensor networks; *IEEE Wireless Communications* 2010; 17(1): 12-19.
- [45] Fanucci L, Saponara S, Bacchillone T, Donati M, Barba P, Sánchez-Tato I and Carmona C. Sensing Devices and Sensor Signal Processing for Remote Monitoring of Vital Signs in CHF Patients. *IEEE Transactions on Instrumentation and Measurement* 2013. 62(3): 553 – 569
- [46] Lee S-J, Kim J and Lee M. The Design of the m-Health Service Application Using a Nintendo DS Game Console. *Telemedicine and e-Health* 2011; 17(2):124-130.
- [47] Dilmaghani RS, Bobarshad H, Ghavami M, Choobkar S and Wolfe C. Wireless sensor networks for monitoring physiological signals of multiple patients. *IEEE Transactions on Biomedical Circuits and Systems* 2011; 5(4):347-56.
- [48] Hii P-C and Chung W-Y. A Comprehensive Ubiquitous Healthcare Solution on an Android™ Mobile Device. *Sensors (Basel)* 2011; 11(7): 6799–6815.
- [49] Cleven NJ, Müntjes JA, Fassbender H, Urban U, Görtz M, Vogt H, Gräfe M, Göttsche T, Penzkofer T, Schmitz-Rode T and Mokwa W. A novel fully implantable wireless sensor system for monitoring hypertension patients. *IEEE Transactions on Biomedical Engineering* 2012; 59(11):3124-30.
- [50] Pitts DG, Patel MK, Lang PO, Sinclair AJ and Aspinall R. A respiratory monitoring device based on clavicular motion. *Physiological Measurements* 2013;34(8):N51-61.
- [51] Anliker U, Ward JA, Lukowicz P, Tröster G, Dolveck F, Baer M, Keita F, Schenker EB, Catarsi F, Coluccini L, Belardinelli A, Shklarski D, Alon M, Hirt E, Schmid R and Vuskovic M. AMON: a wearable multiparameter medical monitoring and alert system. *IEEE Transactions on Information Technology in Biomedicine* 2004;8(4):415-27
- [52] Cheng CM, Hsu YL, Young CM and Wu CH. Development of a portable device for telemonitoring of snoring and obstructive sleep apnea syndrome symptoms. *Telemedicine and e-Health* 2008;14(1):55-68.
- [53] Chun H, Kang J, Kim KJ, Park KS and Kim HC. IT-based diagnostic instrumentation systems for personalized healthcare services. *Studies in Health Technology and Informatics* 2005;117:180-190.
- [54] Yu Y, Li J and Liu J. M-HELP: a miniaturized total health examination system launched on a mobile phone platform. *Telemedicine and e-Health* 2013;19(11):857-65.
- [55] Fong E-M and Chung W-Y. Mobile Cloud-Computing-Based Healthcare Service by Noncontact ECG Monitoring. *Sensors (Basel)* 2013, 13(12), 16451-16473.

- [56] Giansanti D, Morelli S, Maccioni G and Grigioni M. Portable kit for the assessment of gait parameters in daily telerehabilitation. *Telemedicine and e-Health* 2013;19(3):224-32.
- [57] Gómez EJ, Hernando Pérez ME, Vering T, Rigla Cros M, Bott O, García-Sáez G, Pretschner P, Brugués E, Schnell O, Patte C, Bergmann J, Dudde R and de Leiva. A. The INCA system: a further step towards a telemedical artificial pancreas. *IEEE Transactions on Information Technology in Biomedicine* 2008;12(4):470-479.
- [58] D'Arcy RC, Hajra SG, Liu C, Sculthorpe LD and Weaver DF. Towards brain first-aid: a diagnostic device for conscious awareness. *IEEE Transactions on Biomedical Engineering* 2011;58(3):750-4.
- [59] Chen W, Zhu X, Nemoto T, Kitamura K, Sugitani K and Wei D. Unconstrained monitoring of long-term heart and breath rates during sleep. *Physiological Measurements* 2008;29(2):N1-10.
- [60] Nemiroski A, Christodouleas DC, Hennek JW, Kumar AA, Maxwell EJ, Fernández-Abedul MT and Whitesides GM. Universal mobile electrochemical detector designed for use in resource-limited applications;; *Proceedings of the National Academy of Sciences of the United States of America* 2014;111(33):11984–11989.
- [61] Lee Y, Lee B and Lee M. Wearable sensor glove based on conducting fabric using electrodermal activity and pulse-wave sensors for e-health application. *Telemedicine and e-Health* 2010;16(2):209-17. doi: 10.1089/tmj.2009.0039
- [62] Olansen JB and Rosow E. *Virtual Bio-Instrumentation: Biomedical, Clinical, and Healthcare Applications in LabVIEW*. Prentice Hall PTR. December 2001
- [63] *Managing Performance Measurement Data in Health Care Second Edition*; Joint Commission Resources; Jaclyn Graham (Executive Editor), 2008 by Joint Commission on Accreditation of Healthcare Organizations
- [64] Malathi P and Kirthika B. Performance Analysis of Hybrid (SVM+ICA) Method for two class dataset. *International Journal of Advance Research in Computer Science and Management Studies* 2014; 2(1): 656-661.
- [65] Esmaeeli S and Gholampour I. Reduced memory requirement in hardware implementation of SVM classifiers. *Proceedings of the 20th Iranian Conference on Electrical Engineering (ICEE), 2012* May 15-17; p. 46-50. Tehran, Iran
- [66] Harikumar R, Vijayakumar T and Sreejith MG. Performance Analysis of Support Vector Machine (SVM) for Optimization of Fuzzy Based Epilepsy Risk Level, Classifications from EEG Signal Parameters. *Proceedings of Recent Advances in Intelligent Computational Systems (RAICS), Trivandrum, India, 2011* September 22-24: 351-354.
- [67] Sivanandam SN and Deepa SN. *Introduction to Genetic Algorithms*; Springer Berlin, Heidelberg, Germany; 2008
- [68] Jabbar MA, Deekshatulu BL and Chandra P. Heart Disease Prediction System using Associative Classification and Genetic Algorithm. *Proceedings of International*

- Conference on Emerging Trends in Electrical, Electronics and Communication Technologies (ICECIT), 2012 December 21-23: 183-192
- [69] Kew HP and Jeong DU. Variable threshold method for ECG R-peak detection. *J Med Syst.* 2011;35(5):1085-1094
- [70] Wang J, Zhang Z, Li B, Lee S and Sherratt RS. An enhanced fall detection system for elderly person monitoring using consumer home networks. *IEEE Transactions on Consumer Electronics* 2014; 60(1): 23 – 29
- [71] Nandy S, Das A and Sarkar PP. An Improved Gauss-Newtons Method based Back-propagation Algorithm for Fast Convergence. *International Journal of Computer Applications* 2012; 39(8):1-7.
- [72] Jin Z, Oresko J, Huang S and Cheng AC. HeartToGo: a personalized medicine technology for cardiovascular disease prevention and detection. *Proceedings of IEEE/NIH Workshop on Life Science Systems and Applications, Bethesda, USA., 2009 April 9-10: 80-83.*
- [73] Strohmer T. Measure What Should be Measured: Progress and Challenges in Compressive Sensing. *IEEE Signal Processing Letters*; 19(12): 887 - 893.
- [74] Craven D, McGinley B, Kilmartin L, Glavin M, Jones E. Compressed Sensing for Bioelectric Signals: A Review. *IEEE Journal of Biomedical and Health Informatics*; 19(2): 529-540
- [75] Gama J. *Knowledge Discovery from Data Streams.* Chapman and Hall/CRC . 2010
- [76] Zhu W, Zeng N and Wang N. Sensitivity, Specificity, Accuracy, Associated Confidence Interval and ROC Analysis with Practical SAS Implementations. 2010. [Accessed 14 April , 2015]; <http://www.nesug.org/Proceedings/nesug10/hl/hl07.pdf>.
- [77] Codagnone C. *Reconstructing the Whole: Present and Future of Personal Health Systems.* 2009. [Accessed 5 May 2015]. http://www.evia.imasdtic.es/cli_aetic/ftpportalweb/documentos/phs2020-book-rev16082009.pdf
- [78] Hood L. and Rowen, L. The Human Genome Project: big science transforms biology and medicine; *Genome Medicine* 2013, 5(9).
- [79] Deighton, B. Personal health data clouds to give early warning for cancer, other diseases. http://horizon-magazine.eu/article/personal-health-data-clouds-give-early-warning-cancer-other-diseases_en.html [Accessed 5 May 2015].
- [80] *Genomic Medicine: Principles and Practice* (2nd edition). Kumar, D. Eng, C. (Eds). 2014. Oxford University Press; 2 edition
- [81] McDaid, D. *Countering the stigmatisation and discrimination of people with mental health problems in Europe* European Commission, Luxembourg. 2008.
- [82] Islam SK., Fathy A, Wang Y, Kuhn M and Mahfouz M. Hassle-Free Vitals: BioWireleSS for a Patient-Centric Health-Care Paradigm. *IEEE Microwave Magazine*: 15(7): S25 – S33.

- [83] Heurtefeux K., Mohsin N, Hamida EB and Menouar H. Dynamic and Energy Efficient Wireless BAN Platform for Remote Health Monitoring; 2014 IEEE 10th International Conference on Wireless and Mobile Computing, Networking and Communications (WiMob) Larnaca, Cyprus: 548-555.
- [84] Salem O, Liu Y, Mehaoua A and Boutaba R. Online Anomaly Detection in Wireless Body Area Networks for Reliable Healthcare Monitoring. *IEEE Journal of Biomedical and Health Informatics*. 2014. 18(5): 1541-1551
- [85] Gao T, Massey T, Selavo L, Crawford D, Chen, B-r, Lorincz K., Shnayder V, Hauenstein L, Dabiri F, Jeng J, Chanmugam A., White D, Sarrafzadeh M and Welsh M. The Advanced Health and Disaster Aid Network: A Light-Weight Wireless Medical System for Triage. *IEEE Transactions on Biomedical Circuits and Systems*. 2011. 1(3): 203 – 216.
- [86] Chi YM, Jung T-P and Cauwenberghs G. Dry-Contact and Noncontact Biopotential Electrodes: Methodological Review. *IEEE Reviews in Biomedical Engineering*, 2010. 3:106-119.
- [87] Chi YM, Wang Y-T, Wang Y, Maier C, Jung T-P and Cauwenberghs G. Dry and Noncontact EEG Sensors for Mobile Brain-Computer Interfaces. *IEEE Transactions on Neural Systems and Rehabilitation Engineering*, 2012. 20(2): 228-235
- [88] Bernacchia N, Scalise L, Casacanditella L, Ercoli I, Marchionni P and Tomasini EP. Non contact measurement of heart and respiration rates based on Kinect™. 2014 IEEE International Symposium on Medical Measurements and Applications (MeMeA). June 2014; Lisbon, Portugal: 1-5.
- [89] Probing Experience; From Assessment of User Emotions and Behaviour to Development of Products. 2008. Westerink, J., Ouwkerk, M., Overbeek, T.J.M., Pasveer, W.F. (Eds.). Springer Netherlands.
- [90] Meddins R. Introduction to Digital Signal Processing (1st edition). Newnes; 2000.
- [91] Davenport MA, Boufounos PT, Wakin MB and Baraniuk RG. Signal Processing With Compressive Measurements. *IEEE J Selected Topics in Sign Processing*. 2010: 4(2): 445-460
- [92] Zhang Z and Rao BD. Extension of SBL Algorithms for the Recovery of Block Sparse Signals With Intra-Block. *IEEE Transactions on Signal Processing*. 2013. 61(8): 2009-2015
- [93] Zhang Z, Jung T-P, Makeig S and Rao BD. Compressed Sensing of EEG for Wireless Telemonitoring with Low Energy Consumption and Inexpensive Hardware. *IEEE Transactions on Biomedical Engineering* 2013. 60(1): 221-224.
- [94] Map of Life - "Electroreception in fish, amphibians and monotremes" http://www.mapoflife.org/topics/topic_41_Electroreception-in-fish-amphibians-and-monotremes/ (Accessed on February 02, 2015)
- [95] Splinter R (Ed). *Handbook of Physics in Medicine and Biology*; CRC Press; Taylor and Francis Group, USA, 2010.

- [96] Electric Organ Discharge.
http://classic.sidwell.edu/us/science/21bio/new/wef_eod.html
- [97] Snyder JB, Nelson ME, Burdick JW and Maciver MA. Omnidirectional sensory and motor volumes in electric fish. *PLoS Biol* 2007; 11 (e301): 2009-2015
- [98] Scheich H and Bullock TH. The detection of electric fields from electric organs. In *Handbook of Sensory Physiology*, vol. III/3 (ed. A. Fessard). 1974: 201–256. New York: Springer
- [99] von der Emde G and Ronacher B. Perception of electric properties of objects in weakly electric fish: two-dimensional similarity scaling reveals a City-Block metric. 1994. *Journal of Comparative Physiology A*. 175(6): 801-812
- [100] Kramer B. Electric communication and electrolocation. In M. D. Binder, N. Hirokawa & U. Windhorst (Eds) *Encyclopedia of Neuroscience*. 2009: 1038-1045. Berlin Heidelberg: Springer Verlag.
- [101] The energetics of electric organ discharge generation in gymnotiform weakly electric fish; <http://jeb.biologists.org/content/216/13/2459/F1.expansion.html> (Accessed on April 13, 2015)
- [102] Hanika S and Kramer B. Plasticity of electric organ discharge waveform in the South African Bulldog fish, *Marcusenius pongolensis*: tradeoff between male attractiveness and predator avoidance? 2008. *Frontiers in Zoology* 5:7
- [103] Kramer B. Electoreception and communication in fishes. *Progress in Zoology*, 42. Rathmayer W (Ed). 1996. Gustav Fischer, Stuttgart.
- [104] Kramer B and Kuhn B. Electric signalling and impedance matching; The Electric Organ of Mormyrid Fish Actively Adapts to Changes in Water Conductivity. 1993. *Naturwissenschaften* 80: 43-46. Springer-Verlag
- [105] The Physionet Database <http://www.physionet.org/> (Accessed on May 08, 2015)
- [106] Lachaux JP, Rodriguez E, Martinerie J and Varela FJ . Measuring phase synchrony in brain signals. *Human Brain Mapping*, 1999. 8(4): 194-208
- [107] La Rocca D, Campisi P, Vegso B, Cserti P, Kozmann G, Babiloni F, and De Vico Fallani F. Human Brain Distinctiveness Based on EEG Spectral Coherence Connectivity. *IEEE Transactions on Biomedical Engineering*. 2014: 61 (9):2406-2412
- [108] Golinska AK. Coherence function in biomedical signal processing: a short review of applications in Neurology, Cardiology and Gynecology; *Studies in Logic, Grammar and Rhetoric*, 2011. 25(38): 73-82.
- [109] Welch PD. The Use of Fast Fourier Transform for the Estimation of Power Spectra: A Method Based on Time Averaging Over Short, Modified Periodograms. *IEEE Transactions on Audio and Electroacoustics*. 1967. AU-15:70–73.
- [110] Zeng M, Lee J-G, Choi G-S and Lee J-A. Intelligent sensor node based on a low power ECG monitoring system. *IEICE ELEX* 2009: 6(9): 560-565
- [111] Köhler BU, Hennig C and Orglmeister R. *The Principles of Software QRS*

- Detection.; IEEE Engineering in Medicine and Biology Magazine 2002: 21(1):42-57.
- [112] Wang Z and Bovik AC. Mean squared error: Love it or leave it? A new look at Signal Fidelity Measures. Signal Processing Mag. 2009: 26(1):98 - 117.
- [113] Kudeki E. Analog Signals and Systems. 2008. Publisher: Prentice Hall, New Jersey, USA.
- [114] Haliday D. Fundamentals of Physics. 2010. 9th Edition. Wiley, New Jersey, USA.
- [115] Bedard C and Destexhe A. A generalized theory for current-source density analysis in brain tissue 2011. Physical Review E, 84: 041909
- [116] Andrea M, Ettore R, Paolo G, Riccardo B and. Kimimila IL. A New Model to Classify NGS Short Reads by their Allele Origin. 2014 IEEE International Conference on Healthcare Informatics (ICHI), Verona, Italy: 340-342.
- [117] Numez PL and Srinivasan R. Electric Fields of the Brain: The Neurophysics of EEG, Oxford University Press, Oxford, United Kingdom, 2006.
- [118] Xiang Y and Liu S. Coherent high-order harmonic generation by sawtooth-like laser fields. 2013. Optics Express 21(9):11270-11275.
- [119] Berkhout J and Walter DO. Temporal stability and individual differences in the human EEG: An analysis of variance of spectral values. 1968. IEEE Transactions on Biomedical Engineering. 15(3): 165– 168.
- [120] Vogel F and Schalt E. The electroencephalogram (EEG) as a research tool in human behavior genetics: Psychological examinations in healthy males with various inherited EEG variants. 1979. Human Genetics. 47: 81–111
- [121] Campisi P and La Rocca D, Brain waves for automatic biometric based user recognition, IEEE Transactions in Information Forensics and Security. 2014. 9(5): 782 – 800
- [122] Simple Bus Architecture; <http://sba.accessus.com/> (Accessed on May 06, 2015)
- [123] The WISHBONE System-on-Chip (SoC) Interconnect Architecture for Portable IP Cores; <http://opencores.org/opencores,wishbone> (Accessed on May 13, 2015)
- [124] Yang H, Kan C, Liu G and Chen Y. Spatiotemporal Differentiation of Myocardial Infarctions. IEEE Transactions on Automation Science and Engineering, 2013: 938-947
- [125] Nemati E, Deen, MJ and Mondal T. A wireless wearable ECG sensor for long-term applications. IEEE Communications Magazine, 2012. 50(1): 36 - 43,
- [126] Tello JP, Manjarres O, Quijano M, Blanco A, Varona F and Manrique M. Remote Monitoring System of ECG and Human Body Temperature Signals. IEEE (Revista IEEE America Latina) Latin America Transactions. 2013. 11(1): 314 - 318;
- [127] Dong J, Zhang J-w, Zhu H-h., Wang L-p, Liu X. and Li Z-j. A Remote Diagnosis Service Platform for Wearable ECG Monitors. 2012. IEEE Intelligent Systems. 6(27): 36 – 43
- [128] Liu X, Yang J, Zhu X, Zhou S, Wang H and Zhang H. A Novel R-peak

- Detection Method Combining Energy and Wavelet Transformation in Electrocardiogram Signal. Biomedical Engineering: Applications, Basis and Communications. 2014. 26(1)
- [129] What the heart can tell us about the mind: Heart rate variability and PTSD; http://www.research.va.gov/currents/summer2014/summer_2014-25.cfm (Accessed on April 2, 2015)
- [130] Minassian A, Geyer MA, Baker DG, Nievergelt CM, O'Connor DT and Risbrough VB. Heart rate variability characteristics in a large group of active-duty marines and relationship to posttraumatic stress. Psychosomatic Medicine 2014 . 76(4):292-301.
- [131] Freeman R. HRV in Diabetes and Other Disorders; HRV 2006: Techniques, Applications and Future Direction; Boston, USA, April 2006.
- [132] Stein PK. HRV and Risk Stratification:Post-MI; HRV 2006: Techniques, Applications and Future Direction; Boston, USA, April 20, 2006.
- [133] Griffin P and Moorman R. Heart rate characteristics Heart rate characteristics monitoring monitoring to detect neonatal sepsis ; HRV 2006: Techniques, Applications and Future Direction; Boston, USA, April 20, 2006.
- [134] Hossein R, Mahjoob MP, Farahabadi E and Farahabadi A. R Peak Detection in Electrocardiogram Signal Based on an Optimal Combination of Wavelet Transform, Hilbert Transform, and Adaptive Thresholding. 2011. Journal of Medical Systems and Sensors. May-Aug; 1(2): 91–98.
- [135] Jeong CI., Vai MI and Mak PU. QRS Recognition with Programmable Hardware. 2nd International Conference on Bioinformatics and Biomedical Engineering, Shanghai, China, May, 2008: 2028 – 2031.
- [136] Pan J and Tompkins WJ. A Real-Time QRS Detection Algorithm. IEEE Transactions on Biomedical Engineering. 1985. 32(3): 230 - 236;
- [137] Álvarez RA, Penín AJM and Sobrino XAV. A Comparison of Three QRS Detection Algorithms Over a Public Database. 2013. Procedia Technology. 9: 1159–1165
- [138] Citations for "A Real-Time QRS Detection Algorithm";<http://ieeexplore.ieee.org/xpl/abstractCitations.jsp?arnumber=4122029>
- [139] Elgendi M. Fast QRS Detection with an Optimized Knowledge-Based Method: Evaluation on Standard ECG Databases. 2013. PLoS ONE 8(9): e73557.
- [140] Noise Stress Testing. <http://www.physionet.org/physiotools/wag/evnode14.htm> (Accessed on April 6, 2015)
- [141] Afonso VX. ECG QRS detection In: Biomedical digital signal processing 1993: 236-264). Prentice-Hall, Inc.Tompkins, W.J. (Ed)
- [142] Shukla A. and Macchiarulo L. A Fast and Accurate FPGA based QRS detection System. IEEE Engineering in Medicine & Biology Society Conference 2008. Vancouver, Canada: 4828~4831.

- [143] Massachusetts Institute of Technology- Beth Israel Hospital (MIT-BIH) Arrhythmia database ; www.physionet.org/physiobank/database/mitdb/ (Accessed on April 11, 2015)
- [144] Clifford GD, Azuaje F and McSharry P. Advanced Methods and Tools for ECG Data Analysis. Artech House Publishers, 2006
- [145] Cassiano KK and Nadal J. Software Library for Real-Time Cardiac Beat Detection. 17th International Conference on Systems, Signals and Image Processing. Rio de Janeiro, Brazil, June 2009: 546-549.

Appendix A

APPENDIX A. Summary of Studies included in the Review								
S/N	AUTH-ORS	YEAR	JOURNAL	ARCHITECTURE	APPLICATION	ADAPTATION/PERSONALIZATION	STUDY DESIGN	OUTCOME/ RESULTS
1.	Koehler et al. 2-1	2011	Circulation (Journal of the American Heart Association)	12-lead ECG, BP, Weight; Dynamic encryption on cell phone; PDA (Central Device), Bluetooth (Communication)	Impact of remote monitoring on Chronic Heart Failure		710 stable chronic heart failure patients; 17-month (duration); Low statistical power (limitation); Study evaluated effect of remote telemonitoring on mortality.	Primary outcome: Rate of all cause mortality (death) was reduced to 8.4% as compared with 8.7% for normal care; Secondary outcome: Cardiovascular death and hospitalization per 100 person years of follow up reduced to 14.7% as compared to 16.5% for normal care.
2.	Ricci et al 2-2	2009	Eurospace (Europe Society for Cardiology)	Home monitoring, long distance telemetry, automatic transmission of pacemaker data on a daily basis; Implanted cardio device (ICD) with wireless telemetry via a GSM phone as encrypted sms; Data transmitted every night and critical conditions are reported to service center within 3 minutes; Error detection to distinguish between true arrhythmias and R-wave far field oversensing.	Impact of home monitoring on Atrial Fibrillation (AF)	Pacemaker and ICD programming was tailored to patient's individual clinical profile	166 patients for 2 years	Remote monitoring led to AF detection and alert that occurred an average of 148days before scheduled follow up visit Limitation: It was an observational study with no clinical outcome Open issue: how to select appropriate alerts
3.	Guerri et al 2-3	2009	Multimedia Tools and Applications	8-channel Surface EMG, Portable handheld prototype (Platform), connected to phone/PDA via WiFi; PDA: HP IPAQ HX4700, phone: Nokia E41; Includes online telemetry mode and offline mode (with storage on CF card)	Use of mobile devices and wireless networking for assessment of muscular conditions	Configured via a mobile device; Configuration was based on patient's profile or system parameters like duration of exercise, sampling frequency and monitored muscle Config modes: Offline and online	Duration: 55 seconds Phase 1: Feasibility and Reliability: 12 volunteers Phase 2: Usability Assessment: Questionnaires completed by 7 users	Design of a portable device capable of advanced EMG measurements Can be used by both expert and non-expert users
4.	Kang	2006	IEEE	Wrist worn device with 6 biosensors for: (i) Fall detection [2-axis	Wrist-worn		Limitation: Low fidelity	Error Range and Detection

	et al. ²⁻⁴		Transactions on Instrumentation and Measurement	<p>accelerometer, gyroscope and in-house posture sensor] (ii) 1-channel ECG textile electrode (iii) Noninvasive BP [based on a wrist cuff] (iv) SPO2 (v) Respiratory Rate [based on Virtual sensing of r-r intervals of ECG] and (vi) Body Surface Temperature</p> <p>A cellular phone was used as the connection gateway; wireless connection used between wrist worn device and phone; CDMA was used for connection between the phone and medical service center</p> <p>Main algorithms were based on thresholding</p>	<p>device for general health monitoring</p> <p>Anomalies were reported via sms</p>		<p>of biosignals since most measurements were based on readings from the skin. Tests were based on simulated signals and human trials</p>	<p>Rates: ± 5mmHg (NIBP), 2%(SPO2), 1%(ECG), 1.8% (Respiration Rate), 1.5% (Temperature), 91.3% detection rate for 150 simulated falls</p>
5.	Tsanas et al ²⁻⁵	2010	IEEE Transactions on Biomedical Engineering	<p>Virtual sensing based on speech tests from a microphone headset on an Intel AHTD Telemonitoring System for predicting Parkinson's Disease (PD)</p> <p>Algorithm was based on thresholding.</p> <p>Speech signal processing was based on 16 dysphonia measures applied to 5923 sustained phonations.</p>	<p>Accurate system for tracking the progression of Parkinson's Disease Rating Scale (UPDRS).</p> <p>Statistical mapping of a subset of speech features to UPDRS.</p> <p>It showed the potential of sustained vowel phonations in predicting average PD progression.</p>		<p>It was based on 6,000 database recordings from 42 PD patients.</p> <p>Based on objective (rather than subjective) assessment.</p> <p>Human trial was based on a 6 month study of 42 idiopathic PD patients.</p>	<p>This virtual sensing approach can estimate the result within about 7.5. UPDRS points difference from the clinicians' estimates using a simple, self administered non-invasive test.</p>
6.	Dellaca et al ²⁻⁶	2010	Physiological Measurement	<p>Pressure and flow sensors.</p> <p>Respiratory input impedance (Zrs) was measured after a 5Hz pressure stimulus from a loudspeaker was transmitted to the patient through a self-made mesh-type Pneumotachograph (PNT).</p> <p>Zrs was computed using the Least squares algorithm and transmitted over the Internet.</p> <p>Communication was based on GPRS, DSL or WiFi (depending on availability).</p> <p>Encryption was based on Public Key Algorithm.</p> <p>Realtime or scheduled transmission options were available.</p> <p>Reliable and standardized TCP/IP connection was established by using SSH.</p>	<p>Forced Oscillation Technique (FOT) device for unsupervised monitoring to replace supervised spirometry.</p> <p>Useful for diagnosis and staging of obstructive diseases (like COPD and asthma)</p>		<p>5 healthy subjects, 36 consecutive daily home measurements.</p> <p>Reduces the dimensions of current FOT device</p> <p>36 consecutive daily home measurements.</p> <p>Extensive tests on 7 subjects.</p> <p>Limitation: Only 1 COPD patient was used in the tests.</p>	<p>The portable FOT device can be used for unsupervised assessment of airway obstruction over prolonged periods. The maximum error was 10%.</p>
7.	Mesqu	2007	Review of	<p>Photosensor head and photodiodes (Sensors).</p>	<p>Blood flow</p>		<p>Adding a virtual</p>	<p>In vivo tests for 7-10 week old</p>

	ita J Jr et al ²⁻⁷		Scientific Instruments	It was used to implement a virtual velocimeter based on digital cross correlation techniques.	measurements that are less dependent on operator bias. Samples optical signals from microvessel and gives instant velocity.		instrument module to an existing microcirculation hardware reduces operator bias and allows digital signal processing and storage. The manual system depended on the tuning of the system making it susceptible to operator bias.	golden hamsters Pharmacological intervention: successful and accurate monitoring of blood flow velocity in one arteriole analyzed before and after the administration of phenylphrine.
8.	Stichering et al ²⁻⁹	2009	Swiss Medical Weekly	CIED; based on optivol sensor that measured intrathoracic impedance upon the accumulation of intrapulmonary fluid. GSM was used for remote monitoring.	Remote monitoring of ICDs for early detection of disease and device anomaly. It was also used to number of patient visits to the hospital.		It was a survey.	
9.	Wang et al ²⁻¹⁰	2010	IEEE Wireless Communications	It used a 3-lead ECG sensor with a transmission range of 100m. It used a low delay adaptive encryption scheme dependent on the condition of the wireless channel.	Secure and resource aware body sensor network architecture for real-time health monitoring based on unequal resource allocations It used an on-body healthnode data terminal to process and transmit sensor data.		The system allocated extra energy resources to protect the important portion of the transmitted signal.	The tests were based on simulation and real time tests. This lowered energy consumption and gave better signal quality per energy used. Authors stated that shorter QRS windows can improve real-time encryption.
10.	Fanucci et al ²⁻¹¹	2013	IEEE Transactions on Instrumentation and Measurement	7 Sensors: (i) 3-lead ECG (ii) SPO2 (iii) BP (iv) Weight (v) Chest impedance (vi) Respiration (vii) Posture Local-MVI communication: Bluetooth Remote-MVI communication: ADSL or mobile broadband. HTTPS used for security and encryption. A prototype was built and the Pan-Tompkins algorithm was used	Flexible and highly configurable system for monitoring Chronic Health Failure (CHF). It provided alerts	Configuration parameters: Alarm thresholds, transmission policy, selectable symptoms. It also supported	One or few non-continuous daily measurements were made.	ECG simulators and Physionet Toolkit were used for analysis. Pre-prototype tests: 2 patients, 1 month test Post-prototype tests: 30 patients with Chronic Health Failure disease

				for ECG analysis.	for abnormal heart frequency, atrial fibrillation episodes, QRS complexes exceeding 120ms and signs of myocardial ischemia.	remote configuration.		Results: <3% activity misses (mostly in the 1st days). <5% false positive alarms, 95% patients found the system useful and 99% patients were satisfied with system.
11.	Lee et al ²⁻¹²	2011	Telemedicine and e-Health	<p>The system used a Nintendo DS Game Console as the platform. However, the system can also use a PC or PDA.</p> <p>3-channel ECG, 3-axis accelerometer ($\pm 3g$), Tilting (Sensors)</p> <p>1 ECG packet consists of 64 ECG signals</p> <p>ZigBee was used for the local-MVI communication while WiFi was used for the Remote-MVI communication. The system also included a webserver.</p>	Mobile health ECG and gait monitoring system that obviates distance restrictions.			<p>It used a 1 hour test to ensure appropriate wireless connectivity.</p> <p>The Health monitoring test lasted for over 24 hours without any interruption.</p> <p>Packet Loss: <5% for distances less than 20m, much higher and incremental loss beyond 20m</p> <p>For packet error rate (Pe): When Pe=0, no delay; Pe=0.2, 25s delay and Pe=0.4, 157s delay (due to the need for retransmission)</p>
12.	Dilma ghani et al ²⁻¹³	2011	IEEE Transactions on Biomedical Circuits and Systems	<p>ECG (Sensor).</p> <p>Its Wireless Patient Portable Unit (Platform) had a webserver and connected to a central remote node via Internet access provided by a Wireless Access Point Unit (WAPU).</p>	System to monitor patients with chronic diseases in their homes	WPPU can be configured for a variable gain between 500 and 1000.	<p>The study avoided the use of a PC and PDA (to reduce cost).</p> <p>System objectives: Eliminate the need for a PC, eliminate the need for users to configure the system, support automatic transmission of signals, lower cost, increase ease of use.</p>	Same quality of service as PC based systems at a lower cost.
13.	Hii and Chung ²⁻¹⁴	2011	Sensors (Basel)	<p>ECG, Smartphone camera (Sensors).</p> <p>The system was based on 3 layers, namely: (i) Body Sensor Layer [ECG nodes on body] (ii) Personal Network Layer [Mobile phone] (iii) Global Network Layer</p> <p>Platform: Mobile Phone</p> <p>Local-MVI communication: ZigBee</p>	<p>Mobile phone based real time ECG monitoring.</p> <p>It took advantage of the falling cost and rising complexity of mobile phones.</p>			Successful realtime monitoring on a testbed with a human subject.

				<p>Remote-MVI communication: CDMA, GSM, 3G or WiFi</p> <p>Modes: Real-time (immediately viewable on phone) or Store-and-forward (20 byte ECG data and summary reports transferred to the remote end). One ECG data packet contained 10 ECG signals (phone screen could display 5 packets, equivalent to 5s of data).</p> <p>Algorithm: Pan-Tompkins (The analysis was for QRS peaks, QT and RR intervals)</p> <p>The camera was used for scanning the QR barcodes on medicine packs.</p>	A QR code scanner was used to determine patient adherence.			
14.	Cleven et al ²⁵	2012	IEEE Transactions on Biomedical Engineering	<p>Capacitive pressure and temperature (Sensors). Measured intraarterial pressure using an implant consisting of a sensor tip and transponder communicating with a readout station.</p> <p>Local-MVI communication: Inductive coupling.</p> <p>The pressure sensor was powered using wireless magnetic telemetry.</p>	Wireless BP measurement		A batteryless system that uses an implant into the Femoral artery. The implant consists of a pressure sensor and telemetric unit and was placed under the skin.	The trial used an anesthetized sheep and readings were compared to a reference catheter. The system had an accuracy of $\pm 1.0\text{mmHg}$ and a range of 30-300mmHg.
15.	Pitts et al ²⁻¹⁶	2013	Physiological Measurements	<p>Accelerometer (Sensor).</p> <p>The algorithm was based on peak and edge detection.</p> <p>The system provided virtual sensing of respiratory rate based on the longitudinal (Z) axis reading of the accelerometer placed on the patient's clavicle.</p>	Simple low cost device for measuring respiratory rate and inferring disease if the rate falls outside the 12-20 breadth/minute rate of healthy adults.		<p>Respiratory sensor based on clavicular motion</p> <p>A clavicular sensor was used since it gave signals with a greater amplitude and which were more consistent than thoracic sensors.</p> <p>The system was tested on 8 volunteers.</p>	<p>R2 values mean clavicular respiratory rate: 0.89 (lateral) and 0.98 (longitudinal), compared to 0.49 (thoracic).</p> <p>System was unaffected by bioelectrical or electrode problems.</p> <p>A 4-min breath-by-breadth test period was used.</p>
16.	Anlike r et al ²⁻¹⁷	2004	IEEE Transactions on Information Technology in Biomedicine	<p>Blood pressure, SPO2, 1/12-lead ECG, 2-axis accelerometer, pulse, heart rate, temperature (Sensors).</p> <p>Data was encrypted using techniques inherent in GSM/GPRS.</p> <p>Algorithm: Pan-Tompkins.</p>	Unobtrusive wrist-worn multiparametric monitoring system.	Configuration was based on patient specific values: non aerobic/aerobic state (corresponding to level of user activity), age, gender, fitness and medical history.	<p>The study incorporated the patient's profile in order to reduce false alarms.</p> <p>It measured pulse and SPO2 continuously. BP and 30s of ECG were measured 3 times a day or at request of user.</p> <p>The user's health condition/equipment state was grouped into the following zones based on the results:</p>	<p>33 volunteers participated in a 70mins test.</p> <p>Results: For BP, 85% had a difference of less than 5 beats when compared to standard instruments.</p> <p>The ECG results were poor as a result of noise but other readings were ok.</p> <p>70% of users found the system comfortable.</p>

							(i) Normal (ii) Deviant (iii)Risk (iv) High Risk (v) System error																						
17.	Chung et al ²⁻¹⁸	2008	Telemedicine and e-Health	<p>Microphone- an omnidirectional electrets condenser-type (Sensor). System used the measured signals for the virtual sensing of Obstructive Sleep Apnea Syndrome (OSAS)</p> <p>System supported both monitoring and therapeutic applications. The therapeutic application involved nerve stimulation using a low frequency transcutaneous electrical signal.</p> <p>The system included a local webserver.</p> <p>Algorithm: Absolute difference between input voltage and baseline and moving average filter with a window size of 20.</p>	A portable telemonitoring device to recognize sleep-related breathing disorders in real-time	Configuration was based on the detection of a snoring pattern. The detection triggered a system configuration that stimulated the patient's nerve in order to stop the snoring.	5 regular snorers and 5 OSAS patients tested the system.	<p>There was a positive predictivity of 94% and a snoring sensitivity of 94%.</p> <p>The results indicated an OSAS positive predictivity and sensitivity of 73.3% and 81.1% respectively.</p>																					
18.	Chun et al ²⁻¹⁹	2005	Studies in Health Technology and Informatics	<p>Non-Invasive Blood Pressure [NIBP], SPO2, 1-channel ECG textrode electrode, Respiratory Rate [RR], Heart Rate [HR], Body surface temperature, Accelerometer, Posture (Sensors).</p> <p>RR and HR were virtual sensors based on ECG signals.</p> <p>Local-MVI communication: Wireless Remote-MVI communication: sms, cellular</p> <p>The expanded system (Integrated Home Telecare System) comprised the following sensors: 12-channel ECG, Respiratory function, Blood glucose, NIBP, Body fat meter and Spirometer.</p>	Personal Wearable Wristworn Integrated Health Monitoring Device (WIHMD)	<p>System was configured based on patient's diabetic history and postprandial time.</p> <p>The BP tests also considered the patient's history.</p>	<p>The primary system was based on the WIHMD.</p> <p>The secondary system had a number of non intrusive sensors used on the bed, toilet seat and chair. Capacitive sensors were used for the chair.</p> <p>10 volunteers tested the system and authors also used simulations.</p>	<table border="1"> <thead> <tr> <th>Simulation</th> <th>Tests</th> <th>Results</th> </tr> </thead> <tbody> <tr> <td>NIBP</td> <td>100</td> <td>± 4 mmHg</td> </tr> <tr> <td>SPO2</td> <td>100</td> <td>±2%</td> </tr> <tr> <td>HR</td> <td>100</td> <td>±0.9%</td> </tr> <tr> <td>RR</td> <td>50 people</td> <td>±1.8%</td> </tr> <tr> <td>Temp*</td> <td>20</td> <td>±1.5</td> </tr> <tr> <td>Fall#</td> <td>150</td> <td>91.3% #</td> </tr> </tbody> </table> <p>*: Tested in temperature controlled chamber #: Detection rate for simulated falls</p>	Simulation	Tests	Results	NIBP	100	± 4 mmHg	SPO2	100	±2%	HR	100	±0.9%	RR	50 people	±1.8%	Temp*	20	±1.5	Fall#	150	91.3% #
Simulation	Tests	Results																											
NIBP	100	± 4 mmHg																											
SPO2	100	±2%																											
HR	100	±0.9%																											
RR	50 people	±1.8%																											
Temp*	20	±1.5																											
Fall#	150	91.3% #																											
19.	Yu et al ²⁻²⁰	2013	Telemedicine and e-Health	<p>Temperature, mobile phone camera and microphone (Sensors)</p> <p>System used a mobile phone as a miniaturized health exam toolkit.</p> <p>Electronic health records were sent to remote server as e-mails or mms messages.</p> <p>Local-MVI communication: Wireless Remote-MVI communication: Cellular</p> <p>Algorithms: Machine learning</p> <p>System carried out tests for about 12 parameters used in annual physical exams</p>	Mobile phone based system for convenient "annual physical exam".		<p>Eye tests were based on image sizes on phone and feedback from users.</p> <p>The system was trained as follows: 3 deep breaths (for breadth sound), 1 minute data (for heart sound, temperature and ECG).</p> <p>There were 11 volunteers for the test.</p>	The entire test took just about 28 minutes.																					
20.	Fong	2013	Sensors	Platform: Android based phone	Cloud-based Non-	The system	The measurements	The results measured the																					

	and Chung ²⁻²¹		(Basel)	<p>ECG, Heart Rate, Camera (Sensors)</p> <p>Data was shared over the Internet instantaneously using the embedded webserver.</p> <p>Local-MVI communication: Bluetooth communication between capacitive coupled ECG sensor and phone.</p> <p>Inter-MVI communication: WiFi</p> <p>HR was calculated using a virtual sensor based on ECG.</p>	contact ECG monitoring and a QR code based patient adherence scheme.	supported a minimal level of adaptation based on QR code.	required the patient to seat on a chair with capacitive sensors.	website loading times as follows: 1st view load time (2.833ms), repeat view time (0.124ms), the Document Complete parameter, which occurs after all the images content have been loaded (2.833s), the Fully Loaded parameter, which includes any activity triggered by the JavaScript (6.452s).
21.	Giansanti et al ²⁻²²	2013	Telemedicine and e-Health	<p>Sensors: Gastrocnemius Expansion Measurement Unit (GEMU), gyroscope, accelerometer, SECOSP (a step counter)</p> <p>Platform: Custom portable device</p>	Real-time simple portable kit for home-based gait analysis.		<p>The portable kit works with a cascade of Instrumented Walkways (IWs). It also uses walking aids.</p> <p>16 subjects tested the system.</p>	System has a high level of accuracy and costs 948EUR.
22.	Gomez et al ²⁻²³	2008	IEEE Transactions on Information Technology in Biomedicine	<p>Realtime Continuous Glucose Monitoring (CGM) sensor.</p> <p>Platform: PDA (iPAQ hp2210)</p> <p>Local MVI: Bluetooth, Infrared or serial communication</p> <p>Remote MVI: Mobile GPRS for communication to the Telemedicine Central Server (TMCS).</p> <p>The system supports a therapeutic application- the control of an insulin pump.</p>		The PDA was remotely programmed by the TCMS under the doctor's supervision. The insulin pump was configured and controlled remotely in response to the measured CGM values	<p>CGM with real-time programmable insulin pumps.</p> <p>4 system control strategies: (i) Patient control: Manual change supervised by doctor (ii) Doctor control: Come as suggestions that the patient should download and approve (iii) Remote loop control: Programmed by the TCMS under the doctor's supervision. (iv) Personal loop control: Real-time control of the insulin pump based on glucose sensor data</p> <p>The patient has to issue e-consents (digitally signed certificates) before personal data can be accessed.</p>	<p>Only control strategies #1 and #2 were tested and the measured HbA1c values confirmed the effectiveness of the strategy</p> <p>System cost: 7,348 EUR (compared to 5,907 EUR for a CGM system based on a manual approach).</p>

							Feasibility testing phase: 4 Type 1 diabetic patients for 6 months.	
							Clinical testing phase: 10 Type 1 patients for 8 weeks.	
23.	D'Arcy et al 2-24	2011	IEEE Transactions on Biomedical Engineering	EEG sensor. A headset for auditory stimulation. Local-MVI Communication: Bluetooth The algorithm was known as called Halifax Consciousness Scan (HCS). It was based on preprocessing, peak detection and score generation	An approach for replacing the behavioral brain tests with one based on EEG signals. The test provides indicators for 5 identifiable levels of neural processing: sensation, perception, attention, memory and language	The specific parameters of the patient are compared to a normative database.	The portable EEG device for scanning for consciousness awareness addressed 5 challenges/areas: (i) Portability and noise resistance (ii) It has no need for advanced expertise or system training (iii) Addressed the spectrum of EEG-cortical responses (iv) Compared results to a normative database (v) The range of results covered diagnosis, reliability, validity and progression	The authors attempted to provide a solution at the interface between biomedical engineering and neuroscience.
24.	Chen et al 2-25	2008	Physiological Measurements	A pressure sensor was embedded in a pillow for static and dynamic pressure measurements. Wavelet based algorithms were used. Virtual sensing of the pressure was used to reconstruct pulse related waveform information from D4 & D5 components of wavelet transformation. Also, breadth related waveform was reconstructed from the A6 component.	Web-based long term heart and breath rate monitoring during sleep using a single sensor.		The raw pressure was measured under the neck-neck occiput region. The system measures static pressure (based on weight of head) and dynamic pressure (based on fluctuations caused by breathing). Analysis was based on the dynamic pressure. 1 patient was used to test the system over a period of 6 months	The system detected 82.3% of sleep time. The system provided a cheap 1 sensor alternative to replace the traditional \$1,000 11-sensor polysomnography equipment
25.	Nemir oskia et al 2-26	2014	Proceedings of the National Academy of Sciences, USA	A portable system that includes a vibration meter and an audio jack. This system interfaces with a low end mobile phone (Nokia 1100 series model 1112) and can also support 2G, 3G and 4G systems. The system uses a webserver to "geographically decouple" the measurement.	It is an inexpensive device that couples most forms of electrochemical	The system can switch between the following modes: (i) 2 or 3 electrode system.	The system supports cyclic voltammetry, differential phase voltammetry, square wave voltammetry and potentiometry	The system cost just \$25. It is a simple system, much unlike complex microfluidic based system. Latency (transmit and receive) for the blood glucose application was just 2.2s.

				<p>Local-MVI communication: Standard audio cable.</p> <p>Remote-MVI communication: Cellular (based on a live voice link through VoIP Skype between the phone and remote system).</p> <p>The remote server decodes the Frequency Shift Keying (FSK) data and sends an acknowledgement to the phone as an sms to verify the measured value.</p>	<p>analysis directly to the cloud.</p> <p>It uses a handheld device that works in a resource-constrained environment.</p>	<p>(ii) Amperometric (iii) Potentiometric</p> <p>The system can also be configured to accommodate new assays, sequences and standards</p>	<p>It supports low-end phones and does not require apps that are usually required for Smartphone based systems.</p> <p>The proof of concept was demonstrated in 4 application domains: (i) Blood glucose (ii) Trace heavy metals (iii) Sodium in urine and (iv) Test for malaria antigens</p>	<p>The system results for the 4 application domains were compared to results from a commercial bench-top analyzer and the following results were obtained:</p> <p>(i) No difference with respect to performance of the electronics. (ii) Blood glucose standard deviation: 5% (which is much better than most commercial glucometers). (iii) Heavy metals in water: Detection limit of 4μg/L, better than the recommended WHO level of 10μg/L (iii) Sodium in urine: Systematic error of 8%, which is within the certified range of \pm14% (iv) Malaria: Limit of detection was 20ng/mL.</p>
26.	Lee et al ²⁻²⁷	2010	Telemedicine and e-Health	<p>Sensors: Electrodermal Activity [EDA], Pulsewave [Condenser microphone].</p> <p>The EDA sensor was made of conducting fabric lines (instead of AgCl).</p> <p>Platform: Portable arm-band computer</p> <p>Realtime processing supported by a webserver.</p> <p>Local-MVI communication: Serial (RS-232).</p> <p>The algorithm was based on Fast Fourier Transform (FFT).</p>	<p>A system to detect drowsiness based on a correlation between EDA signals and drowsiness.</p>		<p>The system investigated the correlation between skin impedance and drowsiness.</p> <p>The EDA signal was decomposed into 2 signals: (i) Skin Impedance Level (SIL) and (ii) Skin Impedance Response (SIR)</p> <p>The experiment lasted for 30mins.</p>	<p>The detected states: - Aroused condition - Drowsiness - Sleeping</p> <p>The device was able to detect drowsiness before its onset.</p>

저작물 이용 허락서					
학 과	컴퓨터공학과	학 번	20097789	과 정	박사
성 명	아델루이 올루페미 올루월이 ADELUYI OLUFEMI OLUWOLE				
주 소	Chosun University Priv Dorm				
연락처	e-mail : femiadeluyi@yahoo.com				
논문제목	한글 : 신뢰할 수 있는 개인 건강 모니터링을 위한 경량 알고리즘의 설계				
	영문 : Lightweight Algorithms for Reliable Personalized Health Monitoring				
<p>본인이 저작한 위의 저작물에 대하여 다음과 같은 조건 아래 조선대학교가 저작물을 이용할 수 있도록 허락하고 동의합니다.</p> <p style="text-align: center;">- 다 음 -</p> <ol style="list-style-type: none"> 1. 저작물의 DB구축 및 인터넷을 포함한 정보통신망에의 공개를 위한 저작물의 복제, 기억장치에의 저장, 전송 등을 허락함 2. 위의 목적을 위하여 필요한 범위 내에서의 편집과 형식상의 변경을 허락함(다만, 저작물의 내용변경은 금지함) 3. 배포·전송된 저작물의 영리적 목적을 위한 복제, 저장, 전송 등은 금지함 4. 저작물에 대한 이용기간은 5년으로 하고, 기간종료 3개월 이내에 별도의 의사 표시가 없을 경우에는 저작물의 이용기간을 계속 연장함 5. 해당 저작물의 저작권을 타인에게 양도하거나 출판을 허락을 하였을 경우에는 1개월 이내에 대학에 이를 통보함 6. 조선대학교는 저작물 이용의 허락 이후 해당 저작물로 인하여 발생하는 타인에 의한 권리 침해에 대하여 일체의 법적 책임을 지지 않음 7. 소속 대학의 협정기관에 저작물의 제공 및 인터넷 등 정보통신망을 이용한 저작물의 전송·출력을 허락함 <p style="text-align: center;">동의여부 : 동의(0) 반대()</p> <p style="text-align: center;">2015 년 8 월 24</p> <p style="text-align: center;">저작자 : Adeluyi Olufemi Oluwole (인)</p> <p style="text-align: center;">조선대학교 총장 귀하</p>					